Investigating the Role of Nuclear Receptors in HIV/HAART-Associated Dyslipidemic Lipodystrophy

A Thesis

Submitted to the Faculty

of

Drexel University

by

Jennifer Berbaum

in partial fulfillment of the

requirements for the degree

of

Doctor of Philosophy

May 2007

Dedications

To Aslan and Uther….now you can play on Mommy's computer!
Thanks for being patient and understanding that 'Mommy has to work'.
I hope this experience has shown you that learning is for life and that it's never ever too late for accomplishing goals. Love You Guys.

To Mike….the washer of clothes, the washer of dishes, the washer of kids, the food shopper, the bill payer, the house cleaner, the tooth brusher, the fixer of all things and the love of my life…….thanks for letting me drop out for the past four years. I couldn't have done it without you. Now it's your turn!

To Rich….who didn't have to do this. You have reaffirmed my belief that success, fairness and honesty are not mutually exclusive. You've also shown me that 'keeping it real' can sometimes be a rough ride. Thanks for being an advisor in the truest sense. May we have many more adventures…..

To Mom and Dad…who taught me to finish what you start.

Acknowledgement

To the Biology group at Concurrent/Vitae Pharma….I'm sure everyone of you at some point helped me with something concerning this project.

Table of Contents

List of Tables

List of Figures

Abstract

Investigating the Role of Nuclear Receptors in HIV/HAART-Associated Dyslipidemic Lipodystrophy

Jennifer Berbaum

Richard K. Harrison, Ph.D.

The use of highly active antiretroviral therapy (HAART) to manage HIV infection is associated with the development of HIV/HAART-associated dyslipidemic lipodystrophy (HADL). HADL symptoms are comprised of metabolic dysfunctions resulting in hyperlipidemia, fat redistribution, and insulin resistance. The direct interaction of HIV drugs with nuclear receptors involved in metabolic pathways has been largely unexplored. HIV drugs were evaluated for effect on the activation of farsenoid X receptor (FXR), liver X receptor alpha (LXRα), retinoid X receptor alpha (RXRα), pregnane X receptor (PXR) and the peroxisome proliferator-activated receptor family (PPAR α, γ, and δ). Our results indicate direct inhibition of PPARα and PPARγ activation by protease inhibitors (PIs) in both coactivator recruitment and reporter gene assays. Gene chip analysis demonstrated that saquinavir and ritonavir reduced the expression level of PPARγ target genes in primary human hepatocytes. Partial recovery of mRNA levels of glucokinase (GK) and GLUT2 was achieved when hepatocytes were incubated in combination with the PPARγ agonist troglitazone. Decreased glucose sensing capabilities through PI-mediated inhibition of PPARγ activation may be a contributing factor in symptoms of HADL.

PPARα is the nuclear receptor responsible for regulating genes that control lipid homeostasis. Because of this role, PPARα has become a target of interest for the development of drugs to treat diseases such as dyslipidemia, obesity and atherosclerosis.

Assays currently employed to determine potency and efficacy of potential drug candidates typically utilize a truncated form of the native receptor, one which lacks the entire N-terminal region of the protein. We report that differences in PPARα full length and ligand binding domain constructs result in differences in binding affinity for coactivator peptides, but have little effect on potency of agonists in both cell free and cell based nuclear receptor assays.

Chapter 1: General Introduction

1.1 HIV/HAART Associated Dyslipidemic Lipodystrophy (HADL)

1.1.1 Highly Active Antiretroviral Therapy (HAART)

As of 2005, approximately 40 million people world wide are living with HIV [1]. In developed countries, the life expectancy of HIV-infected individuals has increased substantially through the implementation of highly active antiretroviral therapy (HAART) in the management of HIV infection [2-4]. The effectiveness of HAART lies in the co administration of different classes of antiretroviral drugs. These therapies target specific mechanisms within the HIV life cycle and provide a means for simultaneous inhibition of diverse viral processes providing tighter control of HIV replication than could be achieved with single therapy [2]. The three major classes of HIV drugs currently employed in HAART are the non-nucleoside reverse transcriptase inhibitors (NNRTIs), nucleoside/nucleotide analogue reverse transcriptase inhibitors (NRTI and NtRTI) and HIV protease inhibitors (PIs) [5].

Figure 1 shows the life cycle of HIV infection and illustrates the intervention points targeted by each of the three classes of drugs used in HAART. The mechanism of action of the NRTI and NtRTIs class of HIV drugs is the inhibition of transcription of viral ssRNA into ssDNA , an essential first step for viral dsDNA insertion into the host chromosome [6]. NRTI and NtRTIs are designed to structurally resemble the cellular nucleotides needed for reverse transcription of viral RNA [7, 8]. These nucleotide analogues are incorporated into the elongating strand of viral DNA by HIV reverse transcriptase [9]. This drug class does not directly inhibit HIV reverse transcriptase

activity but rather inhibits the elongation process itself. Unlike normal cellular nucleotides, NRTIs and NtRTIs lack the required 3'-hydroxyl group for addition of subsequent nucleotides and causes chain termination once incorporated into the elongating DNA strand. Both NRTI and NtRTIs need to be converted to their triphosphate form by cellular kinases. NtRTIs are monophosphorylated and require fewer metabolic steps to achieve their active form then the NRTI group which requires three phosphorylation events. The class of NRTIs currently includes the drugs zidovudine, didanosine, zalcitabine, stavudine, lamivudine, abacavir, and emtricitabine.

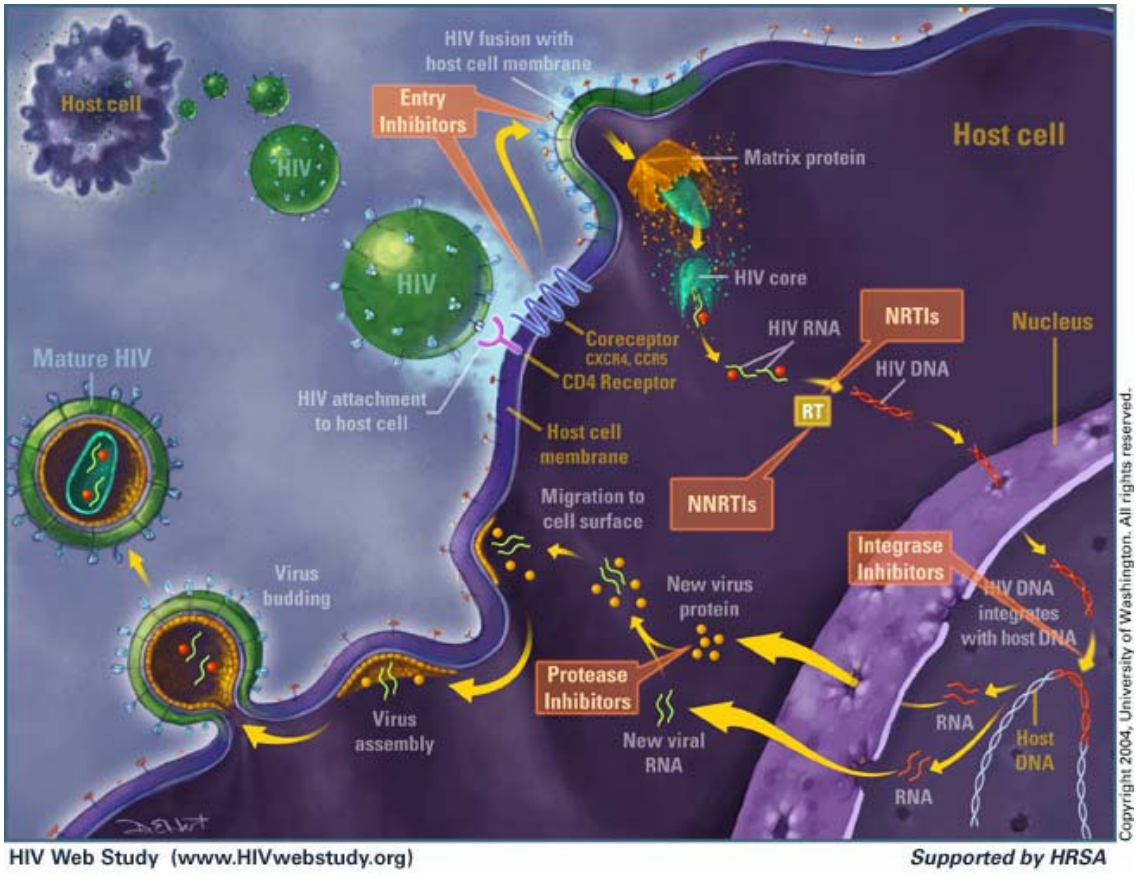

Figure 1. Mechanism of Action of HIV Drug Classes.

The NNRTI class of drugs also inhibit reverse transcription but do so in a more targeted manner than the nucleotide analogue class [6]. NNRTIs bind to a hydrophobic pocket located close to the catalytic domain of the HIV reverse transcriptase enzyme complex and inhibit the movement of protein domains required during DNA synthesis from viral RNA [10, 11]. In addition to target specificity, NNRTIs have an added advantage over the NRTI class because they do not need to be processed by cellular enzymes to become therapeutically active [8]. The class of NNRTIs is currently comprised of nevirapine, delavirdine, efavirenz, and emvirine.

PIs, the most potent therapeutic agent for HIV treatment, prevent viral replication by inhibiting the activity of HIV protease, an enzyme that cleaves nascent viral polyproteins for final assembly of new virons [12-14]. This critical process occurs as new virions bud from the membrane of an HIV-infected cell and continues after the immature virus is released. If the polyproteins are not cleaved, the virus fails to mature and is incapable of infecting a new cell. Five PIs, ritonavir, saquinavir, indinavir, atazanavir and nelfinavir are currently available for use in HAART.

HAART has extended the lives of HIV positive people far beyond what could have been hoped for prior to large scale implementation of the therapy in 1995. Despite the benefits of HAART, acute adverse events often reduce patient compliance and limit the effectiveness of treatment [15, 16]. Within the first year of treatment, ~50% of patients will modify or discontinue HAART altogether [16]. Among the side effects cited for discontinuation or modifications to HAART regimen are persistent diarrhea and nausea with significant weight loss, anemia, psychosis, renal failure, lactic acidosis, pancreatitis, polyneuropathy and hepatotoxicity [16, 17]. Patients who can adjust to

HAART must remain on a cocktail of HIV drugs for the duration of their lives in order to maintain low viral titer. Long-term use of HAART presents additional problems for HIV patients. Continuous long-term use of HAART has been linked to development of a metabolic disorder known as HIV/HAART associated dyslipidemic lipodystrophy. [18, 19].

1.1.2 Symptoms & Health Risks

Lipodystrophy, in patient with HIV, was first described in 1998 by Carr *et al*., approximately three years after PIs were employed in HIV treatment and HAART became the standard of care [20]. HIV/HAART associated dyslipidemic lipodystrophy (HADL) is used to describe a complex assembly of physical and metabolic abnormalities directly associated with the use of HAART in the treatment of HIV infection [19]. In general, HADL is indicated when HIV patients present with a combination of the following: elevated total cholesterol (> 200 mg / dL) combined with a decrease in high density lipoprotein (HDL) levels, increased triglycerides (> 325 mg / dL), insulin resistance and changes in body fat distribution with increased truncal obesity [20, 21]. Manifestation of HADL metabolic symptoms are considered to be significant risk factors for developing cardiovascular disease and type 2 diabetes [22-24].

The first report of body fat redistribution in an HIV patient was described in 1997 preceding the description of associated metabolic effects a year later [18, 25]. The main clinical features described involve the loss of subcutaneous adipose from the face and extremities resulting in an overly muscular appearance with prominent veins and sunken facial features. In conjunction with the loss of peripheral adipose, patients also have

excess deposition of adipose in tissues around the neck (double chin), dorsocervical spine (buffalo hump) and intrabdominal region [26, 27]. While these physical changes are often associated with successful reduction of viral burden and elevated CD4 counts, these changes also carry social stigma by presenting an outward sign of a patients HIV status [26, 28]. The appearance-related side effects have a profound psychological effect on patients and have been shown to impact long-term compliance to treatment [29-31]. In addition to representing HIV status, a shift from subcutaneous to visceral adipose accumulation also represents an underlying dysfunction in metabolic processes.

Visceral adipose is, metabolically speaking, more active than subcutaneous adipose [32]. Gene expression and cytokine release of negative effectors of metabolism such as resistin from visceral adipose is more robust in response to nutrient intake than levels found in subcutaneous adipose [33]. Visceral adipose is less responsive to the antilipolytic effects of insulin and as a result releases more free fatty acids (FFA) and cortisol into circulation than subcutaneous. High FFA and cortisol levels have powerful combined effects, resulting in insulin resistance and increased hepatic gluconeogenesis. Removal of visceral adipose has been shown to reverse peripheral and hepatic insulin resistance providing a direct link between the site of fat storage and the risk of developing insulin resistance, diabetes and dyslipidemia [34].

Dyslipidemia in HADL is characterized by increased levels of triglycerides (hypertriglyceremia) and cholesterol (hypercholesterolemia) with low levels of HDL and increased levels of low density lipoprotein (LDL). It has been well established that dyslipidemia is a significant risk factor for developing coronary artery disease (CAD) [35]. LDL particles are generated from very low density lipoproteins (VLDLs) which are

secreted from the liver and carry excess hepatic cholesterol and triglycerides (TG) to peripheral organs for use as energy or for storage [36]. The action of lipoprotein lipases on cell surfaces strip the VLDL of TGs resulting in formation of intermediate density lipoproteins (IDLs). These particles are taken up by the liver or converted to LDL by hepatic lipase which further strip the IDL of TGs creating a predominantly cholesterol laden particle. One of the first steps in the development of CAD is the movement of LDL into the arterial wall and the chemical modification and oxidation of LDL lipids [37]. Oxidized LDL (oxLDL) stimulates inflammatory signaling and recruitment of monocytes into the arterial wall. The monocytes differentiate into macrophages and internalize oxLDL. Loading of machrophages with oxLDL transforms these cells into foam cells. Foam cells are enlarged and filled with lipids that are released into the arterial wall during cell lysis forming the foundation of atherogenic plaques.

HDL is known as the good component in total cholesterol because of it role in reverse cholesterol transport [38]. Whereas the role of LDL is to transport excess cholesterol and triglycerides from the liver to peripheral tissues, HDL transfers cholesterol from the peripheral tissues back to the liver for excretion as bile acids. This transport is accomplished through the exchange of cholesterol from cells to HDL through the interaction of ATP binding cassette A1 transporters (ABCA1) on cell surfaces and apolipoprotein-AI proteins within the HDL particle [36, 39]. Decreased HDL levels accelerate progression of CAD because of a reduction in cholesterol deloading of macrophages. Even after arterial lesions have been established, increasing HDL levels has been shown to reduce the size and number of lesion in both mice and humans

indicating that HDL levels may be more important in CAD risk than total cholesterol and LDL levels [40, 41].

Clinical reports on the prevalence of HADL are highly variable. The percentage of patients presenting with symptoms associated with lipodystrophy and dyslipidemia range from 20% to as high as 80% [42-44]. The lack of a unifying definition of HADL combined with interpretational differences in the significance of changes in syndrome markers is a likely reason for variability in the incidence of HADL in patient populations [45]. Despite these statistical differences, it is certain that long-term HIV survivors will face additional health risks and quality of life issues associated with HAART.

1.1.3 Risk Factors Associated with HADL

The exact mechanisms that causes HADL is unknown, but certain factors have been associated with an increased risk of developing HADL. PIs have the strongest clinical link to HADL but other factors such as duration of infection and treatment, use of NRTIs, age and gender may contribute to the overall risk of developing HADL [46].

PIs account for the majority of metabolic symptoms of HADL. Many clinical studies have been conducted and have provided strong statistical evidence supporting a direct link between HAART containing PIs and HADL [47-50]. Data are sparse for PI only effects since the majority of HIV patients are on HAART where assignment of side effects to specific drugs is difficult. Studies where patients receiving PIs are switched to a non-PI therapy have shown marked improvement in HADL symptoms especially improvements in cholesterol and triglyceride levels with modest reversal of body fat remodeling [51-53]. Whereas most PIs have been found to induce dyslipidemia in HIV-

positive individuals, short course indinavir treatment had no effect on plasma lipid levels in HIV-negative subjects, and caused only mild hyperlipidemia in HIV-positive individuals [54]. In contrast, both HIV-positive and HIV-negative subjects treated with ritonavir displayed a robust increase in plasma cholesterol and triglyceride after short exposure time [54, 55]. There is little evidence for differential effects of specific PIs regarding the incidence of HADL, with the exception of ritonavir whose association with development of hypertriglyceridemia and hypercholesterolemia is stronger than for other PIs [56]. Atazanavir, a PI approved in 2003 for treatment of HIV infection, has demonstrated comparable antiviral activity to current PIs and has been shown to improve lipid profiles when substituted for other PIs in HAART [57]. Atazanavir may very well serve as the frame work for development of new PIs with decreased side effects, however, data concerning long-term use and the potential for development of HADL is still being collected [58].

The length of infection has been shown to have a negative impact on lipid profiles. Lipid abnormalities have been observed in HIV patients prior to implementation of HAART and in HAART-naïve patients. Lipid abnormalities resulting from HIV infection alone are characterized by a decrease in both LDL and HDL levels and an increase in TGs [59]. After patients begin receiving HAART, the lipid profile is transformed into a proarthrogenic profile by boosting TGs and LDL levels while leaving HDL levels unchanged [59, 60].

Increased risk of developing HADL is also associated with the age and gender of a patient [61]. Older individuals within the patient population tend to have higher cholesterol levels than younger patients at the beginning of treatment, providing a higher

cholesterol baseline for HAART treatment to build on. Male gender is also a risk factor for developing HADL due to a higher baseline of cholesterol and triglyceride levels in this patient population. However, studies have shown that women are more prone to adipose tissue alterations than male patients [62, 63].

Data suggest that use of NRTIs may be a risk factor for developing lipodystrophy associated with HADL. Peripheral loss and visceral accumulation of fat have been reported in PI-naïve patients treated with NRTIs alone [64, 65]. This redistribution of fat is often indistinguishable from those observed in PI-induced lipodystrophy [66]. Data are inconsistent concerning the effects of NRTIs on glucose tolerance and lipid profiles. In fact, patients with NRTI-associated body fat redistribution usually have normal or lower than normal lipid, glucose and insulin levels when compared to PI-related HADL patients. [64, 66].

NRTIs are effective as anti-HIV therapies due to their inhibition of HIV reverse transcriptase. The proposed pathway by which NRTIs cause lipodystrophy is thought to occur through the off-target inhibition of mitochondrial DNA polymerase gamma [6]. Interference in replication of mitochondrial DNA results in overall mitochondrial toxicity, mitochondrial DNA mutations and a reduction in mitochondrial function pertaining to β-oxidation of fatty acids and cytochrome c oxidation [6, 67]. Similar symptoms to HADL lipodystrophy have been reported in patients with the genetic disorder familial multiple symmetric lipomatosis (MSL) [68]. Familial MSL is generally caused by point mutations in mitochondrial DNA resulting in mitochondrial dysfunction and is characterized by marked accumulation of nonencapsulated adipose tissue around the neck (horse collar and buffalo hump), shoulders, and upper torso regions [69, 70].

Current evidence suggests that therapies containing NRTIs may be an aggravating factor for development of HADL by providing an additional risk factor for developing lipodystrophy but lack the metabolic effects observed in therapies containing PIs.

1.1.4 Cellular Mechanisms

The exact mechanism by which PIs initiate metabolic disturbances leading to HADL remains elusive. From the time HADL was first observed in the clinic, researchers have been focused on uncovering the underlying mechanism in the hope of minimizing side effects of current HIV therapies. Clinical observations of altered serum lipid and glucose levels and peripheral lipoatrophy in HADL patients indicate that PIs are likely interfering with effectors of lipid and glucose homeostasis. Some of the metabolic processes shown to be impacted by HIV PIs *in vitro* are inhibition of the glucose transporter-4 (GLUT4), inhibition of apolipoprotein B (ApoB) degradation, inhibition of preadipocyte differentiation and dysregulation of sterol regulatory element binding proteins (SREBPs) [71-73].

Entry of glucose into peripheral tissues is facilitated by GLUT4. After feeding, glucose levels rise, triggering release of insulin from the pancreas. Circulating insulin interacts with cell surface insulin receptors (IR), resulting in a signaling cascade involving various key signaling proteins including insulin receptor substrate 1 (IRS1), phosphatidylinositol 3-Kinase (PI3K) and Akt (Figure 2) [74]. Activated Akt moves from the cell surface back into the cytoplasm where it triggers the movement of GLUT4 to the cell surface. The mechanism through which Akt initiates the movement of GLUT4 is thought to occur through subsequent interactions with unknown cellular components

[75]. GLUT4 is incorporated into the membrane through the interaction of the vesicle-associated membrane protein (VAMP), associated with GLUT4 containing lipid vesicles, and Syntaxin on the membrane surface. Once positioned within the cellular membrane, GLUT4 begins active transport of glucose into the cell.

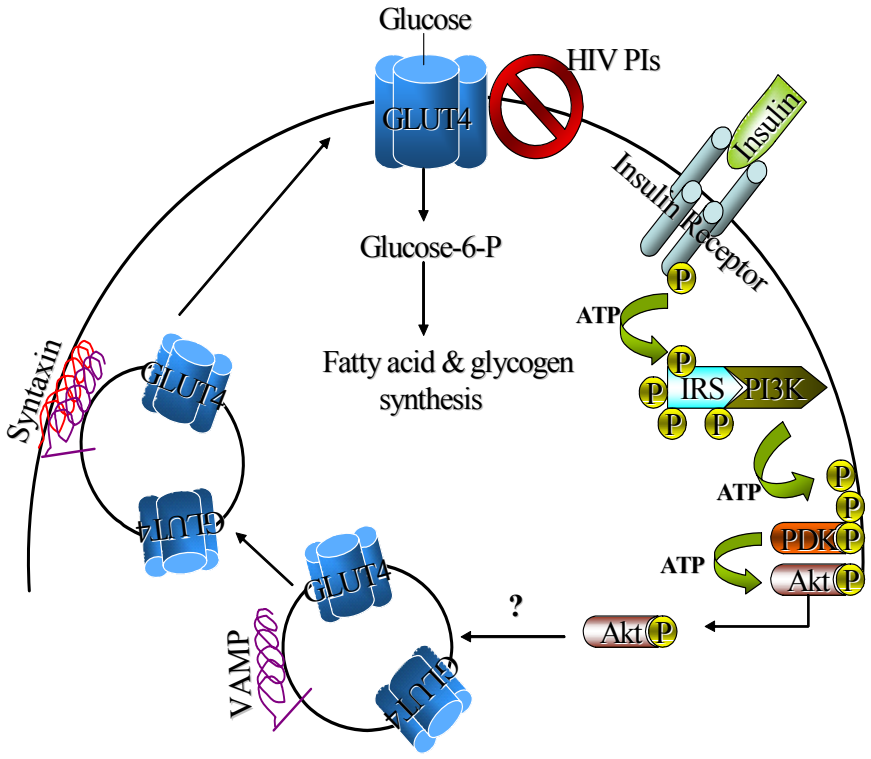

Figure 2. Model of Insulin Signaling and Transport of GLUT4 to the Cell Membrane. Insulin initiates uptake of glucose by triggering a cascade of kinase activity resulting in movement of GLUT4 to the cell surface. After feeding, insulin levels rise and insulin interacts with cell surface insulin receptors. This interaction activates the tyrosine kinase activity of the cytoplasmic portion of the insulin receptor which results in the phosphorylation of IRS. Phosphorylated IRS is then able to bind PI3K. PI3K phosphorylates membrane phospholipids allowing the binding of both PDK and Akt. When PDK and Akt are in close prosimity, PDK is able to phosphorylate Akt. Akt moves away from the cell surface and interacts with cytoplasmic substrates. Interaction with an, as of yet, unidentified substrate causes the movement of GLUT4-containing vesicles to the cell surface. The vesicles are integrated into the plasma membrane through the interaction of Syntaxin and VAMP. Once embedded in the membrane GLUT4 actively transports glucose into the cell where it can be used for energy or stored as glycogen and fatty acids. HIV PIs have been shown to interact directly with GLUT4 and prevent uptake of glucose.

PIs have been shown to act as reversible noncompetitive inhibitors of GLUT4 with binding affinities in the low micromolar range, well within estimated serum concentrations of most PIs [76, 77]. PIs also inhibit glucose transport by other GLUT isoforms although to a lesser extent than that observed with GLUT4. Indinavir is the only PI to show specificity in inhibition of GLUT4 and has been used to investigate the role of different GLUT isoforms in glucose uptake in tissues [78]. PI inhibition of peripheral uptake of glucose from circulation can result in hyperglycemia and insulin resistance, contributing significantly to alterations in glucose homeostasis.

Lipids, phospholipids and cholesterol esters are insoluble in plasma. These lipids combine with apoproteins to form lipoproteins for transport to and from the periphery. Apoproteins are important not only in maintaining the structural integrity of lipoproteins and thereby facilitating the solubilization of lipids, but they also play an important role in lipoprotein receptor recognition and regulation of certain enzymes in lipoprotein metabolism. Apolipoprotein B is the apoprotein associated with chylomicron, LDL, IDL and VLDL lipoprotein particles. An increased ratio of ApoB/ApoA-I containing lipoproteins is predictive of CAD risk [79].

Use of PIs has been shown to increase serum levels and resident time of ApoB containing lipoproteins like VLDL and IDL, independent of other risk factors. Whether the overall increase is due to an actual increase in hepatic lipoprotein production [80-82] or decrease clearance of ApoB lipoproteins through reduced expression of the LDL receptor [83, 84] or a combination of both is uncertain. A recent publication indicates that reduced levels of adiponectin, through loss of peripheral fat, directly correlates with VLDL and LDL clearance rates in treated and non-treated HIV patients [85]. Reduced

adiponectin levels may lead to reduced clearance of ApoB containing lipoproteins through transcriptional repression of lipases. Indicating that increased ApoB lipoproteins levels may be due in part to changes in peripheral and visceral storage of fat and concomitant change in adipokine signaling. Inhibitory effects of PIs on the proteasomal degradation of ApoB may be another contributing factor to the elevated levels of ApoB lipoprotein [80, 86]. The amount of ApoB secreted from the liver is regulated primarily by the rate of ALLN (N-acetyl-leucyl-leucyl-norleucinal)-sensitive proteasomal degradation of newly synthesized ApoB. PIs prevent the degradation of ApoB and lipid biosynthesis resulting in cellular accumulation of ApoB. The ApoB stock pile remains in the liver until lipid availability increases, as occurs in peripheral insulin resistance. Prolonged residence time of ApoB-containing lipoproteins allows for extensive exchange of TGs for cholesterol esters with HDL, increasing clearance rates of HDL and formation of oxLDL, contributing to CAD risk.

Transcription of genes involved in the synthesis of fatty acids, triglycerides, and cholesterol are in part controlled by the sterol regulatory element-binding proteins (SREBPs) [87]. SREBP-1 and -2 are synthesized as precursor proteins bound to the ER membrane and nuclear envelope. In order to enter the nucleus and activate gene transcription, SREBP must be released from the membrane by the SREBP cleavage–activating protein (SCAP). When cells become depleted in cholesterol, SCAP escorts SREBP to two proteases that are responsible for cleavage. Processing by site protease-1 and-2, results in the transcriptionally active SREBPs. The SREBP can be classified based on their transcriptional activity on lipid pathways. SREBP-1a is a general activator of gene expression for all SREBP target genes whereas, SREBP-1c and SREBP-2 are more

restricted to transcriptional activation of gene sets involved in fatty acid and cholesterol synthesis, respectively.

Experiments in mice show that exposure to PIs, especially ritonavir, induces accumulation of SREBP-1 and SREBP-2 in the nucleus of both adipose and liver tissues [88]. However, mRNA levels of SREBPs were unchanged when compared to control animals suggesting that increased levels of nuclear SREBPs were due to mechanisms other than increased transcription of the SREBP gene. The turn over of transcriptionally active SREBPs is also controlled by ALLN (N-acetyl-leucyl-leucyl-norleucinal)-sensitive proteasome degradation involving calpain-like enzymes and the 20S proteasome [89]. PIs have been shown to interfere with ALLN-sensitive proteasome processing of antigens in T cells and the presecretory degradation of ApoB discussed previously [86, 90]. It is through the inhibition of proteasome degradation of nuclear SREBPs that accumulation of active SREBPs is believed to occur [88]. Constitutively active SREBPs would result in increased unregulated transcription of crucial enzymes of *de novo* fatty acid and cholesterol synthesis such as fatty acid synthase (FAS), acyl CoA carboxylase (ACC) and HMG CoA synthase [87]. In fact, transgenic mice over-expressing active SREBP-1 display similar symptoms as those found in HADL including dyslipidemia, insulin resistance and fat remodeling [91].

Despite the progress made towards understanding the off-target cellular interactions of PIs, the redundant nature and complexity of metabolic pathways make it difficult to identify clinically relevant cellular mechanisms in the pathogenesis of HADL. The high dose of PIs required to achieve therapeutic effects further confound the problem by increasing the likelihood of multiple off-target interactions [92, 93]. It is apparent that

HADL likely results from the disruption of multiple pathways involved in energy homeostasis in various tissue types for full manifestation of HADL.

1.1.5 HADL-Like Diseases

Metabolic diseases reminiscent of HADL have been observed outside of the context of HIV infection and HAART. In fact, the first cases of HADL were initially described as a 'pseudo-Cushing's' syndrome due to the similarity in symptoms observed, specifically, peripheral lipoatrophy, truncal obesity and abnormal fat deposit on the upper back and neck [26]. Cushing's syndrome is a disease caused by the prolonged exposure of the body's tissues to high levels of circulating cortisol [94]. The syndrome is used to describe effects of cortisol excess through either hypothalamic-pituitary-adrenal axis (HPA axis) dysfunction or from excessive use of cortisol or other glucocorticoids. Genetic forms of Cushing's syndrome are rare and most cases occur through the use of steroids for treating chronic conditions such as asthma. Cushing's is mainly a lipodystrophy associated syndrome but is also associated with hypertension, insulin resistance and hyperglycemia. Despite the similarities, patients with HADL do not have elevated levels of circulating cortisol characteristic of Cushing's syndrome [26]. Interestingly, Syndrome X (also known as the metabolic syndrome), described as Cushing's syndrome of adipose tissue, also lacks elevated levels of cortisol associated with Cushing's syndrome [95].

Syndrome X is used to describe a cluster of metabolic dysfunctions linked to the dramatic rise of CAD and diabetes in industrialized nations [95]. Metabolic syndrome is associated with increased visceral obesity, dyslipidemia and insulin resistance without the

associated peripheral lipoatrophy observed in HADL. The foundation of metabolic syndrome resides in diet-induced obesity and the concomitant accumulation of visceral adipose. The visceral adipose of obese people has been found to have increased activity of the 11-beta-hydroxysteroid dehydrogenase type 1 (11βHSD1) enzyme when compared to the activity in adipose of non-obese individuals.

11βHSDs are glucocorticoid (GC) metabolizing enzymes that modulate the interconversion of active (cortisol, corticosterone) and inactive (cortisone, dehydroxycorticosterone) GCs in tissues [96]. The primary role of GCs is to mobilize stored fuel sources through gluconeogenesis, lipolysis and mobilization of amino acids [97]. The role of 11βHDs is to control access of GCs to the glucocorticoid (GR) and mineralocorticoid receptors (MR) by either dampening or amplifying the concentration of GCs above circulating levels in specific tissues [96, 98]. In contrast to the effects of Cushing's disease, increased 11βHSD1 activity in adipose tissue does not result in increased circulating levels of cortisol, in fact, serum levels of GCs are normal [99, 100]. The isolated activity of 11βHSD1 directly impacts the composition of serum lipids and peripheral insulin sensitivity through the release of FFAs, adipokines and proinflammatory cytokines from adipocytes into circulation [101].

Research has shown that the adipose tissue of patients with HADL have unusually high levels of 11βHSD1 mRNA, indicating that there is a potential for increased 11βHSD1 activity at these sites [102, 103]. Due to the pandemic nature of the metabolic Syndrome, much interest surrounds the development of therapeutics aimed at the inhibition of 11βHSD1. It is possible that advancements in the treatment of the Metabolic syndrome may also aid in the management and understanding of HADL.

HADL is classified as an acquired lipodystrophy. Lipodystrophies are disorders of adipose tissue characterized by selective loss of fat from various parts of the body [104]. There are several different types of lipodystrophies and can be either inherited or acquired, as in the case of HADL and metabolic syndrome. Inherited lipodystrophies arise from mutations in genes essential to the function and maintenance of adipose tissue. In the context of HADL and similarity in clinical manifestation, the most relevant inherited lipodystrophies are the type 2 and 3 familial partial lipodystrophies (FPLD). FPLD is characterized by fat loss from limbs and the gluteal region at puberty, while central, facial and visceral fat remain unaltered. FPLD2 results from mutations in the nuclear lamin A/C gene, while FPLD3 is linked to a variety of loss of function mutations in PPARγ. The extent of lipodystrophy and metabolic disturbances differ between FPLD2 and FPLD3. Patients with FPLD2 tend to have a more significant reduction in adipose but less metabolic dysfunction when compare to patients with FPLD3. Early investigations into the underlying mechanism of HADL stemmed from the observation that the severe metabolic effects in patients with FPLD3 were similar to HADL patients and that the symptoms of HADL could be due to PI interference of PPARγ activation [18].

1.1.6 HADL and PPARγ

Conflicting results have been reported on the effects of PIs on PPARγ function. Saquinavir and indinavir have been shown to inhibit differentiation of preadipocytes in culture, a function firmly attributed to functional PPARγ. However, levels of aP2 expression, a known PPARγ target gene, were found to be unaffected [105, 106]. Lenhard

et al. also reported decreased adipogensis, lipogenesis and increased lipolysis upon exposure of adipocytes to saquinavir, ritonavir and nelfinavir but with an associated decrease in mRNA levels of adipocyte markers, aP2 and LPL [107]. In contrast, similar experiments performed by Ragnathan and Kern showed decreased activity of LPL in adipocytes without a decrease in mRNA levels upon exposure to saquinavir suggesting PIs may act through alterations in post-translational processing rather than transcription [108]. PI effects on lipolysis, lipogenesis and expression of aP2 and LPL are opposite to effects observed for PPARγ agonists in cultured adipocytes. Further, treatment of HADL patients with rosiglitazone and metformin, known agonists of PPARγ, provides at least moderate improvements in both insulin resistance and fat distribution [109]. Despite circumstantial evidence suggesting involvement of PPARγ in HADL, direct interaction between PIs and PPARγ have yet to be established.

With the exception of PPARγ, nuclear receptors have been largely overlooked as potential targets of PIs in the development of HADL. The severity of metabolic changes observed in patients with HADL suggests that a whole body disruption of energy regulation is occurring. Maintenance of energy homeostasis is achieved through the coordinated control of diverse cellular mechanisms. The activity and availability of key enzymes and transporters within a pathway are modulated by the fine tuning of activation states, allosteric control of substrate binding and gene expression levels in response to nutritional status. Gene expression is controlled by nuclear receptors that are sensitive to fluctuations in concentrations of endogenous and exogenous biological modulators such as drugs, hormones, steroids and metabolic intermediates. Nuclear receptors serve as metabolic sensors whose activation, or suppression, has the potential for long lasting

global effects on pathways of energy utilization. The role of nuclear receptors as major transcriptional regulators directly affecting the abundance of target genes in multiple metabolic pathways and the potential for PI-mediated desensitization to intrinsic ligands, make them ideal candidates in the pathology of HADL.

1.2 Nuclear Receptors

1.2.1 Structure and Function

Gene activation is highly regulated to ensure that appropriate genes are turned on or off according to environmental, developmental and cell cycle controls. The core transcriptional enzyme, RNA polymerase II (Pol II), requires several general transcription factors to perform functions related to DNA unwinding as well as initiation and elongation of transcripts [110]. Pol II and the general transcription factors form what is known as the basal transcriptional machinery. The basal transcriptional complex is sufficient to maintain low levels of cellular gene transcription. However, high levels of regulated, gene-specific transcription require the additional action of ligand-activated transcription factors bound to DNA enhancer element in the promoter region of responsive genes. These ligand-activated transcription factors or nuclear receptors mark a specific gene or a subset of genes for increased transcription by the basal machinery to enhance the transcriptional response to cellular signals [111].

Nuclear receptors are activated primarily through the binding of small, lipophilic ligands that include hormones and endogenous metabolites such as fatty acids, bile acids, oxysterols, and xenobiotics [112]. The activation state of nuclear receptors can also be influenced by other mechanisms including, phosphorylation by cellular kinases in cell

signaling pathways and protein-protein interactions through contacts with other transcription factors [113]. Most members of the nuclear receptor superfamily were originally identified by surveying the genome for stretches of DNA sequences homologous to the classic steroid receptors, GR and estrogen receptor (ER) [114]. The newly discovered receptors were called ‘orphan’ receptors because, at the time, little was known about their function or endogenous ligands. The discovery of these receptors was based on the observation that nuclear receptors are constructed of four independent but interacting functional domains and that the sequence of these domains are conserved across the receptor family [115]. The four functional domains are the modulator domain, DNA binding domain (DBD), hinge region and ligand binding domain (LBD) (Figure 3). The regions of greatest sequence homology among nuclear receptors reside in the LBD and DBD with the hinge and modulator domain having the least similarity. The nomenclature of the nuclear receptor family is based on sequence identity within the LBD and DBD [116]. Receptors within the same group must share at least 80-90% identity within the DBD and at least 40-80% identity within the LBD. The human nuclear receptor superfamily contains a total of 48 nuclear receptors divided into 7 subfamilies and 26 groups.

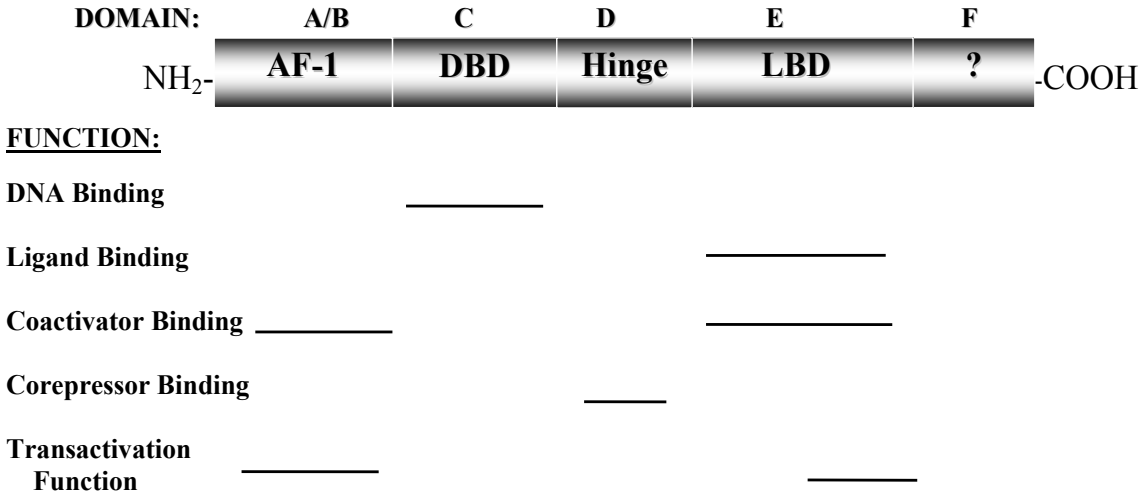

Figure 3. Nuclear Receptor Structural and Functional Domains. The A/B domain, the most variable domain among receptor groups, contains a ligand-independent activation function (AF-1) and coactivator protein binding sites. The C domain is highly conserved and contains zinc finger motifs essential for response element binding. The D domain or hinge region provides flexibility to the nuclear receptor structure as well as binding sites for corepressors. Ligand-dependent transactivation depends on the carboxy-terminal E domains which undergo conformational change upon binding of ligand, allowing for proper positioning of the AF-2 and recruitment of coactivator proteins. The exact function of the F domain is unknown and is present only in certain nuclear receptor groups.

The DBD, also known as the C domain, is highly conserved in sequence across the receptor family due to its function in DNA binding. The function of the DBD is recognition and binding of activated receptors to target gene response element sequences [117]. DNA response elements (RE) are comprised of two hexameric nucleotide sequences known as half sites located in the promoter region of nuclear receptor responsive genes [115]. The sequence, arrangement and spacing of the half sites define the responsiveness of a gene to various nuclear receptors. In general, steroid receptors preferentially recognize AGAACA half sites and bind as homodimers. Receptors that

form a heterodimer pair with RXR typically recognizes AGGTCA as their half site with variable nucleotide spacing between the two half sites. Together with the nucleotide spacing of half sites, the arrangement as either direct, inverted or everted repeats convey receptor specificity. The DBD is GC-rich and contains two zinc finger motifs with a carboxy-terminal extension containing T and A boxes critical for monomeric DNA binding of RE half-sites [112, 117]. The first zinc finger contains amino acid sequences, known as the P box, that are essential for recognition of DNA RE sequences of target genes. The second zinc finger contains the D box which provides an interface for dimerization with the DBD of either a homodimer or heterodimer partner occupying the other half site of the RE.

The LBD, also known as the E/F domain, is a multifunctional domain with sequences critical for ligand binding, ligand-dependent transactivation function (AF-2), receptor dimerization, nuclear localization and the binding of coactivators and heat shock proteins [115, 118]. All nuclear receptor LBDs are comprised of 12 α-helices arranged to form three separate helical sheets that form a hydrophobic pocket suitable for binding of lipophilic ligands [118]. The steroid receptor group members, such as GR and MR, require the binding of heat shock proteins for proper orientation of LBD helices and arrangement of the hydrophobic pocket. Binding of ligand triggers rearrangement of the LBD helices, releasing heat shock proteins and corepressors. The carboxy-terminal helix 12, containing the AF-2, is positioned across the LBD pocket exposing sequences required for coactivator protein interactions rendering the nuclear receptor transcriptionally active.

The hinge region, also known as the D domain, is a stretch of sequence between the DBD and LBD that is variable in both length and sequence between receptor groups [115]. The hinge region contains binding sequences for corepressors, essential for transcriptional silencing. The hinge region also provides flexibility to the receptor domains for proper orientation for both RE binding and dimmer formation.

The amino-terminal modulator domain, also known as the A/B domain, contains amino acid sequences conveying ligand-independent activation function (AF-1) [115]. Truncated expression of receptors, lacking the LBD portion of the receptor sequence, were found to retain functional activation despite the inability to bind ligand. This region also contains sites targeted for phosphorylation by different signaling pathways [119]. Effects on activation due to phosphorylation are receptor-specific and can result in either enhanced or diminished receptor activation. Binding sites for coactivator proteins, essential cofactors for gene transcription, are highly concentrated in the LBD domain and are only accessible upon ligand binding. Coactivator binding sites have also been identified in the modulator region, indicating that transcriptional events mediated through unliganded receptor activation are completely independent of LBD function. Although AF-1 and AF-2 are capable of regulating transcription alone, full transcriptional activation by AF-2 requires functional interactions between the two regions [118, 120]. The interaction facilitates sustained receptor activation and robust gene transcription through stabilization of helix 12 preventing premature dissociation of ligand and mutual binding of coactivators. Although nuclear receptors, in general, share significant homology in both primary amino acid sequence and tertiary structure, the modulator domain shows little or no sequence homology between the different families of receptor

[117]. In fact, the modulator domain is virtually nonexistent in some members of the nonsteroidal receptor group, indicating that these receptors are activated primarily through ligand binding. The nuclear receptor superfamily can be divided into groups based on the specific mechanisms involved in their activation [112, 115]. Type 1 nuclear receptors encompass the steroid hormone binding class of receptors consisting of GR, MR, androgen receptor (AR), progesterone receptor (PR) and ER. While in an unliganded state, these receptors reside in the cytoplasm bound by heat shock proteins (HSPs), specifically HSP90 [121]. Steroid hormones diffuse freely across the plasma membrane and bind to the receptor facilitating the release of HSPs, allowing homodimerization and translocation of the receptor to the nucleus. The remaining members of the nuclear receptor superfamily are classified as type 2 receptors and serve as receptors for nonsteroidal hormones and intermediates of metabolism such as fatty acids, bile acids and oxysterols. Unlike the type 1 receptors, Type 2 receptors do not require association with HSPs and move freely between cytoplasm and the nucleus [122]. In the nucleus, many of these receptors are found to be transiently associated with chromatin, implying that type 2 receptors interact with target gene REs in an inactivated state. Many of the type 2 receptors actively repress basal transcription by recruiting corepressors which are released in the presence of ligand (Figure 4). The majority of type 2 receptors exist as heterodimers with RXR although some receptors from this group, such as NGFI-B and HNF-4, function as monomers and homodimers, respectively [115]. Despite the differences between the type 1 and 2 receptors concerning cellular localization, dimerization and RE binding, both share similar mechanisms in target gene transcription.

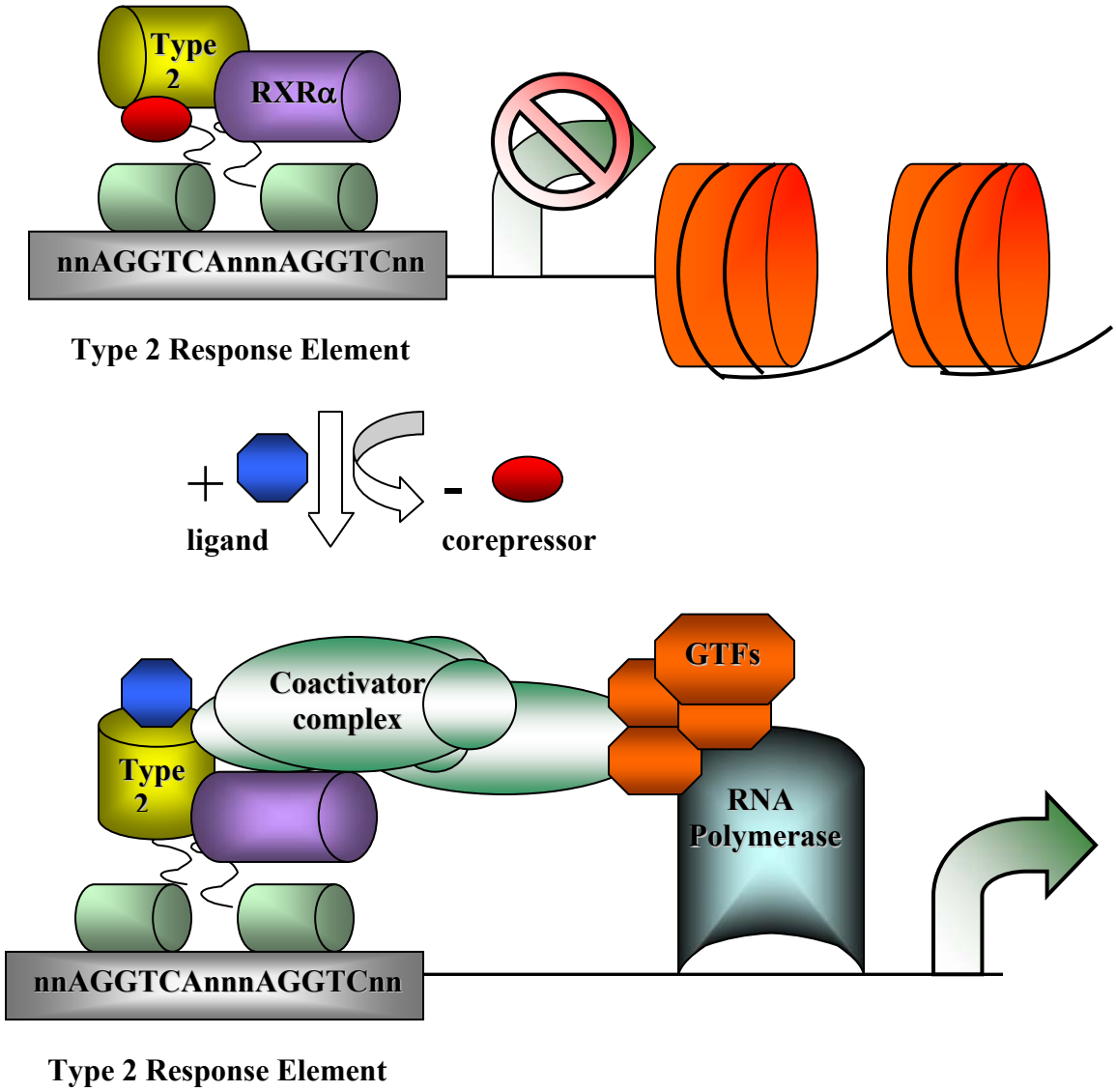

Figure 4. Model of Type 2 Nuclear Receptor Activation. Type 2 nuclear receptors form heterodimers with RXRα. These heterodimers are capable of binding DNA in an unliganded state. Bound to target gene response elements, type 2 receptors can actively repress basal transcription through the binding of corepressors. Binding of ligand triggers conformational changes resulting in release of corepressors and recruitment of coactivators. The coactivator complex removes repressive chromatin structures through the acetylation and methylation of histones providing access to promoter regions for RNA polymerase II and the general transcription factors (GTFs).

Once activated and bound to target gene REs, nuclear receptors must recruit and bind coactivator proteins in order to increase gene transcription. Initially, coactivator proteins were considered silent obligate participants in nuclear receptor transcriptional events, providing a bridge between DNA binding transcription factors and the general transcription machinery, with little influence over the transcriptional event itself [123]. Advancements in the field have shown that the function of coactivator proteins in controlling gene transcription is much more complex.

To date, ~200 members of the coactivator protein family have been identified with 50-70 having been characterized as coactivators exclusive to nuclear receptors [124]. Unlike nuclear receptors, coactivators are structurally and functionally diverse. Not only do coactivators serve as adapters between the receptor and general transcriptional machinery, but also perform enzymatic activities essential to transcription. The primary function of coactivators is the remodeling of chromatin through the modification of histones [125]. Acetylation and methylation of histones by coactivators removes repressive chromatin structures providing access of transcription factors to enhancer and promoter regions of DNA targeted by nuclear receptors. In addition to chromatin remodeling, coactivators also influence the termination of transcriptional events through ubiquitin ligase activities and splicing decisions of the resulting RNA transcripts.

Recruitment of coactivators results in a multifunctional coactivator complex. The assembly and content of the coactivator complex is influenced by many factors including cellular coactivator abundance and affinity as well as the type of RE and ligand bound by the nuclear receptor. Assembly of the complex is initiated through the binding of a core

coactivator which interacts directly with the nuclear receptor through its LXXL motif [126]. Coactivators contain several LXXL motifs with flanking sequences conveying affinity for certain receptors thus enabling coactivators the ability to bind to different combinations of nuclear receptors [127]. The LXXL flanking sequences are subject to posttranslational modifications which influence the binding affinity of coactivators to nuclear receptors and other coactivators [128]. These postranscriptional modifications are mainly phosphorylation events mediated by kinases in cell signaling pathways. Phosphorylation at the LXXL motif and other regions within the coactivator as well as enzymatic actions by other coactivators provides an opportunity for the fine tuning of transcriptional events outside of the context of nuclear receptor activation. The content of the coactivator complex is also dictated, in part, by cellular abundance. Coactivators, like nuclear receptors, have tissue specific expression patterns that change in response to the cellular environment [129, 130]. Peroxisome proliferator-activated receptor gamma coactivator-1 alpha (PGC-1α) has been found to be expressed at higher levels in muscle in response to strenuous exercise [131]. Altered expression levels of coactivators have also been found during embryonic development and in certain cancers, such as prostate and breast cancer [132-135]. Differential expression of coactivators has the potential to influence the content of the coactivator complex and the resulting transcriptional activation of gene subsets by an activated nuclear receptor [136, 137].

Coactivator recruitment is also influenced by the type of ligand bound by the nuclear receptor as demonstrated by the variability of gene responses to different ligands. Binding of tamoxifen instead of the natural ligand, estrogen, to the estrogen receptor alpha (ERα) changes the binding preference of ERα to specific response elements and

alters coactivator preference [138]. Diversity in DNA sequence among target gene REs can cause subtle differences in binding of the DBD of a receptor which in turn influence the conformation of the entire receptor. Differences in RE sequence can change the conformation of the LBD resulting in alterations in both ligand affinity and coactivator preference.

1.2.2. Nuclear Receptors of Metabolism

1.2.2.1 Peroxisome Proliferator Activated Receptors (PPARs)

PPARs, and the potential benefit of PPAR activating drugs, have been the focus of intensive research in the treatment of obesity, diabetes and the metabolic syndrome [139, 140]. Metabolic syndrome is characterized by visceral fat accumulation, hyperlipidemia, elevated triglycerides, elevated blood pressure, and hyperglycemia [141], symptoms similar to those found in HADL and FDLP3, to which PPARγ mutations have already been linked (1.1.5). The PPAR family of nuclear receptors is comprised of three isotypes, α, γ and δ. PPARs are activated by a wide range of endogenous and dietary fatty acids and their derivatives such as prostaglandins and leukotriens [142-144]. PPARs regulate lipid, cholesterol and glucose homeostasis through coordination of gene transcription effects in liver, muscle and adipose tissue. While the PPARs share common ligands, the differential tissue expression pattern, distinct coactivator recruitment preference and variable affinity for ligands results in isotype-specific effects on target gene expression [145, 146].

The primary role of PPARα is the regulation of β-oxidation of fatty acids [142]. PPARα is highly expressed in tissues with high rates of fatty acid catabolism such as the

liver, muscle, kidney and intestine. During fasting, fatty acids are released from adipocytes and transported to the liver. PPARα activation by fatty acids increases transcript levels of genes such as acyl CoA oxidase (ACO) resulting in the increased production of ketone bodies for energy utilization by peripheral tissues [147]. Fatty acid β-oxidation also occurs in skeletal muscle but regulation at this site is not exclusive to PPARα, highlighting the overlapping control of such vital processes. PPARα also enhances uptake and transport of circulating fatty acids through modulation of target genes such as apolipoprotein A (ApoA), fatty acid binding proteins (FABP) and LPL. Activation of PPARα by dietary polyunsaturated fatty acids (PUFAs) and the fibrate class of hyperlipidemic drugs has been shown to have beneficial effects on circulating triglyceride levels and plasma lipid profiles [142]. In addition to its role in lipid metabolism, PPARα also effects gluconeogenesis in the liver and pancreatic islets by promoting the use of pyruvate in gluconeogenesis rather than fatty acid synthesis through upregulation of pyruvate dehydrogenase kinase 4 (PDK4). In general, PPARα serves to direct lipids to the liver while PPARγ activates storage of lipids in peripheral tissues working in concert to maintain balance between energy storage and utilization.

PPARγ is a major regulator of both adipocyte differentiation and the subsequent uptake and storage of lipids in the mature adipocyte. Activation of PPARγ in the preadipocyte promotes cell cycle arrest through the induction of cell cycle inhibitors such as p18 and p21, inhibitors of cyclin-dependent kinase (CDK), along with repression of cyclins [148]. During differentiation, expression of genes essential for transformation of the preadipocyte to a mature adipocyte is increased. Adipose differentiation related protein (ADRP), a well known target gene of PPARγ, is upregulated during

differentiation and is essential to maintenance of lipid droplet structure in adipocytes [149]. Loading of adipocytes with lipid is achieved through the upregulation of PPARγ genes involved in the removal of fatty acids from circulating lipoproteins, such as LPL, and transport of these fatty acids into the adipocyte through fatty acid transport protein (FATP) [147, 150].

PPARγ is also a major regulator of insulin sensitivity and it is this specific function that is the target of therapies directed towards activation of PPARγ. Thiazolidinones or TZDs, such as rosiglitazone and pioglitazone, are marketed PPARγ agonists that are highly effective in the treatment of type 2 diabetes [151]. The insulin sensitizing effects of TZDs are thought to be a result of PPARγ activation in adipose and the beneficial shift of fatty acid storage to adipose rather than muscle and liver, minimizing insulin resistance associated with fatty acid storage in non-adipose tissues. PPARγ activation also results in increased release of adipokines, such as adiponectin, from adipose tissue and may contribute to the insulin sensitivity of TZDs [152]. In addition to expression in adipose, PPARγ is also expressed in tissues essential to glucose homeostasis such as, the liver, pancreas and muscle, but at levels much lower than those observed in adipose tissue. The role of PPARγ in these tissues is poorly understood but has raised questions concerning the possibility of PPARγ playing a direct role in glucose uptake, storage and signaling. PPARγ REs have been located in the glucose transporter 2 (GLUT2) and liver glucokinase (GK) genes, two genes critical to postprandial glucose uptake and signaling in the liver and pancreas [153]. Consistent with these findings, both GLUT2 and L-GK transcript levels increase in the presence of PPARγ agonists in cultured cells [154, 155]. The products of these genes are essential for

the facilitated transport and retention of glucose, allowing efficient glucose stimulated insulin secretion (GSIS) in pancreatic beta cells and storage of glucose as glycogen in the liver. It is possible that the positive effects of TZD through activation of PPARγ may have a direct effect on insulin secretion in addition to improving peripheral insulin sensitivity.

PPARδ, the least characterized of the PPAR family members, is ubiquitously expressed and has been implicated in fatty acid transport and oxidation, as well as, inflammatory responses, wound healing and maintenance of adipocytes [156]. The development of specific, high affinity PPARδ agonists have provided insight into the effect of PPARδ on serum lipid composition and fat deposits in animal models of obesity and diabetes [157]. PPARδ activation has been shown to increase HDL levels by as much as 78% and decrease adipose tissue fat deposits, TGs and LDL particles [158, 159]. The improved serum lipid profile through activation of PPARδ is presumed to result from an increase in expression levels of the reverse cholesterol transporter, ATP binding cassette A1 (ABCA1). These positive effects of PPARδ specific agonists suggest PPARδ may be a suitable target for the treatment of hyperlipidemia.

Skeletal muscle expression of PPARδ has been found to be ~10-50 fold higher than either of the other PPAR family members, making skeletal muscle the primary tissue for PPARδ-specific effects [160]. PPARδ in skeletal muscle is associated with oxidative slow-twitch fibers where it regulates the expression of genes involved in fatty acid transport, oxidation and glucose uptake. Activation of PPARδ has been shown to increase the expression of myoglobin and tropinin 1 slow, which influence the change of muscle fiber type from glycolitic to oxidative [161, 162]. High proportions of oxidative slow-

twitch fibers in muscle have been demonstrated to provide protection against obesity, diabetes and contribute to an overall increase in muscular endurance [161].

1.2.2.2 Farsenoid X Receptor and Liver X Receptor

Farsenoid X receptor (FXR) and liver X receptor alpha (LXRα) play a pivotal role in total body cholesterol homeostasis. LXR activation is triggered by increased levels of oxysterols, which increase in proportion to cellular cholesterol content [163, 164]. LXR facilitates the processing and storage of cholesterol by upregulating cyp7A1 expression, the rate limiting enzyme in the conversion of cholesterol to bile acids. LXR responds to high cholesterol levels by increasing fatty acid synthesis to increase the formation of cholesterol esters, rendering the excess cholesterol pool biologically inactive [165].

LXR also facilitates efflux of cholesterol from the periphery, including macrophages, through the increased expression of ABC transporters [166]. Induction of ABC transporters increases the transfer of cholesterol and phospholipids to ApoA1 containing lipoproteins and may contribute to the increased levels of c-HDL seen with LXR agonist treatment [167]. Activation of LXR also decreases intestinal absorption of cholesterol and appears to also be mediated through the induction of ABC transporters, specifically ABCG5 and ABCG8.

Activation of LXR also has positive effects on glucose metabolism. LXR-mediated improvement in glucose tolerance is associated with decreased expression of rate limiting enzymes of gluconeogenesis such as phophoenolpyruvate carboxykinase (PEPCK) and glucose-6-phosphatase (G6Pase) and the induction of genes for glucose

uptake and utilization in the liver and periphery, such as L-GK and GLUT4, respectively [168]. The effects of LXR on fatty acid synthesis are mediated through the increased expression of SREBP-1, a transcription factor suspected in PI-induced lipodystrophy and discussed in section (1.1.4) [169]. The increased production of liver TGs as well as transient increases in plasma levels resulting from the upregulation of SREBP remains a roadblock in the development of LXR agonists as therapeutics for diabetes.

FXR, the counterbalance of LXR action in the liver, is activated by bile acid accumulation resulting from the LXR-mediated conversion of cholesterol to bile acids [170]. High concentrations of bile acids can be toxic to the cell and FXR functions to minimize this potential by inhibiting further production of bile acids. Inhibition of bile acid synthesis is achieved by increasing expression of the short heterodimer partner (SHP) [171]. SHP represses cyp7A1 expression by binding to promoter sequences and preventing further RE binding of activated LXR. FXR also facilitate elimination of bile acids through the activation of bile acid transporters such as, the bile salt export pump (BSEP) also known as sister of p-glycoprotein (SPGP) and the intestinal bile acid binding protein (IBABP) [172, 173]. Interestingly, PXR is also activated by bile acids, especially lithocholic acid (LCA) [174]. PXR activation results in inhibition of cyp7A1, similar to FXR, although by an unknown mechanism. Recent data suggests FXR may directly regulate PXR transcription levels and may serve to promote robust liver detoxification in the presence of high levels of bile acids [175].

Recent publications concerning FXR and the development of constitutive activating and knockout (KO) models have demonstrated that FXR activation has positive effects on glucose metabolism and has triggered much activity surrounding FXR

as a therapeutic target for diabetes [176]. Positive effects of FXR agonists on glucose tolerance are brought about through the hepatic activation of FXR and the resulting repression of gluconeogenic genes, PEPCK and G6Pase, and increased hepatic glycogen synthesis [177, 178]. In addition to improving glucose tolerance, FXR activation also improves serum lipid profiles through suppression of hepatic triglyceride synthesis via repression of SREBP-1c and increased expression of lipid metabolism genes such as PLTP, LCAT and apoC-II. However, FXR-mediated inhibition of fatty acid synthesis may be transient. Prolonged exposure to high levels of bile acids or potent agonists does not appear to have the same beneficial effects as short term exposure on plasma lipids [179]. SHP-mediated suppression of SREBP-1c via FXR activation appears to be overcome through the direct activation of fatty acid synthase (FAS) by FXR. Direct activation of FAS by FXR is necessary for sufficient fatty acid synthesis under states of cholesterol and bile acid excess in order to continue esterification of cholesterol and avoid cholesterol toxicity. Further research is needed in order to determine whether FXR agonists will be suitable in the treatment of metabolic diseases or whether the multiple gene effects of nuclear receptor activation will provide drug development hurdles as they have done in the development of PPARα/γ and LXR agonists [169, 180] .

1.2.2.3 Pregnane X Receptor

Inclusion of the HIV PI ritonavir in combination therapies has been shown to significantly improve circulating concentrations of coadministered drugs [181, 182]. Improvement in drug serum concentrations have been attributed to a reduction in overall drug metabolism due to direct inhibition of the monoxygenase cytochrome p450 3A4

isozyme (cyp3A4) by ritonavir [183]. Cyp3A4 is responsible for the metabolism of more than 50% of drugs administered to humans. Pregnane X receptor (PXR) RE sequences identified in the promoter region of the cyp3A4 gene have indelibly linked 3A4 transcriptional regulation to the activation of PXR [184]. Activators of PXR are mainly comprised of substrates and inhibitors of cyp3A4, providing a mechanistic loop for effective drug clearance [185]. PXR is expressed predominantly in the liver and is activated by a broad range of structurally diverse xenobiotics and endogenous ligands. PXR REs have been identified in additional p450 enzymes, drug export pumps and phase 2 drug metabolizing enzymes, implicating PXR as the master regulator of xenobiotic metabolism and clearance [186].

In addition to its role as a xenobiotic sensor, PXR has been linked to the regulation of genes within lipid and cholesterol pathways via activation by endogenous sterol metabolites [187-189]. As mentioned in section 1.2.2.2, PXR is activated in the presence of high levels of bile acids, specificically LCA, and oxysterols in the liver [174]. Activation of PXR under these conditions provides an additional route for elimination of cholesterol and bile acids other than through activation of LXR and FXR alone. Target gene expression under these conditions is geared towards increasing the livers capacity to avoid toxicity associated with elevated levels of cholesterol and bile acids through increased expression of export pumps and increased expression of enzymes capable of ‘inactivating’ toxic components through chemical modifications such as cyps and sulfotransferases. PXR also contributes to liver detoxification efforts by ensuring availability of fatty acids for cholesterol ester formation. PXR activation increases

expression of the fatty acid transporter CD36 and several accessory lipogenic enzymes, such as stearoyl-CoA desaturase-1 (SCD-1) and long chain free fatty acid elongase [187].

PXR is also implicated in the regulation of gluconeogenic gene transcription. Regulation of gluconeogenic enzymes by PXR occurs through crosstalk with the forkhead transcription factor, FOXO1 [189]. FOXO1 is an insulin responsive transcription factor that increases transcription of gluconeogenic genes such as PEPCK and G6Pase. FOXO1 activity is inhibited through insulin signaling upon feeding. PXR activation also inhibits FOXO1 activity by blocking the binding of FOXO1 to insulin response sequences in target gene promoters. It is speculated that crosstalk regulation at FOXO1 may be needed in order to regulate the balance between the cofactors, NADPH and NADH. PXR inactivation of gluconeogenesis would increase availability of NADPH for use by drug metabolizing enzyme such as CYP3A4 for which NADPH is an essential electron donor.

PXR does not have a necessary role in lipid and glucose homeostasis. However, PXR activation has been shown to have a profound effect on the expression and activation of key pathway controllers as a consequence of the molecular requirements for robust xenobiotic and endobiotic metabolism. Through activation of PXR, xenobiotics and steroid intermediates can have a wide reaching effect on lipid and glucose homeostasis. HIV PIs are known activators of PXR and have been shown to increase expression of cyp3A4 [185]. How activation of PXR by PIs effect expression patterns in metabolic pathways is yet to be determined.

1.2.2.4 Retinoid X Receptor

A common link between the nuclear receptors involved in the maintenance of energy homeostasis is the requirement of heterodimer formation with the retinoid X receptor (RXR) for proper binding of DNA REs and transcription of target genes. The RXR family of nuclear receptors is comprised of three isotypes, α, β and γ [115]. RXRα is the dominant RXR isoform and the preferred heterodimer partner of metabolic nuclear receptors such as the PPARs, LXR and FXR. RXRα is activated by a product of retinol metabolism, a derivative of vitamin A known as 9-cis retinoic acid [190]. 50-80% of retinoids are stored in liver stellate cells. The remaining 15-20% of retinoids are stored in adipose tissue through the LPL-mediated uptake of retinyl esters from chylomicrons and direct import from the bloodstream through the cellular retinol-binding protein. In addition to retinoids, fatty acids, such as phytanic and docosahexaenoic acids, have been recently identified as endogenous activators of RXR [191, 192]. The discovery of RXR affinity for fatty acids has brought into question the traditional role of RXR as a heterodimer partner.

Transcriptional activation of heterodimers can occur through ligand-specific activation of the 'sensor' receptor, 'non-specific' activation of RXRα or activation of both partners [193]. RXR affinity for fatty acids opens the possibility that RXR, like its heterodimer partners, also operates as a sensor of energy metabolism with the potential to drive metabolic responses through the concerted activation of RXR-containing heterodimers. RXR-specific agonists have been shown to have similar effects as PPARγ activating TZDs on glucose and TG levels as well as improvements in peripheral insulin resistance in mouse models of diabetes and obesity [194]. The similarity of effects is

likely due to the preferentially activation of the RXR/PPARγ heterodimer by RXR activators. While there is similarity between RXR agonists and TZDs in improvement of diabetes markers, treatment with RXR agonists has the added benefit of preventing weight gain usually associated with TZD treatment.

The importance of RXR as both a retinoid receptor and heterodimer partner is made evident through observations of the deleterious effects on survival and metabolism in various RXRα KO models. Whole body RXRα KOs are lethal *in utero* and display myocardial and ocular malformations consistent with fetal vitamin A deficiency syndrome, highlighting the role of RXRα in retinoid signaling [195]. Adipocyte-specific KO models of RXRα are resistant to obesity and have impaired adipocyte differentiation and lipolysis likely due to the lack of PPARγ/RXRα heterodimer formation in these animals [196]. Liver-specific KO models of RXRα are viable but have profound effects on nearly every metabolic pathway where gene regulation is controlled by a nuclear receptor that requires heterodimerization with RXRα [197, 198].

1.3 Thesis Outline

The specific objectives of this research were two-fold. The first objective was to determine direct effects of HIV drugs on the activation of nuclear receptors involved in metabolism. Nuclear receptor activation was determined by *in vitro* methods which measure both the receptors ability to recruit coactivator peptides and increase reporter gene transcription. HIV drugs which elicited an effect were further evaluated by measuring mRNA levels of known target genes in primary hepatocytes. The second task was to determine whether utilizing truncated nuclear receptor constructs in receptor

activation assays effects the rank order potency and efficacy of known agonists of PPARα relative to the full length construct.

Chapter 2: Effect of HIV Drugs on the Activation of Metabolic Nuclear Receptors

2.1 Introduction

In developed countries, the life expectancy of HIV-infected individuals has increased substantially through the use of HAART in the management of HIV infection [2-4]. Despite the benefits of HAART, acute adverse events often reduce patient compliance and limit the effectiveness of treatment [15, 16]. Patients who are tolerant of HAART must remain on a cocktail of HIV drugs for the duration of their lives. Long term use of PIs, the lynch pin of HAART therapy, has been linked to the development of HIV/HAART-associated dyslipidemic lipodystrophy (HADL) [18]. HADL is associated with an increased risk of cardiovascular disease and type 2 diabetes in long-term HIV survivors [22-24]. Increased levels of circulating triglycerides and cholesterol and insulin resistance are early markers in the development of HADL [20, 21]. HADL also causes appearance-related side effects due to abnormal redistribution of fat storage from peripheral to visceral adipose [27, 199]. Changes in body fat distribution have a profound psychological effect on patients and have been shown to increase the risk of non-adherence to therapy by 5 fold [29, 30, 200].

From the time HADL was first observed in the clinic, researchers have focused on uncovering the underlying mechanism in the hope of minimizing side effects of current HIV therapies. Observations of altered serum lipid and glucose levels in HADL patients indicate that PIs are most likely interfering with effectors of lipid and glucose homeostasis. Some of the metabolic processes shown to be impacted by HIV PIs are inhibition of GLUT4 mediated uptake of glucose, inhibition of ApoB degradation and preadipocyte differentiation and dysregulation of sterol regulatory element binding

proteins (SREBPs) [71-73]. However, the redundant nature and complexity of metabolic pathways make it difficult to identify clinically relevant cellular mechanisms in the pathogenesis of HADL. The high dose of PIs required to achieve therapeutic effects, ranging from 300 – 1250 mgs administered 2-3 times daily, further confound the problem by increasing the likelihood of multiple off-target interactions [92, 93]. It is apparent from both clinical and biochemical evidence that HADL likely results from the disruption of multiple pathways involved in energy mobilization, utilization, and storage. The role of nuclear receptors as major transcriptional regulators directly affecting the abundance of target genes in multiple metabolic pathways and the potential for PI-mediated desensitization to intrinsic ligands, make them ideal candidates for investigating the pathology of HADL.

Initial investigations into PI effects on nuclear receptors stemmed from the observation that HIV patients with lipodystrophy presented with symptoms similar to those found in genetic forms of the disease [18]. Familial partial lipodystrophy type 3 has been linked to a P467L mutation in the gene encoding the peroxisome proliferator-activated receptor gamma (PPARγ) [201, 202] . PPARγ is a member of the PPAR family of nuclear receptors whose primary target genes serve as control points in lipid and glucose metabolic pathways [156, 203]. Expression of PPARγ is up regulated during preadipocyte differentiation and is highly expressed in mature adipocytes where PPARγ activation facilitates the uptake and storage of circulating fatty acids through upregulation of genes such as aP2, lipoprotein lipase (LPL), fatty acid transport protein (FATP) and acyl CoA synthetase [204]. Reduction in fatty acid storage capacity in subcutaneous adipose can increase circulating fatty acids and facilitate uptake in non-adipocyte tissues

such as skeletal muscle and liver, leading to insulin resistance and peripheral lipoatrophy [205] . Conflicting results have been reported on the effects of PIs on PPARγ function. Saquinavir and indinavir have been shown to inhibit differentiation of preadipocytes in culture, a function attributed to PPARγ. However, levels of aP2 expression, a known PPARγ target gene, were found to be unaffected by exposure to saquinavir and indinavir [105, 106]. Lenhard *et al*. also reported decreased adipogensis, lipogenesis and increased lipolysis upon exposure of adipocytes to saquinavir, ritonavir and nelfinavir but with an associated decrease in mRNA levels of adipocyte markers, aP2 and LPL [107]. In contrast, similar experiments performed by Ragnathan and Kern showed decreased activity of LPL in adipocytes without a decrease in mRNA levels upon exposure to saquinavir suggesting PIs may act through alterations in post-translational processing rather than transcription [108]. PI effects on lipolysis, lipogenesis and expression of aP2 and LPL are opposite to effects observed for PPARγ agonists in cultured adipocytes. Further, treatment of patients with rosiglitazone and metformin, known agonists of PPARγ, provides at least moderate improvements in both insulin resistance and fat distribution [109]. Despite circumstantial evidence suggesting involvement of PPARγ in HADL, direct interaction between PIs and PPARγ have yet to be demonstrated.

Inclusion of ritonavir in combination therapies has been shown to significantly improve circulating concentrations of coadministered drugs [181, 182]. Improvement in drug serum concentrations have been attributed to a reduction in overall drug metabolism due to direct inhibition of the monoxygenase cytochrome p450 3A4 isozyme by ritonavir [183]. Pregnane X receptor (PXR) response element (RE) sequences identified in the promoter region of the 3A4 gene have indelibly linked 3A4 transcriptional regulation to

the activation of PXR [184]. Ritonavir, as well as other PIs, has been shown to activate PXR-mediated gene transcription and increase levels of 3A4 [185]. RE sequences have also been identified in additional p450 enzymes, drug export pumps and phase 2 drug metabolizing enzymes, implicating PXR as the master regulator of xenobiotic metabolism and clearance [186]. In addition to it role as a xenobiotic sensor, PXR has recently been linked to the regulation of genes within lipid and cholesterol pathways via activation by endogenous sterol metabolites [187-189]. How activation of PXR by PIs effect expression patterns in these pathways has yet to be determined.

Based on the broad effects of nuclear receptor modulation on metabolic pathways and prior evidence of PI interactions with PXR, we set out to explore the possibility of HIV drug interactions with nuclear receptors that were either previously uninvestigated or PI interaction was deemed inconclusive. Selection of the panel members FXR, LXRα, RXRα, PXR and PPAR α,γ, and δ, was based on relevance of target gene activity in metabolic pathways and potential for alterations in expression levels resulting in symptoms of HADL.

Our investigation into HIV drug effects on nuclear receptor binding and activation suggest that HADL symptoms, particularly dysfunctions in glucose processing, may be a direct result of PI inhibition of PPARγ activation, directly impacting expression levels of two key elements in glucose stimulated insulin secretion (GSIS) and glucose metabolism.

2.2 Materials and Methods

2.2.1 Reagents

All solvents and buffer components were purchased from Sigma unless otherwise noted. All media and components for transfections were purchased from Invitrogen except for charcoal-striped fetal calf serum which was purchased from Hyclone. Ligands were purchased from Biomol except for ciprofibrate, TO901317 and GW7647 which were purchased from Sigma. The coactivator peptides, biotinylated steroid receptor coactivator -1 M2 (bSRC-1 M2), biotinylated CREB binding protein (bCBP) and biotinylated PPARγ coactivator –1 (bPGC-1), were synthesized and prepared to 95% purity by Synpep Corp (Table 1). Europium-labeled anti-GST antibody (Eu-αGST) was purchased from CIS-Bio US Inc. Allophycocyan-labeled streptavidin (APC-SA) was purchased from Perkin Elmer. The HIV drug panel was purchased from Sequoia Research Products Ltd. (Table 2). Primary hepatocytes were obtained from Cellzdirect.

Table 1. Sequences of Coactivator Peptides[a,b].

Coactivator Peptide	Sequence and modifications
bSRC-1 M2	Biotin-Ahx-CPSSHSSLTERHKILHRLLQEGSPS-CONH2
bPGC-1	Biotin-Ahx-DGTPPPQEAEEPSLLKKLLLAPANT-CONH2
bCBP	Biotin-Ahx-SGNLVPDAASKHKQLSELLRGGSGS-CONH2

[a] Underlined sequence indicates LXXLL motif involved in receptor binding
[b] Ahx = aminohexanoyl

Table 2. HIV drug panel.

Protease Inhibitors (PIs)	Ritonavir Saquinavir Indinavir Nelfinavir
Nucleoside Reverse Transcriptase Inhibitors (NRTIs)	Zidovudine Zalcitibine Lamivudine Stavudine
Non-Nucleoside Reverse Transcriptase Inhibitors (NNRTIs)	Efavirenz Nevirapine

2.2.2 Cloning and Expression of the Nuclear Receptor Panel

The panel of nuclear receptors was amplified from cDNA utilizing the 5' and 3' primers listed in Table 3. PCR reactions were performed using a combination of GC-2 and HF-2 PCR polymerase mixes (BD Clontech). The purified PCR products were cloned into Invitrogen's Gateway entry vector, pENTR / D-TOPO. Single clones were selected based on their resistance to kanamycin and the isolated plasmids, pENTR:X (X = nuclear receptor), were sequenced to confirm complete gene insertion. The pENTR: X plasmids were then recombined with the Gateway destination vector pDEST15 using LR clonase as per manufacturer's instructions. The pDEST15 expression vector confers an N-terminal GST tag in-frame with the receptor protein for use in purification and detection. Single colonies containing pDEST15: X plasmids were selected based on

resistance to carbenicillin. pDEST15: X plasmids were then transformed into the expression host, BL21(DE3) pLysS, for protein expression.

Table 3. List of Primers and cDNA for PCR Amplification.

Receptor (Genbank accession #)	**cDNA source**	**Amplification primers***
PPARα (L02932) [206]	kidney	5'CACCATGGTGGACACGGAAAGC 3' 5'CTAGTACATGTCCCTGTAGATCTCCTGCAGTAG 3'
PPARα LBD (L02932)	kidney	5' CACCTCACACAACGCGATTCGTT 3' 5'CTAGTACATGTCCCTGTAGATCTCCTGCAGTAG 3'
PPARγ (U79012) [207]	adipose	5'CACCATGGGTGAAACTCTGGGAG 3' 5'CTAGTACAAGTCCTTGTAGATC 3'
PPARδ (L07592) [208]	placenta	5'CACCATGGAGCAGCCACAGGAGG 3' 5'TTAGTACATGTCCTTGTAGATCTC 3'
FXR (U68233) [170]	kidney	5'CACCATGGGATCAAAAATGAATCTCATTG 3' 5'TCACTGCACGTCCCAGATTTCAC 3'
LXRα (U22662) [209]	placenta	5'CACCATGTCCTTGTGGCTGGGGGCCCCTG 3' 5'TCATTCGTGCACATCCCAGATCTCAG 3'
RXRα LBD Ser_{225}- $stop_{263}$ (X52773) [210]	kidney	5'CACCAGCGCCAACGAGGACATGCC 3' 5'CTAAGTCATTTGGTGCGGCGCCTCC 3'
PXR (AF061056)	liver	5'ACGCGTCGACTTATGGAGGTGAGACCCAAAG 3' 5'ATAAGAATGCGGCCGCTCAGCTACCTGTGA 3'

*underlined sequence indicates native start and stop codons

Transformed 1 litre cultures were induced during exponential growth phase, OD_{600} of 0.4 to 0.6, with fresh 400 μM IPTG and grown at room temperature for 4 hours. Cells were harvested by centrifugation at 12,000*g*. Cell pellets were frozen at –20 ºC and lysed by thawing on ice. 50 ml of Buffer A containing 50 mM Tris pH 8.0, 50 mM KCl,

1 mM EDTA, 1 mM DTT, 10% glycerol and 1 mM PMSF were added to the cell pellets. Cell aggregates were disrupted by passage through an 18-gauge syringe or homogenizer. Deoxyribonucease I was added to the lysate at a final concentration of 20 μg/ml and incubated at 37 ºC for 2 hours. The cell lysate was clarified by centrifugation at 50,000*g* and filtered through a PES 0.22 μM filter prior to purification. Purification of the GST-receptor fusions was performed using Glutathione 4B sepharose (Amersham Biosciences). All column equilibration and washing were performed with Buffer A. Proteins were eluted from the column using Buffer A with the addition of 20 mM glutathione pH 8.0. Protein concentrations were determined by Bradford method and purity assessment was determined by SDS-PAGE and western blot analysis using 1:1000 anti-GST mouse antibody.

2.2.3 Coactivator Recruitment Assay

Agonist-HIV drug panel and known ligands

The panel of HIV drugs was evaluated for agonist effects on coactivator recruitment for each receptor. Each receptor assay was validated by titration with reported ligand. All reagent concentrations (GST-receptor, APC-SA and coactivator peptide) were optimized for maximal assay signal. The coactivator recruitment assay was performed for each nuclear receptor in the panel with the exception of PXR. HIV drugs were evaluated against PXR using the cell-based reporter method only.

Table 4. Ligand K_ds for Coactivator Recruitment Assay.

Receptor	Coactivator peptide	Ligand	Saturating ligand (nM)	HTRF K_d (nM) n=3	Lit. K_d (nM)
PPARα	bCBP, bSRC-1 M2 [211]	GW7647	100	5.6 ± 1.4	6 [212]
PPARγ	bSRC-1 M2 [213]	Troglitazone	10 000	1 134 ± 176	274-300 [214, 215]
PPARδ	bPGC-1 [213]	L165,041	10 000	71 ± 4.4	320, 6 [216],[157]
RXRα LBD	bPGC-1 [217]	9-cis-retinoic acid	100	11.4 ± 2.1	14 [218]
LXRα	bSRC-1 M2 [219]	24(s)-hydroxycholesterol	1 000	89.5 ± 25	70 [220]
FXR	bSRC-1 M2 [221]	Chenodeoxycholic acid	100 000	1 125 ± 50.5	4 500 [222]

Titrations of the HIV drug panel and known ligands were prepared at 100 x concentration by performing 8 point two-fold serial dilutions in DMSO with a top concentration of 100 μM (1x). 1 μl of the HIV drug or ligand titrations were dispensed into 96-well black optiplates (Perkin Elmer). 1 μl of DMSO was dispensed to each negative control well. 1 μl of 100 x saturating concentrations of ligand for each receptor were dispensed into the positive control wells (Table 4). 99 μl of assay mix containing

100 nM GST-receptor, 100 nM APC-SA, 3 nM Eu-αGST antibody and 600 nM coactivator peptide (Table 4) in 50 mM Tris pH 8.0, 50 mM KCl, 1 mM EDTA, 1 mM DTT and 1 mg / ml BSA was dispensed to each well [213]. The final assay volume was 100 µl with 1 % total DMSO. The content of the wells were mixed by pippetting and spun at 300*g* to remove bubbles. The plates were covered and incubated at room temperature for 2 hours [216]. Fluorescence was measured by excitation at 340 nm and collection of emission at 615 nm and 665 nm. Measurements were performed on the Perkin Elmer Fusion using the factory settings for time-resolved fluorescence. Nelfinavir mediated FXR activation and recruitment of bCBP and bPGC-1 coactivator peptides was also evaluated using the methods outlined above. All experiments were performed in duplicate.

Antagonist-HIV drug panel

The HIV drug panel was evaluated for antagonist effects on the nuclear receptors by measuring the interference these compounds have on ligand-induced coactivator recruitment. Titrations of the HIV protease inhibitors were prepared at 100 x final assay concentration by performing 8 point two-fold serial dilutions in DMSO with a top concentration of 100 µM (1x). All HIV compounds and ligands were prepared as stock solutions at 100x of the initial concentration. 1 µl of the HIV drug titrations were dispensed into 96-well black optiplates (Perkin Elmer). Along with the HIV drug, 1 µl of ligand at 1.8 K_d (Table 4) was dispensed in each well. The negative control wells received 2 µl of DMSO and the positive control wells received 1 µl of DMSO and 1 µl of 100 x 1.8 K_d ligand. 98 µl of assay mix containing 100 nM GST-receptor, 100 nM SA-

APC, 3 nM Eu-αGST and 600 nM coactivator peptide (Table 4) in 50 mM Tris pH 8.0, 50 mM KCl, 1 mM EDTA, 1 mM DTT and 1 mg / ml BSA was dispensed to each well. The final assay volume was 100 µl with 2 % total DMSO. All experiments were performed in duplicate. Plates were handled identically as described for the agonist assay. In addition to the bCBP peptide, PI effects were also evaluated on PPARα recruitment of the bSRC-1 M2 peptide.

2.3.4 Reporter Gene Assay

Preparation of stable reporter cell line

pG5*luc*, GenBank accession # AF264724, is a reporter vector containing the Gal4 RE upstream from a fire fly luciferase reporter gene (Promega Corp., Madison, WI). The plasmid was converted into a stable reporter plasmid by cloning a neomycin resistance gene at the *BamH*I (2142) / *Sal*I (2148) sites. Wild type HEK293 (ATCC# CRL-1573) cells were transfected with the pG5*luc*+neo plasmid using lipofectamine according to the manufacturer's instructions. Single clones were selected using 800 µg /ml geneticin. Transformed cells were grown in DMEM with 4.5 g / L glucose and 25 mM Hepes supplemented with 10 % charcoal stripped fetal bovine serum, penicillin-streptomycin and glutamine. Cells were maintained at 37°C in a 5 % CO_2 humidified incubator.

Preparation of Gal4 DBD-Nuclear receptor chimeras

pBIND vector, GenBank accession # AF264722, contains a multiple cloning site downstream from the yeast Gal4 DBD (Promega Corp., Madison, WI). The pBind vector was converted into a Gateway destination vector through the insertion of Reading Frame

B (rfb) at the *Ecor*V site (1594) as per manufacturer's instructions. The pENTR: X entry plasmids generated previously for expression of GST-tagged receptor in the coactivator recruitment assay were recombined with the converted destination vector pBIND: rfb using LR clonase. All constructs were 5' sequence confirmed for correct orientation of gene.

Preparation of hPXR and CYP3A4-response element reporter plasmid

Preparation of the CYP3A4 reporter plasmid, p3A4-362 (7836/7208 Ins), was described previously [223] and constructed with the following restriction site usage. The response element sequence, -7836/-7208, was cloned into pGL3-basic (Promega Corp., Madison, WI) at *Kpn*I/*Nhe*I restriction sites and the proximal promoter, -362/+53, was inserted at *Xma*I/ *Hind* III restriction sites. Full-length human pregnane X receptor was amplified from liver cDNA and cloned into pcDNA 3.1 / +Zeo (Invitrogen) at *Nhe*I/ *Xba*I restriction sites using the primers listed in Table 3.

Cell line transfection

pG5*luc* + neo HEK293 stables were batch transfected with pBind: X plasmid at 200 ng /μl using lipofectamine as per manufacturer's protocol. The cells were plated at a concentration of 5 x 10^5 cells per well into black-well clear bottom tissue culture treated plates. The transfected cells were incubated for 24 h, after which an additional 100 μl of media was added to all wells. The same procedure was performed for the cotransfection of pcDNA3.1:hPXR and p3A4-362 (7836/7208 Ins) into HepG2 cells.

Reporter assay-Agonist mode

The panel of HIV drugs was evaluated for agonist effects on receptor-mediated reporter gene transcription. Known ligands for the panel of nuclear receptors listed in Table 5 were also tested for direct comparison to HIV drug-induced reporter gene transcription levels and to ensure accurate determination of EC_{50} values for use in the antagonist mode assay.

Table 5. Ligand EC_{50}s for Cell-Based Gal4 Reporter Assay.

Receptor	Ligand	Cell-Based EC_{50} (nM) N ≤ 3	Lit. EC_{50} (nM)
PPARα	Ciprofibrate	4 613 ± 1 215	6 000 [211]
PPARγ	Troglitazone	1 512 ± 269	550 [224]
PPARδ	L165,041	135 ± 13	530 [224]
RXRα LBD	9-cis-retinoic acid	26.3 ± 7.0	20 [225]
LXRα	TO901317	168 ± 34	50 [166]
FXR	Chenodeoxycholic acid	25 686 ± 3 240	20 000 [170]
PXR	Rifampicin	953 ± 54	1 000 [184]

The ligand and HIV drug titrations were prepared by performing 8 point two-fold serial dilutions in DMSO. The negative control for all constructs was 100 % DMSO and positive controls contained saturating concentration of ligand. 1 µl of the 1000 x drug plate were transferred well to well to a new 96-well polypropylene plate. 200 µl of growth media was added to each well and mixed thoroughly by pipetting. 50 µl of media: drug was added to the respective well in the assay plate containing transfected cells (final

volume 250 µl, 0.1 % DMSO). The cells were returned to the incubator for another 24 hours. Luciferase measurements were conducted using Bright GLO reagents (Promega Corp., Madison, WI) All media was removed from the wells and a 1:1 mixture of phenol red free media and Bright GLO substrate were added at a final volume of 200 µl. The plates were placed on an orbital shaker for 2 minutes to aid in cell lysis then read on a Perkin Elmer Victor V using the factory settings for luminescence readings.

Reporter assay-Antagonist mode

Dilution plates were prepared at concentrations 2000x the final assay concentration in DMSO for both the HIV drug panel and receptor specific agonist. The highest concentration of HIV drug evaluated in experiments was 100 µM. The negative and positive controls for the HIV drug dilution plate were 100 % DMSO. A 0.5 µl aliquot from the HIV drug dilution plate was transferred well to well to a new 96-well polypropylene plate. The receptor specific agonist plate was prepared by dispensing 100 % DMSO to negative control wells and agonist concentrations equal to the EC_{80}, calculated from Table 5, of the receptor specific ligand to all remaining wells. The negative control for the agonist plate was also 100 % DMSO. 0.5 µl of the 2000 x ligand dilution plate was transferred well to well to the same polypropylene plate that the HIV drugs were dispensed. Assay plates were handled identically to procedure described above for the agonist mode assay

2.2.5 Cell Toxicity Assays

Cellular toxicity of HIV protease inhibitors was determined for both primary hepatocytes and the pG5*luc* + neo HEK293 cell line. Toxicity was assessed using two distinct assay techniques. Apo-ONE homogeneous caspase-3/7 and CellTiter-Glo assays were performed as per manufacturer's protocol (Promega Corp., Madison, WI). Hepatocytes were received from Cellzdirect plated in 96-well plates coated with collagen and overlayed with Matrigel. pG5*luc* + neo HEK293 cells and drug plates were prepared as described for the agonist mode cell-based assay with the exception of lipofectamine transfection of the Gal4LBD-receptor plasmid. Drugs were incubated with cells for ~ 24 hours prior to assessment of drug-induced toxicity.

The CellTiter-Glo assay reagents were prepared by mixing CellTiter-Glo substrate with equal volume of phenol red-free media. Media containing drug was removed from all wells and replaced with 200 μl of CellTiter-Glo substrate: media mix. Assay plates were mixed for 2 minutes on an orbital shaker and incubated at room temperature for 10 minutes Well luminescence was read on a Perkin Elmer Victor V using the factory settings for luminescence readings.

Cellular caspase activity was determined using the apo-ONE homogeneous caspase-3/7 assay. 100 μl of apo-ONE substrate were added to all wells for a final reaction volume of 200 μl. The assay plate was incubated at room temperature with shaking for 90 minutes Caspase activity was determined by measuring the fluorescence signal generated by excitation at 485 nm and emission at 530 nm on a Perkin Elmer Victor V.

2.2.6 Gene Expression Analysis

PI treatment of primary hepatocytes and preparation of RNA

Fresh primary hepatocytes were received from Cellzdirect plated in 6-well format on collagen substrata with matrigel overlay. Cells were maintained in Modified Chee's media supplemented with dexamethasone, plus ITS and penicillin-streptomycin (CellzDirect) at 37°C in a 5 % CO_2 humidified incubator. PI selection and concentrations were determined from results obtained in the cell toxicity assay. 15 μM of ritonavir, 15 μM saquinavir with or without 3 μM troglitazone and DMSO control were added to hepatocytes (final DMSO concentration, 0.1%). Hepatocytes were incubated with drug containing media for 24 hours. The hepatocytes were harvested and total RNA extracted using Qiagen's RNAeasy RNA isolation kit. Concentration and purity of samples were determined by $OD_{260/280}$ measurements.

Gene chip analysis

RNA isolated from hepatocytes treated with DMSO, saquinavir and ritonavir were evaluated for drug-induced changes in mRNA transcript levels using GE CodeLink Whole Human Genome Arrays (55K). Sample processing was performed by the Center for Environmental Health, Science and Technology at the University of Massachusetts Boston. Briefly, 2 μg of high quality total RNA was reverse transcribed to produce first-strand and subsequently, second-strand cDNA. The double-stranded cDNA was used as a template for *in vitro* transcription utilizing Ambion's T7 MEGA script reagents and Biotin-11-UTP (PerkinElmer). The resulting biotin labeled cRNA was recovered and purified with Qiagen's RNeasy and quantified. 10 μg of the labeled cRNA, along with

bacterial controls, were hybridized overnight at 37°C to the arrays. After the overnight incubation and a stringent wash at 47°C, the array was incubated with Alexa fluor conjugate. After a three room temperature washes, the slides were spun dry, inspected for gross interference and scanned with a Packard ScanArray 5000 HT, standard setting for CodeLink (100 % laser/ 60 PMT). The generated images were then processed.

Statistical evaluation of gene chip data

The array images were processed using the GE CodeLink expression analysis software. The probe signals were normalized to the median probe intensity of the array. The normalized intensities for each sample were grouped into two classes designated treatment 1 (control) and treatment 2 (ritonavir or saquinavir). The two sided, unpaired t-test were obtained for each gene probe along with the maximum signal in any sample and the ratio of the average experimental signal to the average control signal (AVERAGE(treatment)/ AVERAGE(control)). Genes with p-values ≤ 0.05 were extracted from both treatment groups. Gene sets were then segregated according to known association with either PPARα, PPARγ, SREBP or PXR. Transcriptional dependence was base on literature determinations of response element sequences and/or increased gene transcription due to receptor specific ligands or transgenic models [186, 226, 227].

Quantitation of GLUT2 and GK mRNA levels

Total RNA from each sample was quantified and quality check with Agilent 2100 Bioanalyzer (Agilent Technology). 1 μg of total RNA was treated with DNase I (Ambion, Inc) to remove contaminating DNA from RNA samples.

1 μg of total RNA from each sample was used for each reaction with or without reverse transcriptase (RT) using RETROscript Kit from Ambion (Ambion, Inc). RT reactions were carried out as follows: 1 μg of total RNA (in 5-9 μl nuclease-free water) was mixed with 2 μl Random Decamers and incubated at 70°C for 3 minutes. After cooling on ice, the solution was mixed with 2 μl 10X RT buffer, 4 μl of dNTP mix, 1 μl RNase inhibitor and 1 μl of MMLV-RT and incubated for 60 minutes at 44°C. Reactions were terminated by heating to 92 °C for 10 minutes. After a preliminary RT-PCR assay amplifying the 18S rRNA and GLUT2 and glucokinase (GK) to assess integrity, cDNA was stored at –85 °C until required for real-time PCR.

Primer pairs were designed using Primer Express (Version 1.5, PE Applied Biosystems, Foster City, CA) as close as possible to the 3'-coding region of target gene sequences obtained from GenBank. Where possible, primers were designed based on manufacturer's guidelines, and as described [228]. QuantiTech Primer Assays for GLUT2 and GK (QIAGEN) were used, while for the 18S rRNA the primers used were 18S-FP 5'-GTCTGTGATGCCCTTAGATG-3' and 18S-RP 5'-AGCTTATGACCCGCACTTAC-3'. Amplicons were between 88 (GLUT2), 85 bp (GK) and 177 base pairs (18S rRNA). GLUT2 and GK primers were checked for efficient amplification using cDNA generated from whole blood samples. The resulting PCR products were run on a 2 % agarose gel to verify amplification of a correct sized product.

SYBR-Green assays for each tissue sample as well 18S rRNA were performed in triplicate on cDNA samples in 96-well optical plates on an ABI Prism 7000 Sequence Detection system (PE Applied Biosystems) according to the manufacturer's protocol. For each 25 µl SYBR-Green reaction, 10 ng cDNA (5µl) was mixed with 4.5 µl PCR-grade water, 12.5 µl 2x Power SYBR-Green PCR Master Mix (PE Applied Biosystems), 0.5 µl forward primer (300 nM) and 0.5 µl reverse primer (300 nM). The PCR cycle condition was as follows: an initial step of 2 minutes at 50 $^{\circ}$C was used for AmpErase incubation followed by 10 minutes at 95 $^{\circ}$C to inactivate the AmpErase and to activate the *Taq* polymerase. This was followed by a denaturation step of 95 $^{\circ}$C for 15 seconds and finally annealing/extension at 60 $^{\circ}$C for 1 minute for 45 cycles.

RT-PCR data analysis (Comparative C_T)

All SYBR-Green PCR data were collected using Sequence Detector Software (SDS version 2.0; PE Applied Biosystems. For every sample, an amplification plot was generated showing the increase in the reporter dye fluorescence (ΔRn) with each cycle of PCR. A C_T value, defined as the number of PCR cycles required for the fluorescence signal to exceed the detection threshold value [228, 229] based on the variability of base line data in the first 15 cycles, was calculated for each reaction. C_T values were exported into Microsoft Excel worksheets for further analysis.

The correlation between the C_T value and the fold difference in the concentration was determined individually for each primer set. When PCR efficiency is 100% the C_T values of two separate genes can be compared (ΔC_T) and the relative fold difference can be determined. This was carried out using the Comparative C_T Method (Separate Tubes)

as defined in the ABI analysis manual. The amount of target, normalized to an endogenous reference and relative to a calibrator is given by:

$$2^{-\Delta\Delta C_T}$$

For the $\Delta\Delta C_T$ calculation to be valid, the efficiency of the target and the efficiency of the reference amplification must be approximately equal. The absolute value of the slope of log input amount vs. ΔC_T should be <0.1. The ΔC_T value is determined by subtracting the average 18S RNA C_T value from the average GLUT2 and GK C_T value. The calculation of $\Delta\Delta C_T$ involves subtraction by the ΔC_T calibrator value. The standard deviation of the difference is calculated from the standard deviation of the GLUT2 and GK and 18S RNA values using the following formula:

$$s = \sqrt{s_1^2 + s_2^2}$$

The result represents mean and standard deviation of triplicate samples as reported earlier. Each experiment was repeated three times**.**

2.3 Results

2.3.1 Coactivator Recruitment Assay

Coactivator recruitment – HIV drug panel and ligands

The coactivator recruitment assay is a cell-free assay that is used to measure the potential activation of a receptor through binding of coactivator peptides. Positive interactions between a ligand and receptor result in positive changes in receptor conformation that allow binding of coactivators to coactivator binding sites located in the AF-2 region [230]. Cellular requirements for receptor-mediated up-regulation of target

gene transcription allow for the use of coactivator peptide recruitment as an indicator of receptor activation in a cell-free format. K_d values were obtained for each receptor and it's ligand in the panel to ensure proper evaluation of HIV drugs in the antagonist assay and to provide validity to our assay methods. K_d values obtained in the coactivator recruitment assay are listed in Table 4 and were calculated by fitting data to equation 1 where *y* is the percent activity, *x* is the corresponding concentration and *h* is the Hill coefficient.

$$y = \min + \frac{(\max - \min)}{1 + (\frac{x}{IC_{50}\ or\ EC_{50}})^h} \quad (1)$$

Overall, there was less than two-fold difference between the experimental and literature K_d values. The experimental K_d for troglitazone and CDCA were calculated to be within 4-5 fold of the literature values. The apparent discrepancy between K_d values is most likely an effect of differences in receptor construct design and/or the type of assay format used in determining the literature K_d.

The HIV drug panel was tested to determine whether the selected HIV drugs have the capacity to bind and activate receptors. The HIV drugs tested were considered to be ineffective as an agonist if the % control at the highest concentration tested did not exceed 30 %. Data obtained from the agonist mode coactivator recruitment experiments suggest that the PI, nelfinavir, activates FXR as demonstrated by the dose dependent increase in coactivator recruitment. Receptor activation by nelfinavir was found to be exclusive to FXR (Table 6). The remaining PIs, NNRTIs or NRTIs did not activate any receptor greater than 30 % of control. Dose response data indicate that nelfinavir is a full and potent agonist of FXR with an apparent EC_{50} of 184 ± 11.3 nM. The potency of

activation was dependent on the coactivator peptide used in the experiment. Substitution of bSRC-1 M2 peptide for either bPGC-1 or bCBP in the assay resulted in a 10 or 20 fold decrease in the potency of activation by nelfinavir (Figure 5)

Table 6. Agonist Results for HIV Drugs Tested Against GST-Receptor Panel in HTRF Coactivator Recruitment Assay.

	Ritonavir		Nelfinavir		Saquinavir		Indinavir	
	K_d (nM)	% Control	K_d (nM)	% Control	K_d (nM)	% Control	K_d (nM)	% Control
PPARα	-	-	-	-	-	-	-	-
PPARγ	-	-	-	-	-	-	-	-
PPARδ	-	-	-	-	-	-	-	-
LXRα	-	-	-	-	-	-	-	-
FXR	-	-	**126** ± 11.3	93 ± 2	-	-	-	-
RXRα	-	-	-	-	-	-	-	-

Note: - < 30 % control, K_d not calculated

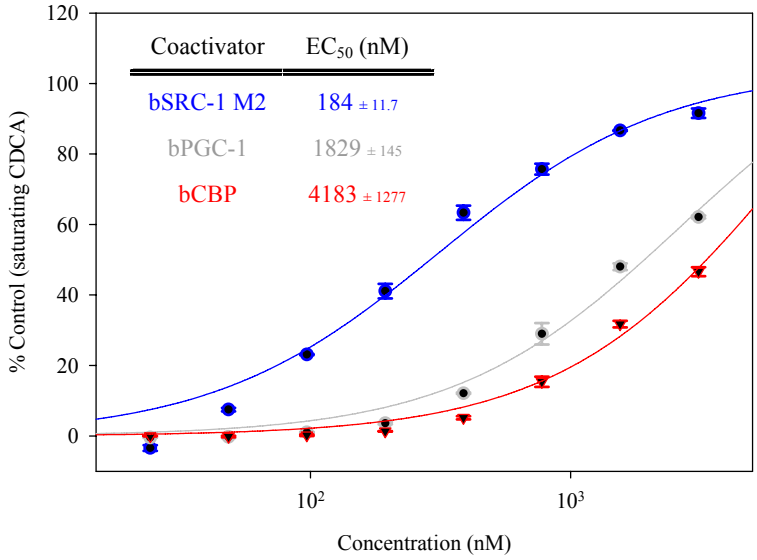

Figure 5. Nelfinavir Activation of FXR with Different Coactivators. Coactivator recruitment levels using either bSRC-1 M2, bPGC-1 or bCBP were measured in the presence of nelfinavir and compared to levels obtained with saturating concentrations of CDCA. Data is plotted as % control versus concentration of nelfinavir. Each data point is the mean of two determinations with error bars representing the standard deviation.

The HIV drug panel was also tested to determine whether HIV therapies have the capacity to interfere with ligand-induced coactivator recruitment. Antagonist effects by the panel would result in reduced coactivator recruitment in the presence of subsaturating agonist concentrations (1.8 K_d or EC_{80}). Maximum % inhibition values reported in Table 7 were calculated from fluorescence ratios obtained at the highest drug concentrations (100 μM). IC_{50} values were calculated by fitting data to equation 1. In cases where a full dose response was not obtained, maximal inhibition levels were estimated by constraining the Hill coefficient (*h*) to 1. An HIV drug was considered to be ineffective as an antagonist if the % inhibition at the highest concentration tested did not exceed 30 %.

Results from the coactivator recruitment assay indicate that the PI class of drugs from the HIV drug panel, with the exception if indinavir, behave as antagonist against distinct members of the receptor panel at micromolar concentrations (Table 7). The NNRTI efavirenz was the only non-PI to show antagonist activity against the receptor panel. Reduction of ligand-induced coactivator recruitment by efavirenz was observed across the entire receptor panel at 100 μM.

Table 7. Antagonist Results for HIV Drugs Tested Against GST-Receptor Panel in HTRF Coactivator Recruitment Assay.

	Ritonavir		Nelfinavir		Saquinavir		Indinavir		Efavirenz	
	IC_{50} (uM)	% INH	IC_{50} (uM)	% INH	IC_{50} (uM)	% INH	IC_{50} (uM)	% INH	IC_{50} (uM)	% INH
PPARα	43 ± 11	54 ± 1.4	13 ± 2.1	75 ± 1.6	26 ± 7.8	132 ± 21	–	–	>100	81
PPARγ	38 ± 6.2	37 ± 9.1	9 ± 1.9	53 ± 4.2	8 ± 4.5	102 ± 0.7	–	–	>100	50
PPARδ	–	–	–	–	–	–	–	–	>100	90
LXRα	> 100	34 ± 2.8	19 ± 8.2	50 ± 6.3	> 100	57 ± 10.6	–	–	>100	87
FXR	> 100	27 ± 9.1	–	–	> 100	44 ± 15.5	–	–	>100	190
RXRα LBD	–	–	–	–	–	–	–	–	>100	35

– = < 30 % inhibition, IC_{50} not calculated
Values in red = > 30% inhibition and IC_{50} calculated

The most robust PI antagonist effects were observed within the PPAR receptor family, specifically PPARα and PPARγ (Figure 6). Saquinavir exhibited full antagonism of ligand-induced recruitment for both receptors. The >100 % inhibition value obtained for PPARα indicates that, in addition to ligand-induced coactivator recruitment, saquinavir also blocks constitutive coactivator recruitment. Nelfinavir inhibited coactivator recruitment in a dose-dependent manner but only showed partial inhibition of

agonist activity. The premature plateau observed in the nelfinavir titrations occurs at concentrations approaching 50-100 μM for both PPARγ and PPARα and can be explained several ways. The effect is likely caused by compound solubility but could also be explained by a mechanism involving non-competitive antagonism. Ritonavir inhibited coactivator recruitment in a dose-dependent manner but with a lower IC_{50} values and % inhibition than both saquinavir and nelfinavir. It is interesting to note that while several PIs inhibited PPARα and PPARγ, there appeared to be no effect on PPARδ.

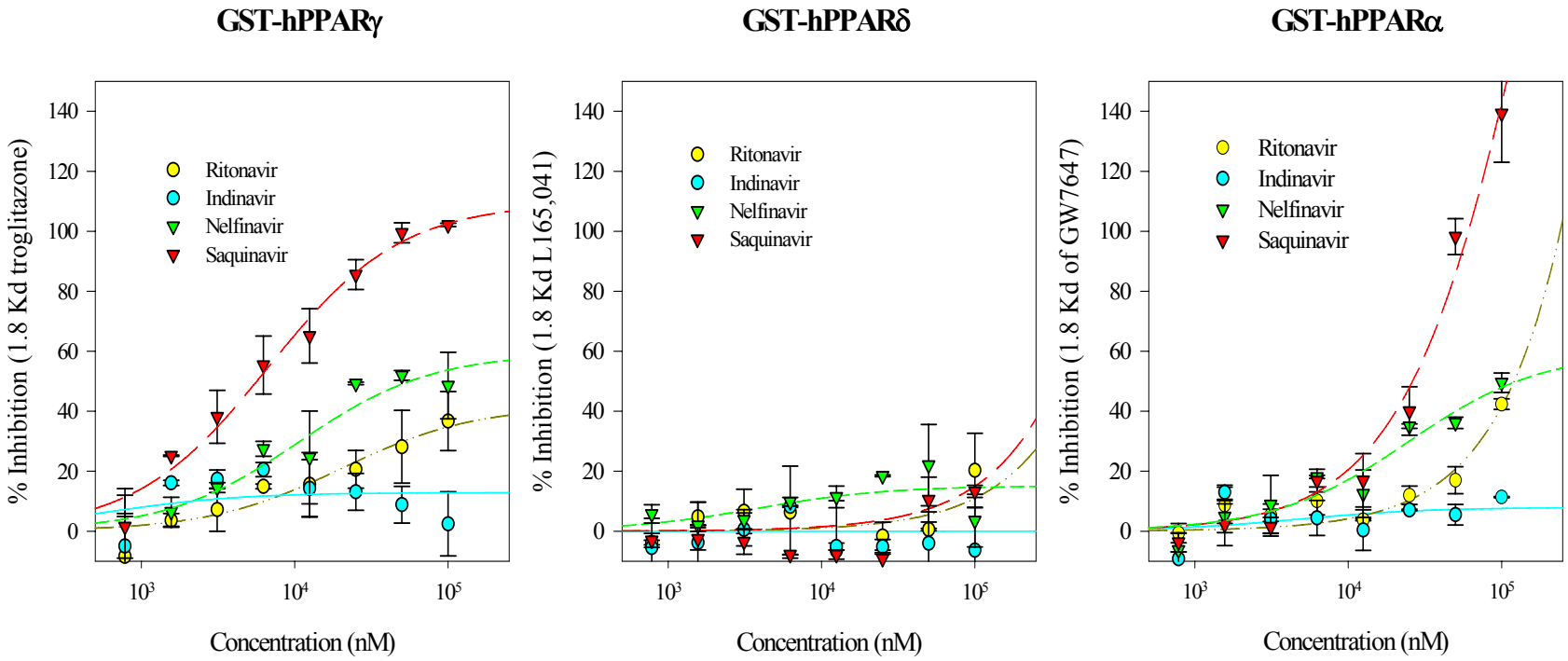

Figure 6. PI Inhibition of PPAR Family Activation. PPAR family member α, γ and δ were evaluated in the HTRF antagonist mode coactivator recruitment assay. The agonists employed in the assay were GW7647 (PPARα), troglitazone (PPARγ) and L165,041 (PPARδ). % inhibition values were obtained by comparing the level of coactivator recruitment in the presence of both PI and subsaturating agonist with levels obtained with agonist only. Data is plotted as % inhibition of coactivator recruitment versus concentration of PI. Each data point is the mean of two determinations with the error bars representing the standard deviation.

In order to determine whether the type of coactivator peptide influences the antagonist effects of PI on PPARα, bSRC-1 M2 peptide was substituted for bCBP in the coactivator recruitment assay. Saquinavir, nelfinavir and ritonavir were found to interfere with PPARα recruitment of bSRC-1 M2 peptide, similar to the effects observed with the bCBP peptide (Figure 7). Saquinavir interfered with both ligand-induced and constitutive bSRC-1 M2 recruitment by PPARα, though the response was slightly higher than for bCBP. Nelfinavir inhibited PPARα recruitment of the bSRC-1 M2 coactivator and was 25% greater than levels achieved with bCBP. The premature plateau in the nelfinavir antagonism of PPARα coactivator recruitment of bCBP was also observed in the recruitment of bSRC-1 M2. Ritonavir was unaffected by the type of coactivator used in the assay.

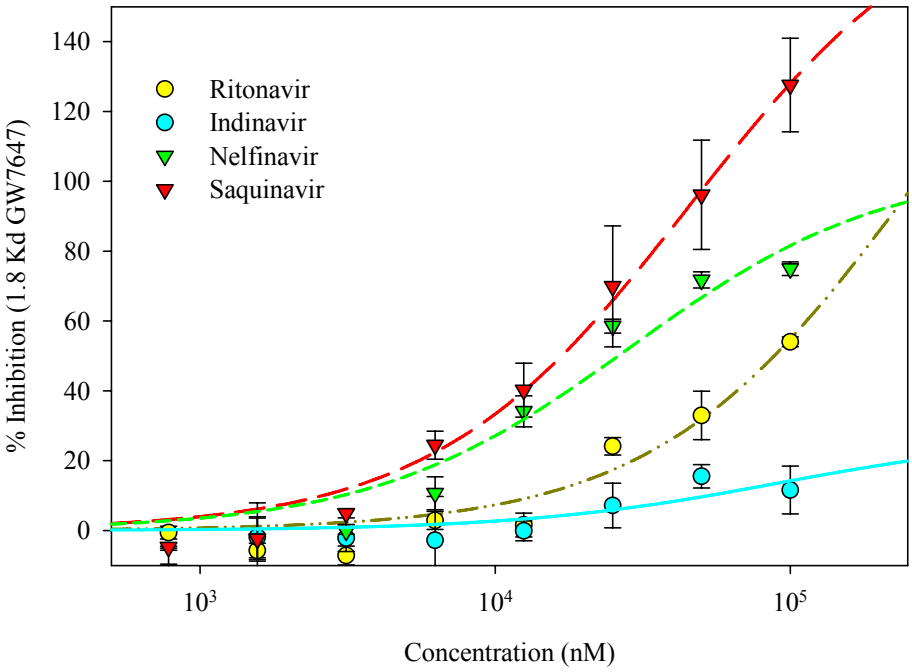

Figure 7. Inhibition of PPARα Activation using bSRC-1 M2 Coactivator Peptide. The bSRC-1 M2 peptide was substituted for bCBP to evaluate whether coactivator type influences potency of PI inhibition of PPARα activation. % inhibition values were obtained by comparing coactivator recruitment levels in the presence of both PI and subsaturating concentration of GW7647 with levels acheived with GW7647 only. Data is plotted as % inhibition versus PI concentration. Data points represent the average of experiments performed in triplicate with the error bars representing the standard deviation.

Antagonist effects of PIs outside of the PPAR receptor family were limited. Nelfinavir was found to interfere with LXRα coactivator recruitment in a dose-dependent manner achieving an inhibition plateau well below maximal inhibition, similar to results observed with nefinavir and other receptors (Figure 8). HIV PIs were found to have minimal effect on the remaining receptor panel with antagonist effects, if any, being observed only at highest drug concentrations.

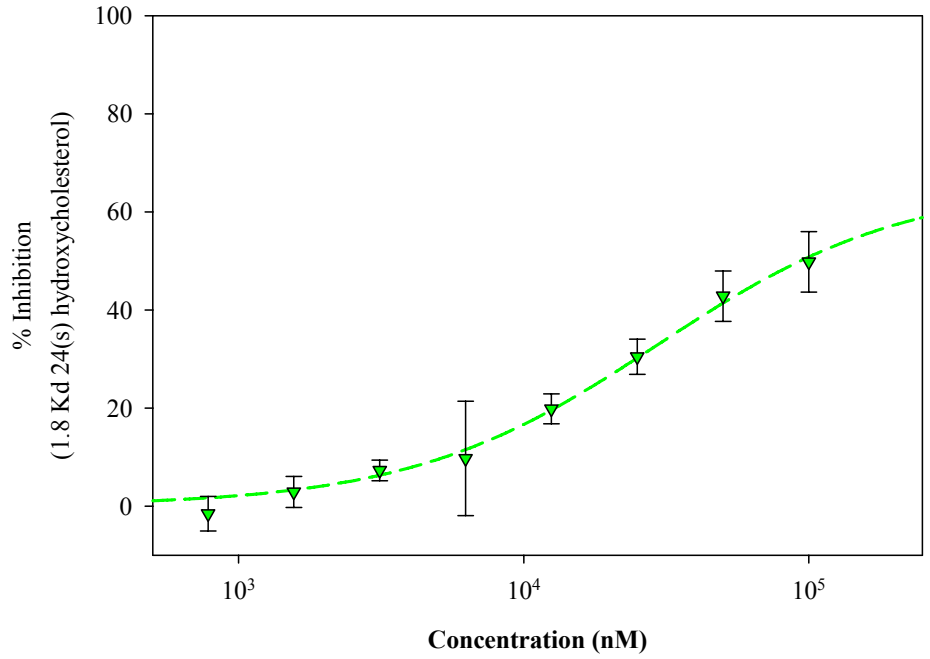

Figure 8. Inhibition of LXRα Coactivator Recruitment by Nelfinavir. Nelfinavir was evaluated for inhibition of LXRα activation and coactivator recruitment in the antagonist mode coactivator recruitment assay. % Inhibition values were obtained by comparing coactivator recruitment levels in the presence of both PI and subsaturating concentration of 24(S)-hydroxycholesterol with levels acheived with 24(S)-hydroxycholesterol only. Data is plotted as % inhibition versus nelfinavir concentration. Data points represent the average of experiments performed in triplicate with the error bars representing the standard deviation.

2.3.2 Reporter Gene Assay

Reporter assay – HIV drug panel and ligands

The Gal4 reporter gene assay is a cell-based assay that measures receptor activation as a function of reporter gene transcription levels. Like the coactivator recruitment assay, the cell-based assay relies on coactivator recruitment by a receptor but also requires successful entry of the compound into the cell and coordinated assembly of transcriptional cofactors and enzymes. EC_{50} values were obtained for each receptor and it's ligand in the panel to ensure proper evaluation of HIV drugs in the antagonist assay and to provide validity to our assay methods. The EC_{50} values and associated ligands are

listed in Table 5. The EC_{50} values were calculated by fitting luminescence data to equation 1. The EC_{50} values were found to be within 3 fold of reported EC_{50} values in literature references listed in Table 5.

HIV compounds were evaluated for induction of reporter gene transcription through agonist interactions with each member of the receptor panel. The efficacy of compounds, as indicated by % control, was determined by comparing reporter gene transcription levels to those achieved with saturating concentrations of receptor specific ligand. HIV compounds were considered to have an agonist effect if there was at least a 30 % increase in signal over background. None of the HIV drugs tested showed any significant agonist activity in the reporter gene assay, confirming results obtained in the coactivator recruitment assay. The potent agonist effects of nelfinavir on FXR were not observed in the reporter assay. The apparent lack of agonist activity was surprising since nelfinavir appeared to be a potent agonist in the coactivator recruitment assay.

In the reporter assay, PXR was found to be activated by all PIs in the drug panel with the exception of indinavir (Figure 9). Ritonavir exhibited a full agonist titration in the range of concentrations tested and induced reporter gene transcription levels comparable to rifampicin. Ritonavir was calculated to have an EC_{50} of 2.6 ±0.4 μM approximating both the efficacy and potency of rifampicin, as previously reported [185]. Nelfinavir and saquinavir both activate PXR in a dose-dependent manner but lack a complete titration range within the concentrations tested. Nelfinavir exhibited a dose dependent response up to 2.5 μM, with decresing response at higher concentrations. EC_{50} values for nelfinavir and saquinavir were 5.1 μM ± 1.3 and 31.8 μM ± 13.3, respectively.

The NRTI and NNRTI compounds were found to have no effect on transcription levels of the reporter gene regardless of the receptor tested.

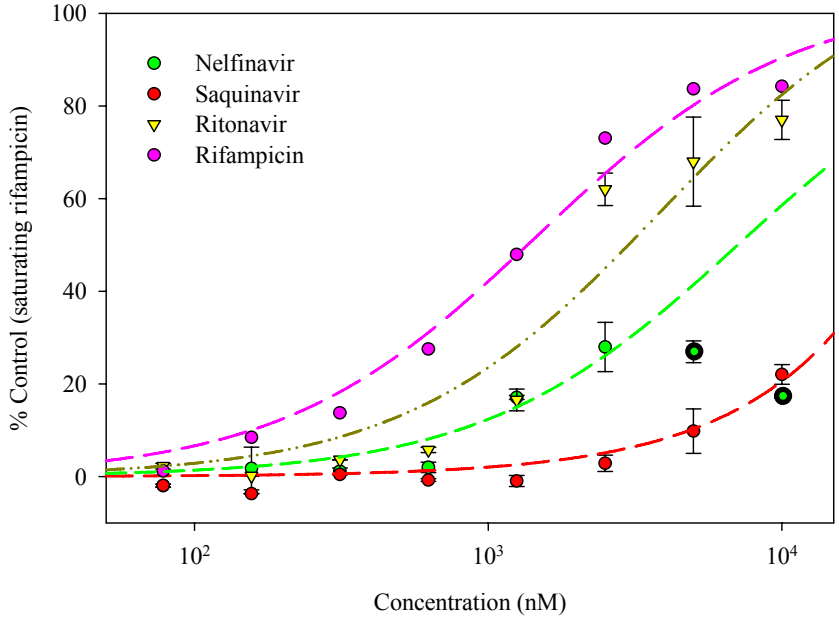

Figure 9. Activation of PXR by PIs. Cells transfected with plasmids containing full length PXR and cyp3A4 RE-luc plasmids were incubated with either rifampicin, saquinavir, ritonavir or nelfinavir for 24 hr. Luminescence generated from expression of the luciferase reporter gene were compared to levels obtained under saturating concentrations of rifampicin. Data points outlined in black were excluded from equations used to generate EC_{50} values and data fitting. Data are plotted as % control versus compound concentration. With the exception of rifampicin, data represents the average of at least two determinations and the error bars are the standard deviation.

Reporter assay – PI toxicity and receptor antagonism

Compounds that interfere with ligand-induced receptor activation reduce levels of reporter gene expression. Any decrease in reporter gene transcription, however, can also result from a decrease in protein expression due to compound toxicity. PIs were evaluated for effects on HEK293 pG5*luc*+neo cell viability and caspase induction. Saquinavir, nelfinavir and ritonavir were found to affect cell viability at concentrations > 12.5 μM

while indinavir had no effect at the concentrations tested. However, increased levels of caspase expression were found at much lower PI concentrations than those found to have an immediate impact on cell viability. The results indicate that PIs trigger induction of the apoptotic pathway which can have generalized effects on rates of transcription and protein synthesis [231]. Therefore, only PI concentrations below induction of caspases could be used reliably for assessment of receptor antagonism. Caspase induction was considered significant if caspase levels were found to be > 1.7 fold over the vehicle control or > 10 standard standard deviations from baseline values (Figure 10 inset). The highest PI concentrations that could be reliably evaluated for antagonist activity were determined to be ≤ 15 μM for ritonavir and saquinavir and ≤ 1.2 μM for nelfinavir. PI receptor antagonism at these concentrations was considered significant if the % inhibition value exceeded 3 standard deviations. Ritonavir and saquinavir met this criterion for both PPARα and PPARγ (Table 8).

Table 8. % Inhibition of PPARα and PPARγ Activation in the Cell-Based Reporter Gene Assay.

	Ritonavir	Saquinavir
PPARα	52 % ± 8	34 % ± 11
PPARγ	64 % ± 12	45 % ± 8

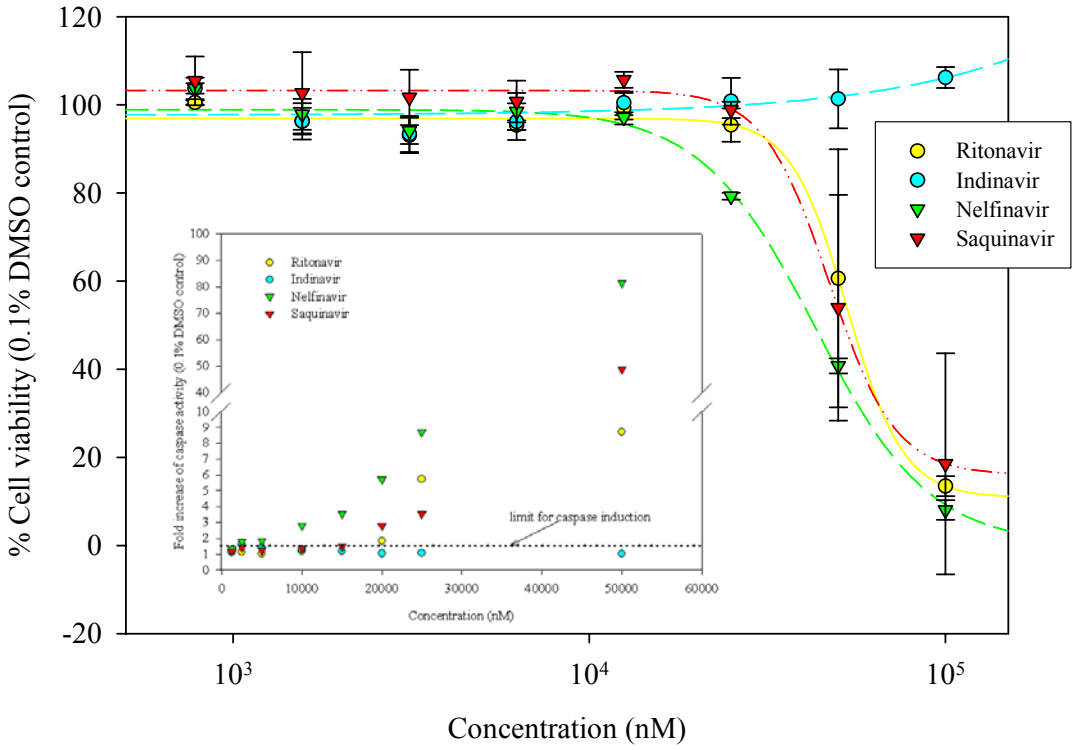

Figure 10. Effect of PIs on Cell Viability and Caspase Induction in HEK293 Cell Line. HEK293 cells were incubated with PIs at various concentrations for 24 hr. Impact of PIs on both cell viability and caspase induction was determined by comparing ATP and caspase levels in control cells exposed to 0.1% DMSO only (vehicle control). Data is plotted as either % cell viability or fold caspase induction versus the concentration of PI. Data is the average of triplicate determinations and the error bars represent the standard deviation.

2.3.3 Gene Expression Analysis

Saquinavir and ritonavir effects on primary hepatocyte gene expression

An exploratory study was performed to determine if gene expression levels in primary human hepatocytes were affected after a 24 hour exposure to media containing ritonavir or saquinavir. Genes with p-values ≤ 0.05 were selected and sorted by treatment group for up-regulated and down-regulated expression compared to the vehicle treatment group. Searches were performed within the treatment groups for genes previously reported to be regulated by PXR, SREBP, PPARα and PPARγ.

Several well characterized PXR target genes were up-regulated by both saquinavir and ritonavir treatments (Table 9). The data set was significantly enriched for genes of both phase I and phase II drug metabolizing enzymes, specifically cyp3A4, cyp2C9 and GSTT2. Interestingly, treatment of hepatocytes with saquinavir increased expression of the lipogenic enzyme, stearoyl CoA desaturase (SCD). SCD transcriptional regulation has recently been associated with the direct activation of PXR [187]. These results confirm that PXR activation in the presence of ritonavir and saquinavir observed in the cell-based reporter assay equates with induction of known PXR target genes in primary hepatocytes providing validation of our experimental design and methods.

Table 9. Effect of Ritonavir and Saquinavir Treatment on the Expression Level of Known PXR Target Genes.

ACCN#	Gene	Ritonavir	Saquinavir
PHASE I			
NM_022820	cytochrome P450, family 3, subfamily A, polypeptide 43 (CYP3A43)	**2.4***	**2.5****
NM_000500	cytochrome P450, family 21, subfamily A, polypeptide 2 (CYP21A2)	**3.3**	**6.4***
NM_000896	cytochrome P450, family 4, subfamily F, polypeptide 3 (CYP4F3)	**2.0**	**3.1***
NM_000783	cytochrome P450, family 26, subfamily A, polypeptide 1 (CYP26A1)	**1.8**	**-1.6***
NM_000771	cytochrome P450, family 2, subfamily C, polypeptide 9 (CYP2C9)	**10.2***	**11.5**
NM_017460	cytochrome P450, family 3, subfamily A, polypeptide 4 (CYP3A4)	**8.8***	**8.1**
NM_000767	cytochrome P450, family 2, subfamily B, polypeptide 6 (CYP2B6)	**3.0****	**1.7**
NM_030622	cytochrome P450, family 2, subfamily S, polypeptide 1 (CYP2S1)	**2.6***	**-1.3**
NM_000777	cytochrome P450, family 3, subfamily A, polypeptide 5 (CYP3A5)	**2.5****	**2.3**
PHASE II			
NM_006588	sulfotransferase family, cytosolic, 1C, member 2 (SULT1C2)	**-2.0****	**-1.6**
NM_000854	glutathione S-transferase theta 2 (GSTT2)	**23.3****	**28.5****
NM_000852	glutathione S-transferase pi (GSTP1)	**4.3**	**7.2****
NM_019093	UDP glucuronosyltransferase 1 family, polypeptide A3 (UGT1A3)	**1.6**	**2.0***
NM_053039	UDP glucuronosyltransferase 2 family, polypeptide B28 (UGT2B28)	**-1.4***	**-2.0***
PHASE III			
NM_033226	ATP-binding cassette, sub-family C (CFTR/MRP), member 12 (ABCC12)	**4.5***	**3.4**
Lipogenic			
NM_005063	stearoyl-CoA desaturase (delta-9-desaturase) (SCD)	**1.2**	**1.9***

* Indicates p value < 0.05, ** < 0.01, all values reported for completeness

Prior evidence suggests that at least some of the dysfunction of cholesterol and fatty acid regulation found in HADL is due to HIV PI inhibited degradation of nuclear SREBP [88]. Comparison of published results of gene expression profiles obtained in transgenic mice over expressing SREBP isoforms with our data identified several overlapping genes [227]. Increased expression levels of genes involved in both fatty acid and cholesterol synthesis pathways were identified in both treatment groups (Table 10). The most significant changes were observed in the saquinavir treatment group with respect to both statistical merit and magnitude of change. The only gene found to be significantly increased by both treatment groups was SPOT14. With the exception of fatty acid desaturase (FADS) and SPOT14, modest increases in SREBP target genes were observed, ranging from 1.3 to 2.5 fold. These increases are similar to those obtained in studies using normal mice treated with ritonavir [88]. SCD was included in both the SREBP and PXR gene list due to overlapping control of SCD expression by these transcription factors [87, 187].

Table 10. Effect of Ritonavir and Saquinavir Treatment on the Expression Level of Known SREBP Target Genes.

ACCN#	Gene	Ritonavir	Saquinavir
	Fatty Acid Synthesis		
AI659296	acetyl-Coenzyme A carboxylase alpha γ	**1.5***	**2.0****
NM_018677	acetyl-Coenzyme A synthetase 2 (ADP forming) (ACAS2), transcript variant 1	**1.0, 1.2**	**1.5*, 1.6***
NM_005063	stearoyl-CoA desaturase (delta-9-desaturase) (SCD) γ	**1.2**	**1.9***
NM_013402	fatty acid desaturase 1 (FADS1) delta-5-desaturase	**1.4**	**5.6***
NM_020918	glycerol-3-phosphate acyltransferase, mitochondrial (GPAM)	**2.5***	**1.2**
NM_004092	enoyl Coenzyme A hydratase, short chain, 1, mitochondrial (ECHS1), nuclear gene encoding mitochondrial protein γ	**1.0**	**1.5****
NM_004104	fatty acid synthase (FASN) γ	**1.3**	**1.8***
NM_003251	thyroid hormone responsive (SPOT14 homolog, rat) (THRSP)	**3.5***	**2.7****
	Cholesterol Synthesis		
NM_001096	ATP citrate lyase (ACLY), transcript variant 1 γ	**1.2**	**1.3****
NM_004458	acyl-CoA synthetase long-chain family member 4 (ACSL4), transcript variant 1 γ	**1.2***	**1.3***
NM_004508	isopentenyl-diphosphate delta isomerase (IDI1)	**1.2**	**1.4***
NM_005891	acetyl-Coenzyme A acetyltransferase 2 (acetoacetyl Coenzyme A thiolase) (ACAT2)	**1.7**	**2.3***
BU741861	2,3-oxidosqualene:lanosterol cyclase	**1.1**	**1.6***
	Miscellaneous		
NM_014573	hypothetical protein MAC30 (MAC30)	**1.3***	**1.3**
NM_018645	hairy and enhancer of split 6 (Drosophila) (HES6)	**1.5***	**1.1**
NM_001169	aquaporin 8 (AQP8)	**1.2**	**1.9***

* indicates p value <0.05, ** <0.01, all values reported for completeness

γ also target gene of PPARγ

In general, PPARγ target genes identified in the data sets were down regulated by both saquinavir and ritonavir treatments supporting observations of inhibition of PPARγ activation in both the coactivator and cell-based transcription assays (Table 11). The PPARγ gene set contains down regulated genes of various activity within biological processes rather than enrichment of any particular pathway. GLUT2 and glucokinase (GK), major mediators of glucose uptake and metabolism, were down regulated with significant reduction of glucokinase observed in both treatment groups. Reduction in expression levels > 2 fold were also observed for the fatty acid metabolism enzymes glycerol-3-phosphate dehydrogenase (GPD) and mitochondrial 3,2 trans-enoyl-CoA as well as insulin-like growth factor-1 (IGF-1) and promethin. No PPARα target genes, meeting statistical criteria, were found in the microarray data set.

Table 11. Effect of Ritonavir and Saquinavir Treatment on the Expression Level of Known PPARγ Target Genes.

ACCN#	Gene	Ritonavir	Saquinavir
NM_000340	solute carrier family 2 (facilitated glucose transporter), member 2 (SLC2A2)	**-2.0***	**-1.2**
NM_033507	glucokinase (hexokinase 4, maturity onset diabetes of the young 2) (GCK)	**-2.9****	**-4.6****
NM_000041	apolipoprotein E (APOE)	**-1.2***	**1.0**
NM_002970	spermidine/spermine N1-acetyltransferase 1 (SAT1)	**1.2****	**1.6****
NM_005693	nuclear receptor subfamily 1, group H, member 3 (NR1H3), LXRα	**-1.5****	**-1.2**
NM_005276	glycerol-3-phosphate dehydrogenase 1 (soluble) (GPD1)	**-2.0***	**-1.6***
NM_032564	diacylglycerol O-acyltransferase (DGAT2)	**-1.5***	**1.0**
BF002257	phospholipid transfer protein (PLTP precursor)	**-1.7***	**-1.2***
NM_020672	S100 calcium binding protein A14 (S100A14)	**-1.5****	**1.1**
NM_018441	peroxisomal trans-2-enoyl-CoA reductase (PECR)	**-1.4****	**1.0**
NM_000618	insulin-like growth factor 1 (somatomedin C) (IGF1)	**-1.6**,-2.3***	**-1.1,-3.4***
NM_004092	enoyl Coenzyme A hydratase, short chain, 1, mitochondrial (ECHS1)	**1.0**	**1.5****
NM_021814	ELOVL family member 5, elongation of long chain fatty acids (FEN1/Elo2, SUR4/Elo3-like, yeast) (ELOVL5)	**-1.3***	**1.0**
NM_021213	phosphatidylcholine transfer protein (PCTP)	**1.3**	**1.5***
AA581670	mitochondrial 3,2 trans-enoyl-CoA isomerase	**-2.1****	**-1.6***
NM_020422	transmembrane protein 159 (Promethin)	**-2.0**	**-4.7***

* indicates p value <0.05, ** <0.01, all value reported for completeness

Saquinavir and ritonavir effects on GK and GLUT2 expression in primary hepatocytes

qRT-PCR experiments confirmed treatment effects on expression levels of GK and GLUT2 in primary hepatocytes (Table 12). Troglitazone, a PPARγ specific agonist, also increased the transcription of GLUT2. A slight increase in GK was observed but did not reach statistical significance. Incubation of troglitazone in combination with the PIs overcame the decrease of both GK and GLUT2 mRNA when compared to treatment with saquinavir and ritonavir alone.

Table 12. qRT-PCR Analysis of GK and GLUT2 Expression in Primary Human Hepatocytes.

		ritonavir	saquinavir	troglitazone
GLUT2	array†	-2.0*	-1.2	-
	qRT-PCR†	-2.6*	1.0	2.3*
	qRT-PCR + troglitazone‡	1.5**	1.5*	-
GK	array†	-2.9**	-4.6**	-
	qRT-PCR†	-2.1*	-5.5*	1.4
	qRT-PCR + troglitazone‡	-1.5**	-1.4**	-

† p-values based on DMSO
‡ p-values based on troglitazone
indicates p-value * <0.05, **<0.01

2.4 Discussion

The use of HAART in the treatment of HIV infection has resulted in a dramatic decline in AIDS-related deaths [2-4]. However, it is widely recognized that HAART, especially those containing the PI class of antiretroviral drugs, is also associated with a variety of metabolic side effects. These side effects include hypertriglyceridemia, insulin resistance, hypercholesteremia and body fat redistribution, collectively known as HADL [20, 21]. The cause of HADL appears to be multifactorial, involving the disruption of multiple pathways, which have only complicated a detailed understanding of the mechanisms involved. Despite many advances in unraveling the complex events and pathway perturbations involved in the development of HADL, a complete understanding of the biological processes involved for the totality of symptoms observed in the clinical definition of the syndrome, as well as, mechanistic difference between members of the PI class, have yet to be fully defined.

The goal of this project was to investigate the role of nuclear receptor activation in the development of HADL, with a specific interest in receptors whose target genes reside in pathways that regulate energy storage and metabolism. The panel of HIV drugs listed in Table 2 was evaluated for effects on nuclear receptor activation using both cell-free and cell-based methods measuring coactivator binding and reporter gene transcription.

Coactivator recruitment results indicated that nelfinavir was a full and potent activator of FXR. The potency of nelfinavir activation was dependent on the coactivator peptide recruited by FXR in the order of potency bSRC-1 M2 > bPGC-1 > bCBP. However, this robust activation could not be confirmed in the cell-based reporter assay.

Failure to reproduce the activity of a potent FXR agonist in cell-based systems has been reported previously and was attributed to issues concerning compound solubility [232]. Intrinsic FXR activators, such as bile acids, are derived from cholesterol and, therefore, hydrophobic in nature. Exogenous compounds that activate FXR must retain the chemical characteristics of the intrinsic ligand in order to form positive interactions with amino acids in the ligand binding pocket. Studies using various pharmaceutical formulations of nelfinavir report a maximum solubility of ~10 μM in aqueous solutions, with higher concentrations attainable in solutions containing DMSO [233]. Therefore, solubility of nelfinavir could not have been a factor in the cell-based assay since a measurable transcriptional response should have been possible with concentrations < 10 μM. In addition, nelfinavir has been shown to rapidly accumulate in cultured cells with concentrations greater than 30-fold over media concentrations having been reported [234]. This suggests that neither solubility nor inadequate intracellular accumulation provide an explanation for the lack of transcriptional response. The coactivator recruitment results were scrutinized for any indication of assay interference which could have been interpreted as potent activation of FXR. Values from the raw fluorescence readings did not indicate interference in absorption or emission readings. Fluorescence interference by nelfinavir is highly unlikely due to the time resolved nature of fluorescence energy transfer of europium. In addition, general assay interference by nelfinavir would have been observed in other receptor assays since the assay components, including GST-tag and inclusion of bSRC-1, were common to other receptors in the panel.

The reason for the apparent discrepancy in nelfinavir effects may lie in the nature of the assays. The methods used to evaluate drug effects on nuclear receptor activation may not accurately represent the *in vivo* requirements for efficient gene transcription. Coactivator assembly by an activated receptor entails the recruitment of a primary coactivator, binding directly to the AF-2 region, through which the remaining coactivator complex is anchored [126]. The coactivator complex is comprised of many coactivator proteins with diverse roles in facilitating recruitment of transcriptional machinery such as chromatin remodeling, DNA unwinding and interaction with general transcription factors [125]. The composition of the coactivator complex and the order of recruitment are influenced by many factors. Cell-type coactivator abundance, as well as, agonist and response element binding effects on LBD conformation all influence the order of complex assembly, composition of the complex and ultimately the level of transcriptional response [136-138]. In this instance, use of the Gal4 system, rather than a system relying on direct binding of FXR to target gene RE sequences may have prevented an efficient transcriptional response. Experiments utilizing full length FXR and RE sequences from different target genes or quantitation of protein levels of target genes, such as the bile salt export pump (BSEP) and short heterodimer partner (SHP), in relevant cell lines need to be performed in order to determine the potential for *in vivo* activation of FXR by nelfinavir [171, 173].

Analysis of inhibitor effects on nuclear receptor activation in the coactivator assay indicated that micromolar concentrations of ritonavir, saquinavir and nelfinavir prevent ligand-induced activation of PPARα and PPARγ. Nelfinavir was shown to inhibit the activation of LXR but to a lesser extent than effects observed for PPARα/γ. Unlike the

other PPAR family members, PPARδ activation was unaffected by HIV PIs. This result was not surprising since ligands that activate both PPARα/γ often have little to no effect on the activation of PPARδ [224]. While the sequence homology between the LBDs of the PPAR family members is 60-70 %, the ligand binding pockets of PPARα and PPARγ are spatially much larger than PPARδ [235]. Minor differences in the amino acid sequence surrounding the binding pocket of PPARδ cause a narrowing of the LBD close to the AF-2 helix [235]. This excludes the productive binding of many large and potent ligands of the PPARα/γ subtypes, such as thiazolidinones (TZDs) and fibrates [235]. The narrow binding pocket of PPARδ together with the large structures of PIs provides a reasonable explanation for the subtype specific effects of PIs within the PPAR family.

Direct measurement of PI effects on receptor activation in the cell-based reporter gene assay proved problematic. All PIs, with the exception of indinavir, were found to decrease cell viability at concentrations exceeding 12.5 μM. Others have reported similar effects on the viability of B and T-cell lines at concentrations greater than 10 μM and caution the interpretation of PI-mediated cellular effects under such conditions [90, 236]. However, the cellular toxicity of PIs at these concentrations do highlight the global effects these drugs have on normal cellular function and are responsible, in part, for the development of acute side effects, such as hepatotoxicity and gastrointestinal disturbances [237] Lower concentrations, while not impacting cell viability directly, were found to induce expression of caspases, indicating induction of apoptotic pathways and the possibility of negative effects on cellular rates of transcription and translation [231]. Transcriptional effects at PI concentrations low enough to avoid caspase induction, confirmed the inhibition of PPARα/γ activation by saquinavir and ritonavir observed in

the coactivator recruitment assay. However, we were unable to confirm the inhibitory effects of nelfinavir due to significant toxicity at concentrations that would have been required for inhibition of both LXR and PPARα/γ activation.

Therapeutic drug monitoring studies indicate that maximal plasma concentrations (C_{max}) of ritonavir, under recommended doses, are in the range of 15 μM [93]. Saquinavir, administered as a monotherapy, has a reported C_{max} of 300 nM. However, current guidelines require coadmistration of saquinavir with small doses of ritonavir in order to 'boost' saquinavir exposure, resulting in an improved C_{max} of ~10 μM [92, 238]. Based on the pharmacokinetic data of PIs, inhibition of PPARα/γ activation by ritonavir and saquinavir at micromolar concentrations is possible under current dosing guidelines.

Microarray analysis was performed on mRNA transcripts from primary human hepatocytes to determine whether partial inhibition of PPARα/γ activation would be significant enough for measurable effects on the abundance of known target genes. Changes in PXR target genes abundance, as well as those of SREBP, were also evaluated. We expected that PXR activation by saquinavir and ritonavir in the reporter gene assay would result in increased expression of genes involved in drug metabolism pathways in hepatocytes. Even though SREBP was not included in our initial experimental design, evaluation of changes in target gene expression was included due to expected effects on SREBP target gene transcription with ritonavir and saquinavir and the overlap of transcriptional control of lipogenic pathways with PPAR and PXR.

Microarray analysis of differentially expressed genes in primary human hepatocytes with either ritonavir or saquinavir treatment demonstrated robust induction of drug metabolizing enzymes consistent with transcriptional activation of PXR in the

reporter gene assay. Activation of PXR by the PI class of HIV drugs has been described previously [185]. A recent publication examining changes in liver gene expression profiles among different PIs, failed to show changes in transcriptional response indicative of PXR activation. The microarray data obtained in these experiments were derived from transcriptional responses in the HepG2 cell line. Wilkening *et al*. compared the drug metabolizing capabilities of primary hepatocytes and HepG2 cells and demonstrated that HepG2 cells do not retain drug metabolizing characteristics of the primary cell line [239]. The expression of all p450 enzymes was found to be 100 to 1000 fold less when compared to primary hepatocytes. In addition, Jover *et al.* found that liver-specific transcription factors such as, hepatocyte nuclear factors and C/EBPα, are also expressed at lower levels in HepG2 [240]. In contrast, primary human hepatocytes have been shown to be equally effective as liver slices in their ability to reproduce drug effects on gene expression profiles observed *in vivo* [241]. The absence of crucial drug metabolizing capabilities, as well as transcription factors and cofactors, requires that claims based on gene effects in the HepG2 cell line be considered with caution.

Recent studies indicate that PXR activation has the potential to induce lipogenic pathways through mechanisms independent of SREBP activation [187]. PXR mediated hepatic lipid accumulation correlated with increased expression of SCD-1, fatty acid elongase (FAE) and FAT/CD36 as well as suppression of β-oxidation pathways. The implications of PI-mediated PXR activation on lipid and fatty acid synthesis are unknown. While we were unable to identify the majority of lipogenic genes currently linked to PXR activation, SCD-1 was found to be up regulated in response to saquinavir treatment. Increased expression and activity of SCD-1 has been linked to the onset of

diet-induced hepatic insulin resistance [242]. Whether this increased expression is a direct result of PXR activation remains uncertain since transcriptional control of SCD-1 overlaps with SREBP [87, 187]. Since PIs have been shown to prevent degradation of SREBP directly, SREBP KO models would be required to determine PXR specific effects on SCD-1 expression. In addition, experiments employing an extended time course of treatment and transcriptional analysis would provide an opportunity to capture transcriptional changes in other PXR lipogenic genes currently absent from our data set. Although hepatic steatosis in PI treatments has been linked to uncontrolled transcription of SREBP target genes, activation via PXR could provide an additive effect in saquinavir based therapies.

Consistent with increased accumulation of nSREBP due to proteasome inhibition, several genes implicated in SREBP-mediated lipogenic pathways were up regulated in response to both ritonavir and saquinavir treatments. Increased expression of ATP-citrate lyase and acetyl-CoA synthetase indicate cellular conditions favorable for production of acetyl-CoA, an essential precursor for both monounsaturated fatty acid and cholesterol biosynthetic pathways. A significant increase of SPOT14 expression was observed in both treatment groups. While expression of SPOT14 has been directly correlated with SREBP activity, the function of SPOT14 in lipogenic processes is unknown. The development of SPOT14 KO models suggest that SPOT14 may function as a transporter of fatty acids [243]. SPOT14 KOs have been shown to accumulate malonyl-CoA, the product of acetyl-CoA carboxylase and the substrate of FAS. It is hypothesized that SPOT14 serves to eliminate product inhibition of FAS through transport of fatty acids, promoting a favorable environment for fatty acid accumulation.

The microarray gene set did not contain PPARα target genes meeting statistical significance. Due to the low number of samples submitted for microarray analysis, a relatively small number of genes meet criteria for statistical significance. The limited sample set certainly resulted in exclusion of differentially expressed genes due to statistical failure. For this reason, many SREBP and PXR target genes, whose expression levels were described to be affected by PI treatment, such as the drug export pump, MDR1 and HMGCoA synthase, were excluded from the data set [88, 244]. Failure to achieve statistical significance combined with the modest inhibitory effects predicted from the reporter assay may provide an explanation for the absence of differentially expressed PPARα target genes. In order to rule out inhibition of PPARα activation as a potential mechanism towards development of HADL, additional experiments, consisting of greater replicates, as well as, time course evaluation of transcriptional change, need to be conducted.

In contrast to PPARα, several PPARγ target genes were identified in the microarray gene set in both treatment groups. In general, expression levels of these target genes were decreased by both ritonavir and saquinavir treatment, consistent with inhibitory effects on receptor activation in both the coactivator and reporter gene assays. Target gene assignment was based on both experimental and bioinformatic evidence suggesting that PPARγ was responsible, in part, for modulation of transcript abundance [146, 226, 245]. However, transcriptional control for many of these genes overlap with other transcription factors such as LXRα, PPARα and SREBP, providing a monumental hurdle in establishing a direct relationship between the state of PPARγ activation and gene expression [246, 247] . Several fatty acid and cholesterol biosynthetic genes listed

in the SREBP target gene table ($^{\gamma}$ notation) are also controlled by PPARγ [226, 227]. Cross talk between nuclear factors in the regulation of fatty acid and cholesterol pathways, especially those shared with SREBP, prevented general conclusion from being made pertaining to the effects of PI-mediated inhibition of PPARγ activation within the context of the microarray experimental methods.

However, qRT-PCR results indicate that negative effects on GK and GLUT2 gene expression by ritonavir and saquinavir treatments may occur through direct inhibition of PPARγ activation. This conclusion is based on the observation that treatment of hepatocytes with troglitazone in combination with either ritonavir or saquinavir results in partial reversal of inhibitory effects on GK and GLUT2 expression levels when compared to ritonavir/saquinavir treatment groups. Supporting this observation, Goetzman *et al.* also noted partial inhibition of rosiglitazone–induced expression of the PPARγ target genes, PEPCK and UCP-2, in the adipose tissue of mice when rosiglitazone was coadministered with ritonavir [248]. In addition, troglitazone treatment of hepatocytes resulted in a 2 fold increased expression of GLUT2, indicating direct transcriptional control of this gene by ligand-activated PPARγ. These observations are consistent with previous reports of increased GLUT2 mRNA in hepatocytes treated with rosiglitazone as well as the identification of PPAR RE sequences in the +68/+89 and -197/-184 region of the rat and mouse GLUT2 promoters, respectively [155, 249]. While we were unable to establish a direct connection between GK and PPARγ activation due to statistical constraints, positive effects on GK transcription levels have been reported by others. Kliewer et al. reported increased levels of GK mRNA in the liver of diabetic ZDF rats treated with the PPARγ-specific agonist GW1929. Kim *et al.* reported similar effects on

GK expression in rat hepatocytes treated with troglitazone [154]. This group also identified a functional PPAR RE sequence in the -116/-104 region of the rat GK gene suitable for direct binding of PPARγ/RXRα heterodimers.

Identification of several cis and trans-activating sites within the GLUT2 promoter region indicate the interplay of multiple transcription factors in tissue-specific gene regulation [250]. Hepatocyte nuclear factor-6 (HNF6) influences the expression levels of both GK and GLUT2 in pancreatic β-cells [251]. Inactivation of the HNF6 gene was associated with a 50 % decrease of GK mRNA compared to controls, confirming compensatory mechanisms and overlap of transcriptional control [252]. Other transcription factors, such as the PDX-1 homeobox factor and SREBP-1c, have also been implicated in the transcriptional control of GLUT2 and GK, respectively [253]. Therefore, the possibility that transcriptional repression is occurring through PPARγ-independent mechanisms, which are overcome by increasing transcription via troglitazone-activated PPARγ, can not be ruled out.

GLUT2 and GK play an important role in GSIS and the postprandial processing of glucose and are expressed in the liver, as well as pancreatic β-cells [254-256]. GLUT2 and GK are low affinity binders of glucose and provide liver and β-cells with increased sensitivity to high levels of circulating glucose. The K_m of most glucose transporters are between 2 - 5 mM [256]. GLUT2, however, has a high transport capacity and a higher K_m for glucose (> 6 mM) and is better suited to decrease high levels of circulating glucose after feeding [257]. When blood glucose levels exceed 5.5 mM, glucose is transported by GLUT2 into cells where it is rapidly phosphorylated to glucose-6-phosphate (G-6-P) by hexokinases, trapping glucose within the cell. GK, also known as hexokinase 4, is one of

four hexokinases found in humans [254] . Like GLUT2, GK also has a low affinity for glucose (K_m 6-15 mM) and is the primary hexokinase involved in G-6-P formation under high glucose conditions [254]. GK has an additional advantage over other hexokinases in that it is not subject to product inhibition by physiological concentrations of G-6-P ensuring sustained processing of glucose. GK activity is the rate-limiting step for glucose metabolism in both β-cells and liver. The concerted actions of GLUT2 and GK result in the intracellular accumulation of G-6-P which facilitates fatty acid synthesis and glycogen storage in the liver and insulin secretion in β-cells. Proper function of GLUT2 and GK are essential for reduction of circulating glucose levels through induction of insulin-mediated peripheral cellular uptake and glycogen storage in the liver [258].

Loss of function mutations of GK have been identified in families with maturity onset diabetes of the young (MODY2) [259]. MODY2 mutations are located throughout the GK gene and produce GKs with lower kinetic rates in the formation of G-6-P. Decreased rates in the formation of G-6-P delay insulin secretion, as well as hepatic glycogen synthesis, in response to high glucose levels, highlighting the importance of GK in the maintenance of glucose homeostasis [260]. Reduced levels of liver GK activity have also been reported in diabetic patients negative for MODY2 [261-263]. Hepatocytes isolated from diabetic Zucker rats were found to have 4.5 fold less GK activity compared to normal rats [264]. Transgenic models have demonstrated that relatively modest increases in liver GK expression levels can lead to substantial changes in blood glucose concentrations [264, 265]. Increasing liver GK activity by 20 % in transgenic mice was shown to improve glucose tolerance, insulin secretion and reduce body weight [266].

Small molecule GK activators are currently being investigated as potential therapies in the treatment of diabetes [267, 268].

While the role of GK in the pathogenesis of diabetes has been firmly established, the role of GLUT2 is less certain. Reduction of β-cell GLUT2 transcripts have been observed in many rodent models of diabetes [269]. However, comparison of human and rodent GLUT2 mRNA in β-cells indicate that GLUT1 may be the primary glucose transporter for humans at this site and has brought into question the relevance of GLUT2 in the manifestation of diabetes in humans [270, 271]. Despite these observations, there is direct evidence supporting a role for GLUT2 in the dysfunction of glucose uptake and GSIS. In diabetic islets from human cadavers, mRNA expression of GLUT1, GLUT2 and glucokinase was reduced by 20, 50 and 30 %, respectively [272]. The reduction of GK and GLUT2 expression, not GLUT1, was found to correlate directly with a 50 % reduction of glucose oxidation in the islets. Mutations of liver GLUT2 found in Fanconi-Bickel syndrome, a rare autosomal recessive disorder of glucose metabolism, results in fasting hypoglycemia and postprandial glucose intolerance [273]. In addition, polymorphisms in the promoter region of the GLUT2 gene have been associated with an increased risk of developing type 2 diabetes through decreased expression of GLUT2 [274].

HIV patients receiving PI-containing therapies often display impairments in glucose processing and β-cell function. PIs, especially indinavir, have been shown to interfere with peripheral glucose uptake through direct binding of GLUT4. Other GLUT isoforms are also targets of PI inhibition but to a lesser extent than GLUT4. Suppression of glucose stimulated insulin release has also been observed in mouse pancreatic islets

and MIN6 cells [275]. Indinavir treatment reduced insulin release by 50 % at concentrations > 2 μM. Indinavir was shown to have no effect on GK activity at these concentrations, suggesting glucose signaling was being blocked at the transport level. Similar observations were made with ritonavir and saquinavir treatment but at concentrations 10 fold higher than those required for inhibition with indinavir. The concentrations of saquinavir/ritonavir required for GLUT4 inhibition are above C_{max} values and, therefore, may not be relevant *in vivo*. Unfortunately, GK activity levels were not determined for these PIs. A single dose of 1200 mg indinavir administered to healthy volunteers was found to increase insulin resistance by 35 %, supporting the rapid effects of indinavir on peripheral glucose transport [276]. Similar studies with ritonavir showed no significant change in insulin resistance, confirming differences in glucose processing between indinavir and other PIs [277]. However, long-term administration of ritonavir did cause significant changes in glucose tolerance upon administration of the oral glucose tolerance test. These findings suggest that individual PIs may have differential effects on glucose metabolism resulting in similar long term risks of developing diabetes.

Differences between indinavir and other PIs were also observed in our evaluation of PI effects on metabolic nuclear receptors. Saquinavir and ritonavir both inhibited the activation of PPARα/γ while indinavir had no effect. Formulation studies of indinavir indicate that indinavir is soluble in aqueous solution up to ~25 μM, excluding solubility as a potential reason for the lack of indinavir effects [233]. Intracellular accumulation of indinavir is limited and often approximates concentrations in culture media [234]. In fact, cell lines engineered to overexpress MDR1, reduce indinavir concentrations below limits of detection. While active efflux of indinavir by MDR1 may explain the lack of cellular

toxicity at concentrations approaching 100 μM, lack of inhibitory effects on receptor activation in the cell-free coactivator recruitment assay are likely mechanistic. The differential effects observed in PPAR α/γ activation may provide insight into the metabolic differences between saquinavir/ritonavir and indinavir based therapies and deserves further investigation.

Our research has confirmed that saquinavir/ritonavir based therapies influence the transcription of genes involved in drug metabolism through direct activation of PXR and suggest that induction of lipogenic processes are possible through PXR activation. Saquinavir and ritonavir also increased the expression of genes within cholesterol and fatty acid biosynthetic pathways providing further confirmation of PI lipogenic effects through nuclear accumulation of SREBP. Inhibitory effects were also observed in the activation of PPARα/γ, suggesting a role for metabolic nuclear receptors in the manifestation of HADL. Reduced expression and activity of GLUT2 and GK has been directly linked to development of diabetes and may contribute to insulin resistance and glucose intolerance in HIV patients receiving saquinavir/ritonavir based therapies, as well. TZDs have demonstrated some usefulness in the alleviation of HADL symptoms in HIV patients by decreasing insulin resistance, increasing subcutaneous body fat with modest effects on circulating triglycerides [278, 279] . These effects have been attributed primarily to improvements in subcutaneous adipose depots, increased efficiency in fatty acid uptake and favorable adipokine secretion at this site [205]. Our research has shown that positive effects on the expression of GK and GLUT2 in the liver and possibly pancreatic β-cells may also contribute to the positive effect of TZDs in treating HADL symptoms.

Chapter 3: Comparison of Full Length Versus Ligand Binding Domain Constructs in Cell Free and Cell Based PPARα Assays

Publication: Jennifer Berbaum and Richard K. Harrison, Analytical Biochemistry, 339 (2005) 121-128.

3.1 Introduction

Peroxisome proliferator-activated receptor alpha (PPARα) is a ligand-induced transcription factor belonging to the super family of nuclear hormone receptors [280]. The PPAR family consists of three members, alpha, gamma and delta, all of which are involved in the regulation of genes that control glucose, lipid, and cholesterol metabolism [224, 281]. PPARα has been shown to play a direct role in lipid homeostasis through the regulation of PPARα responsive genes [280]. These genes contain peroxisome proliferator responsive elements (PPREs) within the promoter region of the gene, where the ligand-activated PPARα and its obligate heterodimer partner, retinoid X receptor, bind and modulate gene transcription through recruitment of transcriptional machinery [193]. Most genes found to contain PPREs are involved in lipid catabolism, transport and storage pathways [280, 282]. PPARα is known to be activated by a variety of compounds including fatty acids and the fibrate class of hypolipidemic drugs [283]. Because of its role in dietary lipid regulation, PPARα has become an attractive target for drug development [224]. The potential role of PPARα in diseases such as diabetes, obesity and atherosclerosis has resulted in a considerable effort towards developing methods to accurately evaluate effects of drugs on PPARα receptor activation and subsequent gene regulation [203, 284].

The assays developed to analyze both PPARα activation and gene transcription exploit the unique structure and function of nuclear receptors. All nuclear receptors

contain six functional domains [115]. The N-terminal A/B domain contains the ligand-independent activation function (AF-1), which allows for constitutive expression of genes while the receptor is in an unliganded state. The C domain encodes the DNA binding domain (DBD) containing characteristic GC-rich regions and zinc finger motifs. The DBD interacts directly with receptor-specific gene response elements. The D domain, also known as the hinge region, connects the ligand binding domain (LBD) to the DBD. The hinge region is thought to play a role in transcriptional silencing and modulation of binding of the receptor to DNA. The E/F domain contains the LBD, a ligand-dependent activation function AF-2, dimerization sequences, and nuclear localization sequences. These distinct functional domains have allowed for development of cassettable systems for analyzing drug interaction with nuclear receptors [285].

Historically, assays such as the Gal4 transactivation and coactivator recruitment assays have relied solely on the LBD of the receptor in order to determine potency and efficacy of potential PPARα agonists. Coactivator recruitment assays assess agonist potency through measurement of the receptors ability to recruit coactivator peptides [283, 286]. Binding of the coactivator occurs due to conformational changes brought about by agonist binding [287]. The level of recruitment is measured through the transfer of energy between molecules such as allophycocyan (APC) and europium (Eu), which only occurs when the two are in close proximity [211]. Receptor constructs for these assays typically involve the use of GST, c-myc or His_6 N-terminal tags for detection purposes and a truncated form of the receptor for agonist binding.

The cell based Gal4 transactivation assay utilizes the 1-147 amino acid sequence of the yeast Gal4 transcription factor as a generic DBD [288]. The resulting chimera,

composed of an artificial DBD and native LBD, relies on the LBD for agonist binding and the Gal4 DBD for DNA binding. The chimera must be able to bind agonist and recruit transcriptional machinery in order for reporter gene expression to occur. The level of reporter gene induction indicates agonist efficacy on downstream gene transcription. This assay format is useful because it eliminates the need to generate specific response element reporter systems for each receptor to be investigated. However, like the coactivator recruitment assay, the Gal4 chimeras only include the LBD portion of the nuclear receptor. The reason for exclusion of full length nuclear receptors in these assay formats is unclear. Perhaps it is thought that inclusion of the native DBD in a Gal4 system would decrease overall transcription of reporter gene because of binding of the DBD to native RE in the cell. A recent publication concerning estrogen receptor alpha suggests that there are differences in LBD and full length receptor conformations upon binding of the same ligand [289]. These conformational differences appear to influence the binding of coactivator peptides and consequently agonist efficacy [289].

To determine whether similar effects would be seen for PPARα, we examined the potency and efficacy of several well characterized PPARα agonists using full length and LBD constructs. The results from these assays lead to an increased understanding of the binding and efficacy results from nuclear receptor assays, and suggest subtitle differences in the binding of coactivators to full length and ligand binding domain constructs.

3.2 Materials and Methods

The preceding methods have been described previously in Chapter 2 sections 2.2.2 thru 2.2.4. The methods were included in order to maintain the integrity of the published work.

Reagents

All solvents and buffer components were purchased from Sigma unless otherwise noted. cDNA was purchased from Invitrogen corp. Cell culture media and reagents were purchased from both Mediatech and Invitrogen except for charcoal stripped fetal bovine serum, which was purchased from Hyclone.

The coactivator peptides bSRC-1 M2, bPGC-1 and bCBP were synthesized and prepared to 95 % purity by Synpep Corp (Table 1). Europium-labeled anti-GST antibody was purchased from CIS-Bio US Inc. Allophycocyan-labeled strepavidin was purchased from Perkin Elmer. GW7647 was purchased from Sigma. Bezafibrate, Ciprofibrate and WY 147647 were purchased from Biomol.

Cloning and Expression of GST-PPARα FL and LBD constructs

The full length (FL) and the ligand binding domain (LBD) (166-468 aa) of the human PPARα gene, Genbank accession # L02932, were amplified from kidney cDNA using the primers in (Table 3). PCR reactions were conducted using BD Clontech's GC-2 and HF-2 PCR polymerases. PCR products were gel purified and TOPO cloned into Invitrogen's Gateway entry vector, pENTR / D-TOPO. Single clones were selected based on their resistance to kanamycin and the isolated plasmids, pENTR: PPARα FL /

LBD, were sequenced to confirm complete gene insertion. The pENTR: PPARα FL / LBD plasmids were then recombined with the Gateway destination vector pDEST15 using LR clonase as per manufacturer's procedure. pDEST15 confers a C-terminal glutathione-S-transferase (GST) tag in-frame with PPARα FL / LBD receptor. Single colonies containing pDEST15: PPARα FL / LBD plasmids were selected based on resistance to carbenicillin. pDEST15: PPARα FL / LBD plasmids were then transformed into BL21 (DE3) pLysS for protein expression.

Transformed 1 liter cultures were induced at an OD_{600} of 0.4 to 0.6 with fresh 0.4 mM IPTG and grown at room temperature for 4 hours. Cells were harvested by centrifugation at 12,000*g*. Cell pellets were frozen at –20ºC and lysed by thawing on ice. 50 ml of Buffer A containing 50 mM Tris pH 8.0, 50 mM KCl, 1 mM EDTA, 1 mM DTT, 10 % glycerol and 1 mM PMSF were added to the cell pellets. The cell aggregates were disrupted by passage through an 18-gauge syringe or homogenizer. Deoxyribonucease I (DNaseI) was added to the lysate at a final concentration of 20 μg/ml and incubated at 37 ºC for 2 hours. The cell lysate was clarified by centrifugation at 50,000*g* and filtered through a PES 0.22 μM filter prior to purification. Purification of the GST-receptor fusions was performed using Glutathione 4B resin (Amersham Biosciences). Column equilibration and washing were performed with Buffer A. Proteins were eluted from the column using Buffer A with the addition of 20 mM glutathione (pH 8.0). Protein concentrations were determined by Bradford assay and the protein was <95% pure as visualized by SDS-PAGE and western blot.

Coactivator titrations

Coactivator recruitment was determined by a homogenous time-resolved coactivator recruitment assay. Each coactivator assay contained 100 nM GST-PPARα FL or LBD, 100 nM streptavidin-APC, 3 nM europium (Eu)-labeled anti-GST antibody and 1 μM GW7647 / DMSO in assay buffer (50 mM Tris pH 8.0, 50 mM KCL, 1 mM EDTA, 1 mM DTT and 1 mg / ml BSA). All components were optimized for maximal assay signal. The coactivator peptides bSRC-1 M2, bPGC-1 and bCBP were diluted in dH_2O to a final stock concentration of 1 mM. A 10 μL aliquot of various concentrations of coactivator were added to the complete assay mix (final assay volume 100 μl, 1 % DMSO) in 96-well black optiplates (Perkin Elmer). Contents were mixed by pipetting, and the plates were spun at 300*g* for 1 minute to remove bubbles. Plates were covered and incubated for 2 hours at room temperature. Fluorescence was measured by excitation at 340 nm and reading of emission at 615 nm and 665 nm. Measurements were performed on the Perkin Elmer Fusion using the factory settings for time-resolved fluorescence.

Agonist titrations

Agonist potency was determined using the same assay format as the coactivator titrations with one exception. Instead of varying coactivator concentration, the concentration of agonist was varied in the experiment. Each HTRF assay contained 100 nM GST-PPARα FL or LBD, 100 nM streptavidin-APC, 3 nM Eu-labeled anti-GST antibody and 600 nM bSRC-1 M2 in 50 mM Tris pH 8.0, 50 mM KCL, 1 mM EDTA, 1 mM DTT and 1 mg / ml BSA. All agonists were solubilized in DMSO. Agonist titrations were prepared in DMSO at 100x assay concentration. Prior to addition of the assay mix,

1 µl of agonist titration was dispensed to the 96-well assay plate (final DMSO conc. 1%). Plates were mixed well by pipetting and handled identically as described above.

Preparation of stable reporter cell line

pG5*luc*, GenBank accession number AF264724, is a reporter vector containing the Gal4 response element upstream from a fire fly luciferase reporter gene (Promega). The plasmid was converted into a stable reporter plasmid by cloning a neomycin resistance gene at the BamHI (2142) / SalI (2148) sites. Wild type HEK293 (ATCC# CRL-1573) cells were transfected with the pG5*luc*+neo plasmid using lipofectamine according to the manufacturer's instructions. Single clones were selected using 800 µg /ml geneticin. Transformed cells were grown in DMEM with 4.5 g / L glucose and 25 mM Hepes supplemented with 10 % charcoal stripped fetal bovine serum, penicillin-streptomycin and glutamine. Cells were maintained at 37°C in a 5 % CO_2 humidified incubator.

Preparation of Gal4 DBD PPARα FL and LBD chimeras

pBIND vector, AF264722, contains a MCS downstream from the yeast Gal4 DBD (Promega). The pBind vector was converted into a Gateway destination vector through the insertion of Reading Frame B (rfb) at the *Ecor*V site (1594) as per manufacturer's instructions. The pENTR: PPARα FL / LBD plasmids were then recombined with the converted destination vector pBIND: rfb using LR clonase. All constructs were 5' sequence confirmed for correct orientation of gene (described previously in section 2.2.4).

Gal4 reporter assay- Agonist titrations

The pG5*luc* + neo HEK293 stables were batch transfected with either pBind: hPPARα or hPPARα LBD plasmid at 200 ng /μl using lipofectamine as per manufacturer's protocol. The cells were plated at a concentration of 5 x 10^5 cells per well into black-well clear bottom tissue culture treated plates. The transfected cells were incubated for 24 hours, after which the media was replaced with 100 μl of fresh media. Either DMSO or agonists were added to the cells (0.1 % DMSO final). The cells were returned to the incubator for another 24 hours. Luciferase measurements were conducted using Promega's Bright GLO reagents. All media was removed from the wells and a 1:1 mixture of phenol red free media and Bright GLO substrate were added at a final volume of 200 μl. The plates were placed on an orbital shaker for 2 minutes to aid in cell lysis then read on a Perkin Elmer Victor V using the factory settings for luminescence readings.

3.3 Results and Discussion

PPARα FL and LBD display differences in coactivator recruitment

PPARα FL and LBD were tested in the coactivator recruitment assay to determine their relative affinity and total fluorescence signal for the three coactivator peptides. The measurement of coactivator recruitment is determined by the amount of energy transferred from europium (λex 335 / λem 615) to allophycocyan (λex 615 / λem 665) [290]. Figure 11 illustrates the transfer of energy between these two molecules when they are brought within close proximity of each other. This event occurs when the receptor assumes a suitable conformation that allows for binding of the coactivator LXXLL

sequence [291]. Considering that the FL and LBD receptor could potentially assume different conformations based on the inclusion or exclusion of the highly structured N-terminal domain, it was important to determine whether this would convert into a measurable difference between the coactivator binding affinity and / or total fluorescence of the assay. Titrations for all assay components were performed for both full length and LBD construct to ensure that maximal interaction signals could be generated.

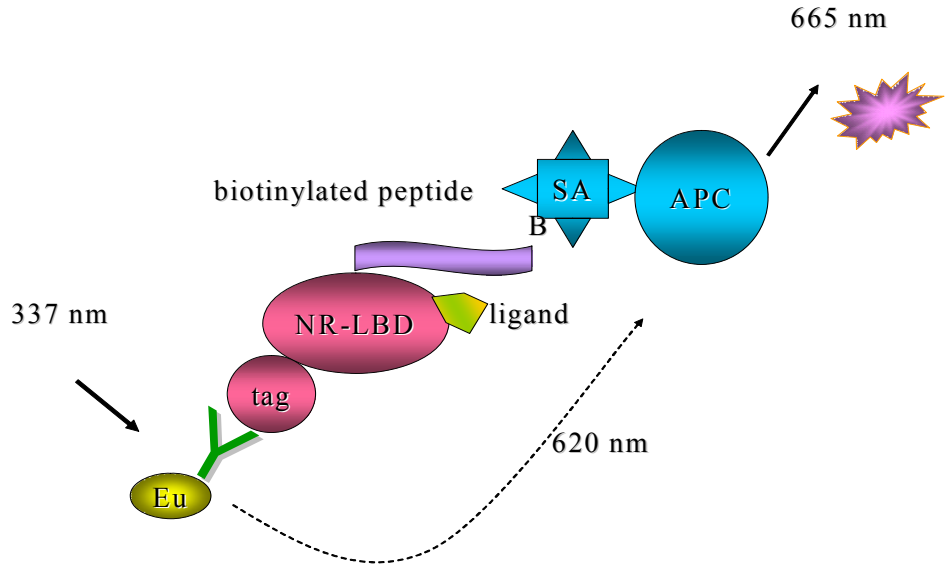

Figure 11. Illustration of Homogeneous Time-Resolved Fluorescence (HTRF) Assay for Detection of Coactivator Recruitment. Ligand activation of the labeled receptor results in conformational changes allowing for recruitment of coactivator peptides. The interaction between the labeled coactivator peptide and tagged receptor are detected by monitoring changes in energy transfer levels between Eu and APC.

Coactivator recruitment levels for the FL receptor, in the absence of ligand, are 2-3 fold greater than those observed for the LBDA. This increase in constitutive coactivator recruitment by FL PPARα is consistent for all three coactivator peptides tested. High levels of constitutive recruitment of coactivator peptides by PPARs have been reported

previously using a tagged PPAR LBD [213, 292]. Since the FL receptor includes the complete LBD, it would be reasonable to expect similar constitutive interactions to occur. However the level of increase in coactivator recruitment for the FL PPARα was unexpected, and may suggest interactions with regions outside the LBD.

Ligand-induced coactivator recruitment increases the total level of fluorescent signal for both constructs. Two of the coactivator peptides, bCBP and bPGC-1, show similar levels of recruitment for both FL and LBD constructs. bSRC-1 M2 peptide is recruited at a level ~ 5 fold greater for FL PPARα than LBD in the presence of saturating amounts of ligand (GW7647) (Figure 12). Since the previous experiments were conducted using saturating concentrations for all assay components, including coactivator peptide, the observed increase in fluorescence for the FL construct is most likely due to a favorable receptor conformation which allows a more efficient energy transfer between Eu and APC rather than an actual increase in affinity for the coactivator peptides. To rule out the possibility of increased affinity due to additional coactivator-binding sites in the N-terminus, titrations were performed for each coactivator and binding constants were determined.

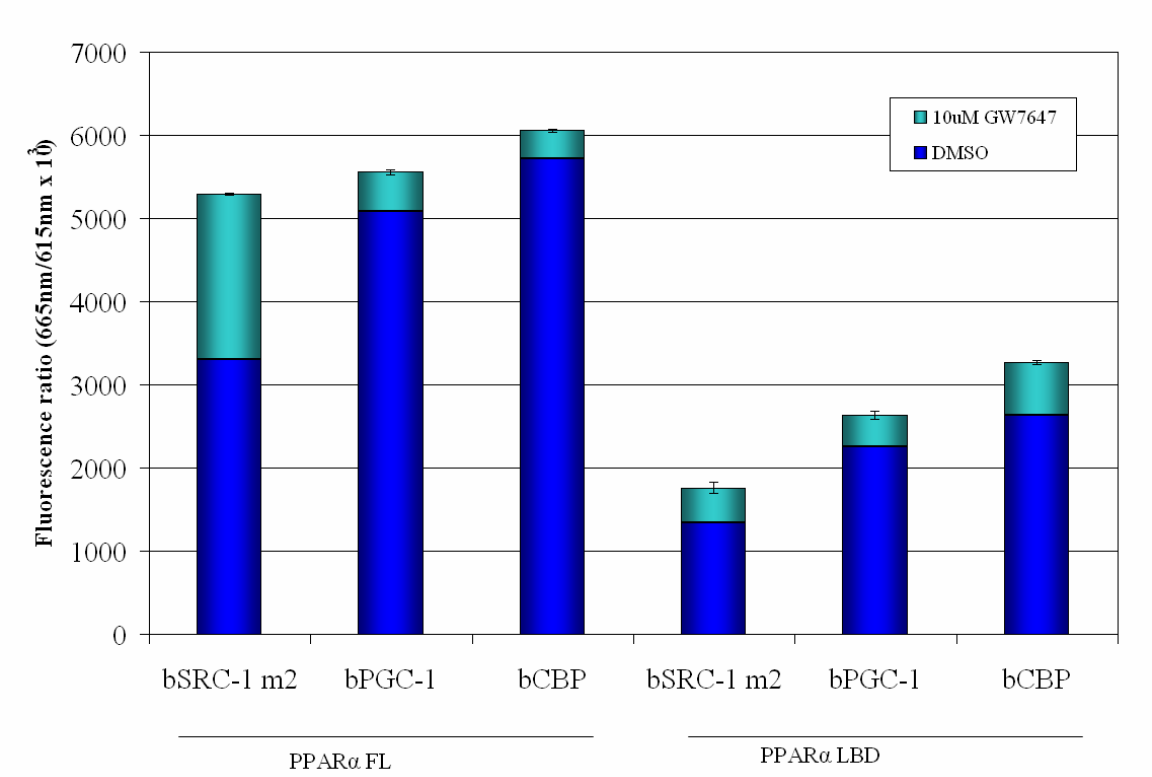

Figure 12. Levels of Constitutive and Ligand-Induced Coactivator Recruitment Obtained in Cell-Free Assays for Each Construct Using Three Different Coactivators. Each bar is the average of three or more determinations, and the error bars signify the standard deviation. The agonist employed for induction of coactivator recruitment is GW7647 at 10 μM. Each data point is the mean of a duplicate, and the error bars represent the standard deviation.

Figure 13 shows the titration of the coactivator peptide bSRC-1 M2 in the presence of the agonist GW7647 with both receptor constructs. All data sets were fit to a single site saturation equation, and the K_d determined (Table 12) The affinity of the FL receptor for bCBP is 115 nM , bPGC-1 is 83 nM and bSRC-1 M2 is 73.9 nM. These K_d values are 2- fold (bCBP and bPGC-1) and 5-fold less, respectively, than those observed for LBD receptor. The hill coefficient for all the coactivator titrations were determined to be 1, suggesting binding of only one coactivator peptide per receptor. It appears unlikely that coactivator binding is occurring in regions other than the LBD.

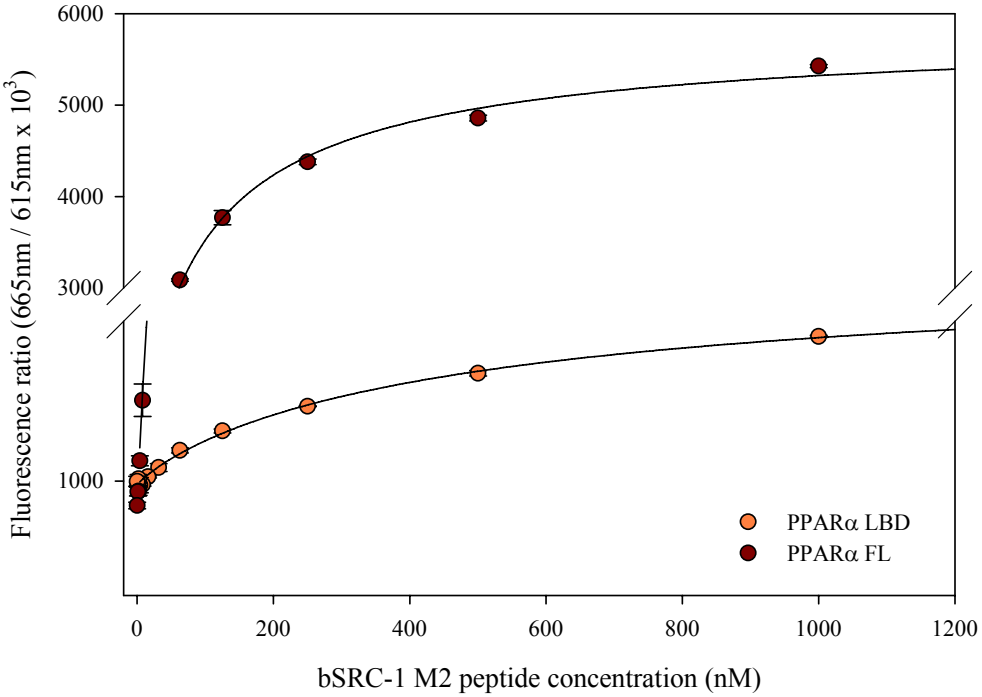

Figure 13. Change in the Fluorescence Ratio as a Function of the Coactivator Peptide bSRC-1 M2. The assay was conducted at room temperature and pH 7 under saturating conditions for Eu antibody, Streptavidin-APC and receptor. The agonist employed for induction of coactivator recruitment is GW7647 at 10 μM. Each data point is the mean of a duplicate, and the error bars represent the standard deviation.

Table 13. Equilibrium Constants for Coactivator Peptide Binding to PPARα FL and LBD.

	K_d (nM)	
Coactivator peptide	**PPARα FL**	**PPARα LBD**
bSRC-1 M2	73.9 +/- 1.4	364.5 +/- 2.7
bCBP	115.0 +/- 5.9	246.5 +/- 20.3
bPGC-1	83.0 +/- 4.6	237.6 +/- 23.5

Although there is no evidence of direct binding of our panel of coactivators to the AF-1, other coactivators have been found to not only bind directly but bind exclusively to the AF-1. A binding site for the coactivator peroxisomal enoyl-CoA hydratase/ 3-hydroxyacyl-CoA dehydrogenase (bifunctional enzyme, BFE) has been mapped to the AF-1 region of the PPARα receptor and has been found to act constitutively [293]. GST-pull down experiments performed by Juge-Aubrey *et al.* provide no evidence that coactivators involved in ligand-induced activation of PPARα , to include our panel, are also bound by the AF-1 region. This however does not exclude the need for nonspecific interaction of the obligate AF-2 coactivators with the N-terminal AF-1 domain for high affinity binding to occur, as our data suggests. It has been determined that phosphorylation of the AF-1 is required for ligand-independent coactivator recruitment for some nuclear receptors including estrogen receptor β and PPARα [294, 295]. However, other member of the PPAR family, such as PPARγ, do bind supposed ligand-dependent coactivators in the AF-1 region without the requirement of phosphorylation [296]. While the data analysis from binding experiments suggests that there are no additional binding sites for the panel of coactivators in the AF-1 domain, further investigation into potential interactions is warranted.

PPARα FL and LBD display differences in reporter gene expression

In order to determine if the difference in affinity of coactivator peptides in the HTRF assay would result in a direct effect on gene transcription levels, both constructs were analyzed in a Gal4 reporter assay. Briefly, Gal4 DBD fusions were created for both FL and LBD PPARα. Either the FL or LBD constructs were batch transfected with the

reporter vector pG5 *luc*+, containing the fire fly luciferase gene downstream from the Gal4 response element. Any observed increase in luminescence signal would be a direct result of PPARα activation. Levels of luciferase transcription, in the absence of ligand, were found to be 2-3 fold higher for the FL receptor than the LBD under similar conditions. It was also determined that the FL receptor displayed a much stronger transcriptional activation than LBD in the presence of the agonist ciprofibrate (Figure 14). The increase in transcriptional activation of FL receptor was consistent for all agonists tested, and may arise from the FL PPARα receptor assuming a more suitable conformation for assembly of enzymes and coactivators involved in transcription. Our results are similar to previous observations concerning the additive role of the mouse PPARα AF-1 domain in gene transcription [297]. The increase in transactivation may also be due in part to the increase in affinity for coactivators that was observed in the coactivator recruitment assay.

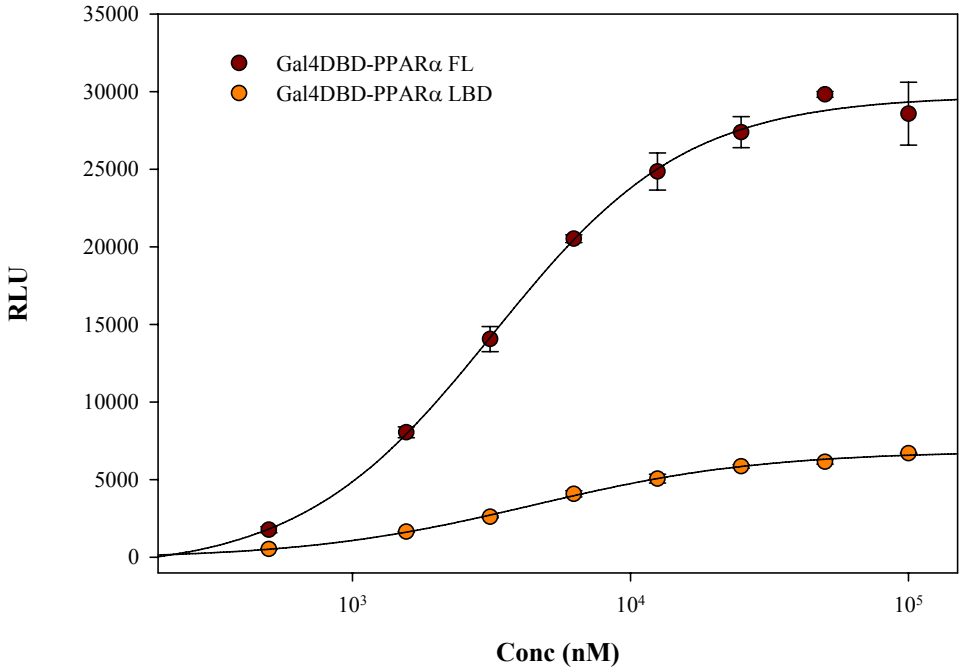

Figure 14. Change in Luminescence as a Function of the Concentration of Ciprofibrate for the Gal4DBD-PPARα LBD and FL Receptors in the Cell-Based Reporter Assay. Background luminescence was subtracted (DMSO) from each point, and contributed less than 20% of the total signal. Each data point is the mean of two determinations, and the error bars are the standard deviation.

PPARα FL and LBD show no difference in affinity for agonists

Figure 15 shows agonist titrations in the coactivator recruitment assay for both PPARα FL and LBD constructs. The figure is a good illustration of the benefit obtained from utilizing the FL receptor in the coactivator recruitment assay. In addition to achieving greater assay signal, the agonist affinity remains consistent between the two constructs. Table 14 lists K_d values in cell free and and EC_{50} values for cell based assays obtained for a panel of agonists. The data indicates that there is no significant difference in agonist K_d and EC_{50} values between constructs.

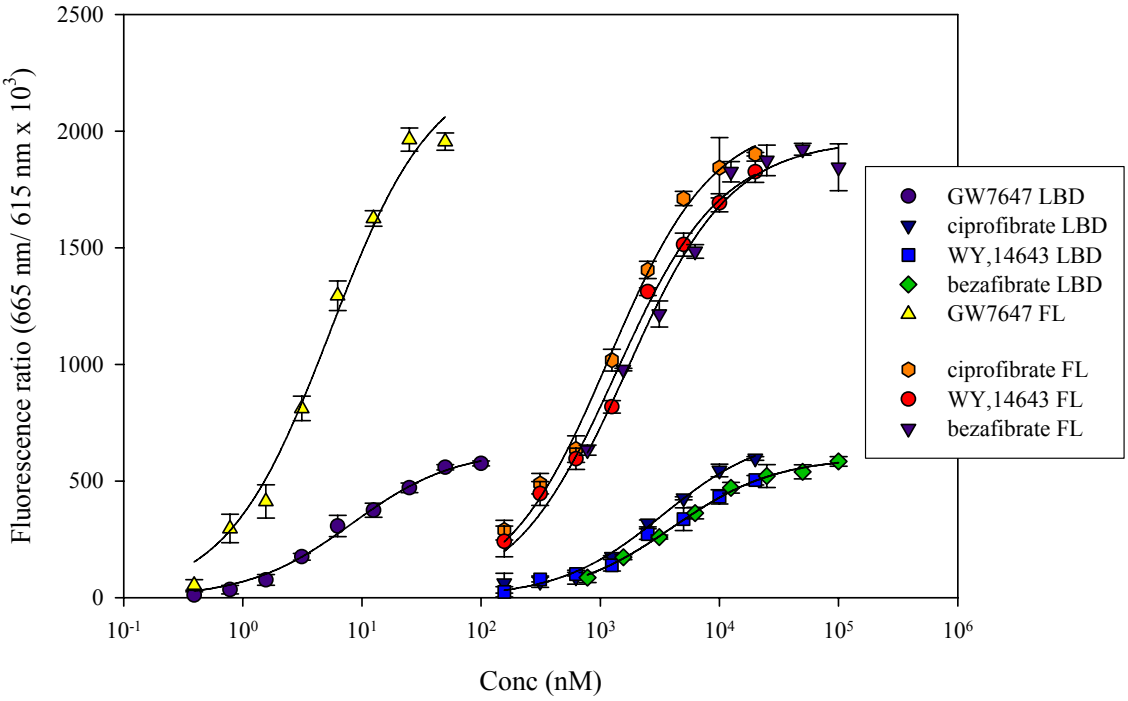

Figure 15. Change in Fluorescence as a Function of Concentration of Agonist in the Coactivator Recruitment Assay. A total of four ligands were titrated against both full length and ligand binding domain constructs. Assays were conducted under saturating conditions for all components with the exception of agonist. Coactivator peptide used in assays is bSRC-1 M2. All values corrected for background fluorescence which never exceeded 20% of the total signal. Each data point is the mean of three determinations and the error bars represent standard deviation.

Table 14. EC_{50} Values for Agonist Activity of Various Ligands Vs. PPARα FL and LBD

	Coactivator recruitment K_d (μM)		Gal4 reporter EC_{50} (μM)	
Agonist	PPARα FL	PPARα LBD	PPARα FL	PPARα LBD
ciprofibrate	1.4 ± 0.03	2.2 ± 0.14	6.9 ± 1.7	5.2 ± 1.8
WY,14643	1.6 ± 0.16	2.3 ± 0.28	15.1 ± 4.3	16.5 ± 4.4
GW7647	$4x10^{-3}$ ± 0.3	$5x10^{-3}$ ± 0.1	$2x10^{-3}$ ± 0.4	$5x10^{-3}$ ± 2.0
Bezafibrate	4.8 ± 0.4	7.2 ± - 0.8	15.4 ± 1.1	17.6 ± 9.0

In summary, PPARα FL and LBD constructs do display differences in agonist efficacy in both cell free and cell based assays. They do not, however, display differences in agonist affinity. The increase in agonist efficacy for FL PPARα is consistent for all agonists tested. In the cell free assay, FL PPARα was shown to have a higher affinity for coactivators along with significantly higher assay signal when compared to the LBD construct. Upon analysis of the data, it was determined that the increase in assay signal was not a direct result of the increased affinity for coactivators. It appears as thought FL PPARα is able to adopt a more favorable conformation for efficient energy transfer between fluorescence groups. The increased fluorescence from these conformational differences results in a more robust assay system for analyzing agonists.

The higher binding affinity for coactivators that was observed for the FL PPARα in the cell free system may explain the differences in gene expression levels between FL and LBD in the Gal4 assay system. Increased affinity for coactivators would most likely convert into increased efficiency in assembly of transcription machinery, resulting in higher levels of gene expression. Therefore, the FL PPARα construct seems to be more suitable for use in receptor assays due to the increase transcription and fluorescence signal obtained and the overall similarity to the native receptor.

References

1. Joint United Nations Programme on HIV/AIDS (2005) AIDS epidemic update, UNAIDS, Geneva.

2. N. F. Crum, R. H. Riffenburgh, S. Wegner, B. K. Agan, S. A. Tasker, K. M. Spooner, A. W. Armstrong, S. Fraser, and M. R. Wallace, Comparisons of causes of death and mortality rates among HIV-infected persons: analysis of the pre-, early, and late HAART (highly active antiretroviral therapy) eras, J Acquir Immune Defic Syndr 41 (2006) 194-200.

3. F. J. Palella, Jr., K. M. Delaney, A. C. Moorman, M. O. Loveless, J. Fuhrer, G. A. Satten, D. J. Aschman, and S. D. Holmberg, Declining morbidity and mortality among patients with advanced human immunodeficiency virus infection. HIV Outpatient Study Investigators, N Engl J Med 338 (1998) 853-860.

4. R. D. Moore, and R. E. Chaisson, Natural history of HIV infection in the era of combination antiretroviral therapy, Aids 13 (1999) 1933-1942.

5. Z. Temesgen, D. Warnke, and M. J. Kasten, Current status of antiretroviral therapy, Expert Opin Pharmacother 7 (2006) 1541-1554.

6. K. E. Squires, An introduction to nucleoside and nucleotide analogues, Antivir Ther 6 Suppl 3 (2001) 1-14.

7. P. L. Sharma, V. Nurpeisov, B. Hernandez-Santiago, T. Beltran, and R. F. Schinazi, Nucleoside inhibitors of human immunodeficiency virus type 1 reverse transcriptase, Curr Top Med Chem 4 (2004) 895-919.

8. A. S. Ray, Intracellular interactions between nucleos(t)ide inhibitors of HIV reverse transcriptase, AIDS Rev 7 (2005) 113-125.

9. V. Idemyor, Human immunodeficiency viruses and drug therapy: resistance and implications for antiretroviral therapy, Pharmacotherapy 22 (2002) 659-662.

10. J. Balzarini, Current status of the non-nucleoside reverse transcriptase inhibitors of human immunodeficiency virus type 1, Curr Top Med Chem 4 (2004) 921-944.

11. M. Gotte, Inhibition of HIV-1 reverse transcription: basic principles of drug action and resistance, Expert Rev Anti Infect Ther 2 (2004) 707-716.

12. B. Dauer, Protease inhibitors: the current status, J HIV Ther 10 (2005) 72-74.

13. T. Robins, and J. Plattner, HIV protease inhibitors: their anti-HIV activity and potential role in treatment, J Acquir Immune Defic Syndr 6 (1993) 162-170.

14. T. D. Meek, Inhibitors of HIV-1 protease, J Enzyme Inhib 6 (1992) 65-98.

15. D. S. Schiller, Identification, management, and prevention of adverse effects associated with highly active antiretroviral therapy, Am J Health Syst Pharm 61 (2004) 2507-2522.

16. A. d'Arminio Monforte, A. C. Lepri, G. Rezza, P. Pezzotti, A. Antinori, A. N. Phillips, G. Angarano, V. Colangeli, A. De Luca, G. Ippolito, L. Caggese, F. Soscia, G. Filice, F. Gritti, P. Narciso, U. Tirelli, and M. Moroni, Insights into the reasons for discontinuation of the first highly active antiretroviral therapy (HAART) regimen in a cohort of antiretroviral naive patients. I.CO.N.A. Study Group. Italian Cohort of Antiretroviral-Naive Patients, Aids 14 (2000) 499-507.

17. V. Montessori, N. Press, M. Harris, L. Akagi, and J. S. Montaner, Adverse effects of antiretroviral therapy for HIV infection, Cmaj 170 (2004) 229-238.

18. A. Carr, K. Samaras, S. Burton, M. Law, J. Freund, D. J. Chisholm, and D. A. Cooper, A syndrome of peripheral lipodystrophy, hyperlipidaemia and insulin resistance in patients receiving HIV protease inhibitors, Aids 12 (1998) F51-58.

19. A. Balasubramanyam, R. V. Sekhar, F. Jahoor, P. H. Jones, and H. J. Pownall, Pathophysiology of dyslipidemia and increased cardiovascular risk in HIV lipodystrophy: a model of 'systemic steatosis', Curr Opin Lipidol 15 (2004) 59-67.

20. A. Carr, K. Samaras, D. J. Chisholm, and D. A. Cooper, Abnormal fat distribution and use of protease inhibitors, Lancet 351 (1998) 1736.

21. C. A. Wanke, Epidemiological and clinical aspects of the metabolic complications of HIV infection the fat redistribution syndrome, Aids 13 (1999) 1287-1293.

22. M. J. Glesby, Coronary heart disease in HIV-infected patients, Curr HIV/AIDS Rep 2 (2005) 68-73.

23. G. M. Behrens, D. Meyer-Olson, M. Stoll, and R. E. Schmidt, Clinical impact of HIV-related lipodystrophy and metabolic abnormalities on cardiovascular disease, Aids 17 Suppl 1 (2003) S149-154.

24. B. Salehian, J. Bilas, M. Bazargan, and M. Abbasian, Prevalence and incidence of diabetes in HIV-infected minority patients on protease inhibitors, J Natl Med Assoc 97 (2005) 1088-1092.

25. R. L. Hengel, N. B. Watts, and J. L. Lennox, Benign symmetric lipomatosis associated with protease inhibitors, Lancet 350 (1997) 1596.

26. K. K. Miller, P. A. Daly, D. Sentochnik, J. Doweiko, M. Samore, N. O. Basgoz, and S. K. Grinspoon, Pseudo-Cushing's syndrome in human immunodeficiency virus-infected patients, Clin Infect Dis 27 (1998) 68-72.

27. D. N. Stocker, P. J. Meier, R. Stoller, and K. E. Fattinger, "Buffalo hump" in HIV-1 infection, Lancet 352 (1998) 320-321.

28. R. Viraben, and C. Aquilina, Indinavir-associated lipodystrophy, Aids 12 (1998) F37-39.

29. A. Marin, J. L. Casado, L. Aranzabal, J. Moya, A. Antela, F. Dronda, A. Moreno, and S. Moreno, Validation of a Specific Questionnaire on Psychological and Social Repercussions of the Lipodystrophy Syndrome in HIV-infected Patients, Qual Life Res 15 (2006) 767-775.

30. C. P. Santos, Y. X. Felipe, P. E. Braga, D. Ramos, R. O. Lima, and A. C. Segurado, Self-perception of body changes in persons living with HIV/AIDS: prevalence and associated factors, Aids 19 Suppl 4 (2005) S14-21.

31. S. Duran, M. Saves, B. Spire, V. Cailleton, A. Sobel, P. Carrieri, D. Salmon, J. P. Moatti, and C. Leport, Failure to maintain long-term adherence to highly active antiretroviral therapy: the role of lipodystrophy, Aids 15 (2001) 2441-2444.

32. P. Bjorntorp, Metabolic implications of body fat distribution, Diabetes Care 14 (1991) 1132-1143.

33. F. H. Einstein, G. Atzmon, X. M. Yang, X. H. Ma, M. Rincon, E. Rudin, R. Muzumdar, and N. Barzilai, Differential responses of visceral and subcutaneous fat depots to nutrients, Diabetes 54 (2005) 672-678.

34. N. Barzilai, L. She, B. Q. Liu, P. Vuguin, P. Cohen, J. Wang, and L. Rossetti, Surgical removal of visceral fat reverses hepatic insulin resistance, Diabetes 48 (1999) 94-98.

35. A. M. Gotto, G. A. Gorry, J. R. Thompson, J. S. Cole, R. Trost, D. Yeshurun, and M. E. DeBakey, Relationship between plasma lipid concentrations and coronary artery disease in 496 patients, Circulation 56 (1977) 875-883.

36. P. Linsel-Nitschke, and A. R. Tall, HDL as a target in the treatment of atherosclerotic cardiovascular disease, Nat Rev Drug Discov 4 (2005) 193-205.

37. T. Kita, N. Kume, M. Minami, K. Hayashida, T. Murayama, H. Sano, H. Moriwaki, H. Kataoka, E. Nishi, H. Horiuchi, H. Arai, and M. Yokode, Role of oxidized LDL in atherosclerosis, Ann N Y Acad Sci 947 (2001) 199-205; discussion 205-196.

38. F. M. Sacks, The role of high-density lipoprotein (HDL) cholesterol in the prevention and treatment of coronary heart disease: expert group recommendations, Am J Cardiol 90 (2002) 139-143.

39. J. Y. Lee, and J. S. Parks, ATP-binding cassette transporter AI and its role in HDL formation, Curr Opin Lipidol 16 (2005) 19-25.

40. S. E. Nissen, T. Tsunoda, E. M. Tuzcu, P. Schoenhagen, C. J. Cooper, M. Yasin, G. M. Eaton, M. A. Lauer, W. S. Sheldon, C. L. Grines, S. Halpern, T. Crowe, J. C. Blankenship, and R. Kerensky, Effect of recombinant ApoA-I Milano on coronary atherosclerosis in patients with acute coronary syndromes: a randomized controlled trial, Jama 290 (2003) 2292-2300.

41. R. K. Tangirala, K. Tsukamoto, S. H. Chun, D. Usher, E. Pure, and D. J. Rader, Regression of atherosclerosis induced by liver-directed gene transfer of apolipoprotein A-I in mice, Circulation 100 (1999) 1816-1822.

42. A. M. Sanchez Torres, R. Munoz Muniz, R. Madero, C. Borque, M. J. Garcia-Miguel, and M. I. De Jose Gomez, Prevalence of fat redistribution and metabolic disorders in human immunodeficiency virus-infected children, Eur J Pediatr 164 (2005) 271-276.

43. S. Safrin, and C. Grunfeld, Fat distribution and metabolic changes in patients with HIV infection, Aids 13 (1999) 2493-2505.

44. L. Calza, R. Manfredi, and F. Chiodo, Hyperlipidaemia in patients with HIV-1 infection receiving highly active antiretroviral therapy: epidemiology, pathogenesis, clinical course and management, Int J Antimicrob Agents 22 (2003) 89-99.

45. C. J. Smith, and C. A. Sabin, The problems faced when assessing the prevalence and incidence of antiretroviral-related toxicities, Antivir Ther 9 (2004) 865-878.

46. D. Chen, A. Misra, and A. Garg, Clinical review 153: Lipodystrophy in human immunodeficiency virus-infected patients, J Clin Endocrinol Metab 87 (2002) 4845-4856.

47. E. Martinez, A. Mocroft, M. A. Garcia-Viejo, J. B. Perez-Cuevas, J. L. Blanco, J. Mallolas, L. Bianchi, I. Conget, J. Blanch, A. Phillips, and J. M. Gatell, Risk of lipodystrophy in HIV-1-infected patients treated with protease inhibitors: a prospective cohort study, Lancet 357 (2001) 592-598.

48. K. A. Lichtenstein, D. J. Ward, A. C. Moorman, K. M. Delaney, B. Young, F. J. Palella, Jr., P. H. Rhodes, K. C. Wood, and S. D. Holmberg, Clinical assessment of HIV-associated lipodystrophy in an ambulatory population, Aids 15 (2001) 1389-1398.

49. R. Thiebaut, V. Daucourt, P. Mercie, D. K. Ekouevi, D. Malvy, P. Morlat, M. Dupon, D. Neau, S. Farbos, C. Marimoutou, and F. Dabis, Lipodystrophy, metabolic disorders, and human immunodeficiency virus infection: Aquitaine Cohort, France, 1999. Groupe d'Epidemiologie Clinique du Syndrome d'Immunodeficience Acquise en Aquitaine, Clin Infect Dis 31 (2000) 1482-1487.

50. P. Bonfanti, C. Gulisano, E. Ricci, L. Timillero, L. Valsecchi, S. Carradori, L. Pusterla, P. Fortuna, S. Miccolis, C. Magnani, A. Gabbuti, F. Parazzini, C. Martinelli, I. Faggion, S. Landonio, T. Quirino, and G. Vigevani, Risk factors for lipodystrophy in the CISAI cohort, Biomed Pharmacother 57 (2003) 422-427.

51. E. Negredo, R. Paredes, A. Bonjoch, A. Tuldra, C. R. Fumaz, S. Gel, B. Garces, S. Johnston, A. Arno, M. Balague, A. Jou, C. Tural, G. Sirera, J. Romeu, L. Cruz, E. Francia, P. Domingo, J. Arrizabalaga, I. Ruiz, J. R. Arribas, L. Ruiz, and B. Clotet, Benefit of switching from a protease inhibitor (PI) to nevirapine in PI-experienced patients suffering acquired HIV-related lipodystrophy syndrome (AHL): interim analysis at 3 months of follow-up, Antivir Ther 4 Suppl 3 (1999) 23-28.

52. C. Fisac, E. Fumero, M. Crespo, B. Roson, E. Ferrer, N. Virgili, E. Ribera, J. M. Gatell, and D. Podzamczer, Metabolic benefits 24 months after replacing a protease inhibitor with abacavir, efavirenz or nevirapine, Aids 19 (2005) 917-925.

53. J. A. Arranz Caso, J. C. Lopez, I. Santos, V. Estrada, V. Castilla, J. Sanz, J. P. Molina, M. Fernandez Guerrero, and M. Gorgolas, A randomized controlled trial investigating the efficacy and safety of switching from a protease inhibitor to nevirapine in patients with undetectable viral load, HIV Med 6 (2005) 353-359.

54. M. A. Noor, R. A. Parker, E. O'Mara, D. M. Grasela, A. Currie, S. L. Hodder, F. T. Fiedorek, and D. W. Haas, The effects of HIV protease inhibitors atazanavir and lopinavir/ritonavir on insulin sensitivity in HIV-seronegative healthy adults, Aids 18 (2004) 2137-2144.

55. V. Puro, Effect of short-course of antiretroviral agents on serum triglycerides of healthy individuals, Aids 14 (2000) 2407-2408.

56. S. Tsiodras, C. Mantzoros, S. Hammer, and M. Samore, Effects of protease inhibitors on hyperglycemia, hyperlipidemia, and lipodystrophy: a 5-year cohort study, Arch Intern Med 160 (2000) 2050-2056.

57. G. Haerter, B. J. Manfras, M. Mueller, P. Kern, and A. Trein, Regression of lipodystrophy in HIV-infected patients under therapy with the new protease inhibitor atazanavir, Aids 18 (2004) 952-955.

58. B. G. Gazzard, and G. Moyle, Does atazanavir cause lipodystrophy?, J HIV Ther 9 (2004) 41-44.

59. S. A. Riddler, E. Smit, S. R. Cole, R. Li, J. S. Chmiel, A. Dobs, F. Palella, B. Visscher, R. Evans, and L. A. Kingsley, Impact of HIV infection and HAART on serum lipids in men, JAMA 289 (2003) 2978-2982.

60. B. F. Asztalos, E. J. Schaefer, K. V. Horvath, C. E. Cox, S. Skinner, J. Gerrior, S. L. Gorbach, and C. Wanke, Protease inhibitor-based HAART, HDL, and CHD-risk in HIV-infected patients, Atherosclerosis 184 (2006) 72-77.

61. J. M. Leitner, H. Pernerstorfer-Schoen, A. Weiss, K. Schindler, A. Rieger, and B. Jilma, Age and sex modulate metabolic and cardiovascular risk markers of patients after 1 year of highly active antiretroviral therapy (HAART), Atherosclerosis 187 (2006) 177-185.

62. M. Galli, F. Veglia, G. Angarano, S. Santambrogio, E. Meneghini, F. Gritti, A. Cargnel, F. Mazzotta, and A. Lazzarin, Gender differences in antiretroviral drug-related adipose tissue alterations. Women are at higher risk than men and develop particular lipodystrophy patterns, J Acquir Immune Defic Syndr 34 (2003) 58-61.

63. C. Gervasoni, A. L. Ridolfo, G. Trifiro, S. Santambrogio, G. Norbiato, M. Musicco, M. Clerici, M. Galli, and M. Moroni, Redistribution of body fat in HIV-infected women undergoing combined antiretroviral therapy, Aids 13 (1999) 465-471.

64. T. Saint-Marc, M. Partisani, I. Poizot-Martin, F. Bruno, O. Rouviere, J. M. Lang, J. A. Gastaut, and J. L. Touraine, A syndrome of peripheral fat wasting (lipodystrophy) in patients receiving long-term nucleoside analogue therapy, Aids 13 (1999) 1659-1667.

65. S. A. Mallal, M. John, C. B. Moore, I. R. James, and E. J. McKinnon, Contribution of nucleoside analogue reverse transcriptase inhibitors to subcutaneous fat wasting in patients with HIV infection, Aids 14 (2000) 1309-1316.

66. A. Carr, J. Miller, M. Law, and D. A. Cooper, A syndrome of lipoatrophy, lactic acidaemia and liver dysfunction associated with HIV nucleoside analogue therapy: contribution to protease inhibitor-related lipodystrophy syndrome, Aids 14 (2000) F25-32.

67. A. M. Martin, E. Hammond, D. Nolan, C. Pace, M. Den Boer, L. Taylor, H. Moore, O. P. Martinez, F. T. Christiansen, and S. Mallal, Accumulation of mitochondrial DNA mutations in human immunodeficiency virus-infected patients treated with nucleoside-analogue reverse-transcriptase inhibitors, Am J Hum Genet 72 (2003) 549-560.

68. K. Brinkman, J. A. Smeitink, J. A. Romijn, and P. Reiss, Mitochondrial toxicity induced by nucleoside-analogue reverse-transcriptase inhibitors is a key factor in the pathogenesis of antiretroviral-therapy-related lipodystrophy, Lancet 354 (1999) 1112-1115.

69. T. Klopstock, M. Naumann, B. Schalke, F. Bischof, P. Seibel, M. Kottlors, P. Eckert, K. Reiners, K. Toyka, and H. Reichmann, Multiple symmetric lipomatosis: abnormalities in complex IV and multiple deletions in mitochondrial DNA, Neurology 44 (1994) 862-866.

70. T. Klopstock, M. Naumann, P. Seibel, B. Shalke, K. Reiners, and H. Reichmann, Mitochondrial DNA mutations in multiple symmetric lipomatosis, Mol Cell Biochem 174 (1997) 271-275.

71. D. Y. Hui, Effects of HIV protease inhibitor therapy on lipid metabolism, Prog Lipid Res 42 (2003) 81-92.

72. A. Rudich, R. Ben-Romano, S. Etzion, and N. Bashan, Cellular mechanisms of insulin resistance, lipodystrophy and atherosclerosis induced by HIV protease inhibitors, Acta Physiol Scand 183 (2005) 75-88.

73. J. Hertel, H. Struthers, C. B. Horj, and P. W. Hruz, A structural basis for the acute effects of HIV protease inhibitors on GLUT4 intrinsic activity, J Biol Chem 279 (2004) 55147-55152.

74. M. Ver, Hu Chen, Michael Quon, Insulin Signaling Pathways Regulating Translocation of GLUT4, Current Medicinal Chemistry - Immun., Endoc. & Metab. Agents 5 (2005) 159-165.

75. M. Ishiki, and A. Klip, Minireview: recent developments in the regulation of glucose transporter-4 traffic: new signals, locations, and partners, Endocrinology 146 (2005) 5071-5078.

76. R. Ben-Romano, A. Rudich, D. Torok, S. Vanounou, K. Riesenberg, F. Schlaeffer, A. Klip, and N. Bashan, Agent and cell-type specificity in the induction of insulin resistance by HIV protease inhibitors, Aids 17 (2003) 23-32.

77. H. Murata, P. W. Hruz, and M. Mueckler, Investigating the cellular targets of HIV protease inhibitors: implications for metabolic disorders and improvements in drug therapy, Curr Drug Targets Infect Disord 2 (2002) 1-8.

78. H. Murata, P. W. Hruz, and M. Mueckler, Indinavir inhibits the glucose transporter isoform Glut4 at physiologic concentrations, Aids 16 (2002) 859-863.

79. G. Walldius, I. Jungner, A. H. Aastveit, I. Holme, C. D. Furberg, and A. D. Sniderman, The apoB/apoA-I ratio is better than the cholesterol ratios to estimate the balance between plasma proatherogenic and antiatherogenic lipoproteins and to predict coronary risk, Clin Chem Lab Med 42 (2004) 1355-1363.

80. T. M. Riddle, N. M. Schildmeyer, C. Phan, C. J. Fichtenbaum, and D. Y. Hui, The HIV protease inhibitor ritonavir increases lipoprotein production and has no effect on lipoprotein clearance in mice, J Lipid Res 43 (2002) 1458-1463.

81. J. M. Petit, M. Duong, E. Florentin, L. Duvillard, P. Chavanet, J. M. Brun, H. Portier, P. Gambert, and B. Verges, Increased VLDL-apoB and IDL-apoB production rates in nonlipodystrophic HIV-infected patients on a protease inhibitor-containing regimen: a stable isotope kinetic study, J Lipid Res 44 (2003) 1692-1697.

82. M. Schmitz, G. M. Michl, R. Walli, J. Bogner, A. Bedynek, D. Seidel, F. D. Goebel, and T. Demant, Alterations of apolipoprotein B metabolism in HIV-infected patients with antiretroviral combination therapy, J Acquir Immune Defic Syndr 26 (2001) 225-235.

83. A. M. Umpleby, S. Das, M. Stolinski, F. Shojaee-Moradie, N. C. Jackson, W. Jefferson, N. Crabtree, P. Nightingale, and M. Shahmanesh, Low density lipoprotein apolipoprotein B metabolism in treatment-naive HIV patients and patients on antiretroviral therapy, Antivir Ther 10 (2005) 663-670.

84. J. M. Petit, M. Duong, L. Duvillard, E. Florentin, H. Portier, G. Lizard, J. M. Brun, P. Gambert, and B. Verges, LDL-receptors expression in HIV-infected patients: relations to antiretroviral therapy, hormonal status, and presence of lipodystrophy, Eur J Clin Invest 32 (2002) 354-359.

85. S. Das, M. Shahmanesh, M. Stolinski, F. Shojaee-Moradie, W. Jefferson, N. C. Jackson, M. Cobbold, P. Nightingale, and A. M. Umpleby, In treatment-naive and antiretroviral-treated subjects with HIV, reduced plasma adiponectin is associated with a reduced fractional clearance rate of VLDL, IDL and LDL apolipoprotein B-100, Diabetologia 49 (2006) 538-542.

86. J. S. Liang, O. Distler, D. A. Cooper, H. Jamil, R. J. Deckelbaum, H. N. Ginsberg, and S. L. Sturley, HIV protease inhibitors protect apolipoprotein B from degradation by the proteasome: a potential mechanism for protease inhibitor-induced hyperlipidemia, Nat Med 7 (2001) 1327-1331.

87. J. D. Horton, J. L. Goldstein, and M. S. Brown, SREBPs: activators of the complete program of cholesterol and fatty acid synthesis in the liver, J Clin Invest 109 (2002) 1125-1131.

88. T. M. Riddle, D. G. Kuhel, L. A. Woollett, C. J. Fichtenbaum, and D. Y. Hui, HIV protease inhibitor induces fatty acid and sterol biosynthesis in liver and adipose tissues due to the accumulation of activated sterol regulatory element-binding proteins in the nucleus, J Biol Chem 276 (2001) 37514-37519.

89. M. Bochtler, L. Ditzel, M. Groll, C. Hartmann, and R. Huber, The proteasome, Annu Rev Biophys Biomol Struct 28 (1999) 295-317.

90. P. Andre, M. Groettrup, P. Klenerman, R. de Giuli, B. L. Booth, Jr., V. Cerundolo, M. Bonneville, F. Jotereau, R. M. Zinkernagel, and V. Lotteau, An inhibitor of HIV-1 protease modulates proteasome activity, antigen presentation, and T cell responses, Proc Natl Acad Sci U S A 95 (1998) 13120-13124.

91. I. Shimomura, R. E. Hammer, J. A. Richardson, S. Ikemoto, Y. Bashmakov, J. L. Goldstein, and M. S. Brown, Insulin resistance and diabetes mellitus in transgenic mice expressing nuclear SREBP-1c in adipose tissue: model for congenital generalized lipodystrophy, Genes Dev 12 (1998) 3182-3194.

92. R. K. Zeldin, and R. A. Petruschke, Pharmacological and therapeutic properties of ritonavir-boosted protease inhibitor therapy in HIV-infected patients, J Antimicrob Chemother 53 (2004) 4-9.

93. U. S. Justesen, Therapeutic drug monitoring and human immunodeficiency virus (HIV) antiretroviral therapy, Basic Clin Pharmacol Toxicol 98 (2006) 20-31.

94. J. Newell-Price, X. Bertagna, A. B. Grossman, and L. K. Nieman, Cushing's syndrome, Lancet 367 (2006) 1605-1617.

95. P. M. Stewart, Tissue-specific Cushing's syndrome uncovers a new target in treating the metabolic syndrome--11beta-hydroxysteroid dehydrogenase type 1, Clin Med 5 (2005) 142-146.

96. P. M. Stewart, and Z. S. Krozowski, 11 beta-Hydroxysteroid dehydrogenase, Vitam Horm 57 (1999) 249-324.

97. D. N. Brindley, Role of glucocorticoids and fatty acids in the impairment of lipid metabolism observed in the metabolic syndrome, Int J Obes Relat Metab Disord 19 Suppl 1 (1995) S69-75.

98. C. B. Whorwood, J. A. Franklyn, M. C. Sheppard, and P. M. Stewart, Tissue localization of 11 beta-hydroxysteroid dehydrogenase and its relationship to the glucocorticoid receptor, J Steroid Biochem Mol Biol 41 (1992) 21-28.

99. I. J. Bujalska, S. Kumar, and P. M. Stewart, Does central obesity reflect "Cushing's disease of the omentum"?, Lancet 349 (1997) 1210-1213.

100. E. Rask, B. R. Walker, S. Soderberg, D. E. Livingstone, M. Eliasson, O. Johnson, R. Andrew, and T. Olsson, Tissue-specific changes in peripheral cortisol metabolism in obese women: increased adipose 11beta-hydroxysteroid dehydrogenase type 1 activity, J Clin Endocrinol Metab 87 (2002) 3330-3336.

101. H. Masuzaki, J. Paterson, H. Shinyama, N. M. Morton, J. J. Mullins, J. R. Seckl, and J. S. Flier, A transgenic model of visceral obesity and the metabolic syndrome, Science 294 (2001) 2166-2170.

102. J. Sutinen, K. Kannisto, E. Korsheninnikova, T. Nyman, E. Ehrenborg, R. Andrew, D. J. Wake, A. Hamsten, B. R. Walker, and H. Yki-Jarvinen, In the lipodystrophy associated with highly active antiretroviral therapy, pseudo-Cushing's syndrome is associated with increased regeneration of cortisol by 11beta-hydroxysteroid dehydrogenase type 1 in adipose tissue, Diabetologia 47 (2004) 1668-1671.

103. J. C. Krause, M. P. Toye, B. W. Stechenberg, E. O. Reiter, and H. F. Allen, HIV--associated lipodystrophy in children, Pediatr Endocrinol Rev 3 (2005) 45-51.

104. R. A. Hegele, and R. L. Pollex, Genetic and physiological insights into the metabolic syndrome, Am J Physiol Regul Integr Comp Physiol 289 (2005) R663-669.

105. J. M. Wentworth, T. P. Burris, and V. K. Chatterjee, HIV protease inhibitors block human preadipocyte differentiation, but not via the PPARgamma/RXR heterodimer, J Endocrinol 164 (2000) R7-R10.

106. B. Zhang, K. MacNaul, D. Szalkowski, Z. Li, J. Berger, and D. E. Moller, Inhibition of adipocyte differentiation by HIV protease inhibitors, J Clin Endocrinol Metab 84 (1999) 4274-4277.

107. J. M. Lenhard, E. S. Furfine, R. G. Jain, O. Ittoop, L. A. Orband-Miller, S. G. Blanchard, M. A. Paulik, and J. E. Weiel, HIV protease inhibitors block adipogenesis and increase lipolysis in vitro, Antiviral Res 47 (2000) 121-129.

108. S. Ranganathan, and P. A. Kern, The HIV protease inhibitor saquinavir impairs lipid metabolism and glucose transport in cultured adipocytes, J Endocrinol 172 (2002) 155-162.

109. T. Feldt, M. Oette, A. Kroidl, K. Goebels, R. Fritzen, J. Kambergs, G. Kappert, C. Vogt, M. Wettstein, and D. Haussinger, Evaluation of Safety and Efficacy of Rosiglitazone in the Treatment of HIV-Associated Lipodystrophy Syndrome, Infection 34 (2006) 55-61.

110. A. M. Naar, B. D. Lemon, and R. Tjian, Transcriptional coactivator complexes, Annu Rev Biochem 70 (2001) 475-501.

111. B. M. Spiegelman, and R. Heinrich, Biological control through regulated transcriptional coactivators, Cell 119 (2004) 157-167.

112. V. Giguere, Orphan nuclear receptors: from gene to function, Endocr Rev 20 (1999) 689-725.

113. N. L. Weigel, Steroid hormone receptors and their regulation by phosphorylation, Biochem J 319 (Pt 3) (1996) 657-667.

114. V. Giguere, N. Yang, P. Segui, and R. M. Evans, Identification of a new class of steroid hormone receptors, Nature 331 (1988) 91-94.

115. T. Burris, and E. McCabe (Eds.) (2001) Nuclear Receptors and Genetic Disease, Academic Press, Academic Press, San Diego.

116. A unified nomenclature system for the nuclear receptor superfamily, Cell 97 (1999) 161-163.

117. A. Aranda, and A. Pascual, Nuclear hormone receptors and gene expression, Physiol Rev 81 (2001) 1269-1304.

118. A. Warnmark, E. Treuter, A. P. Wright, and J. A. Gustafsson, Activation functions 1 and 2 of nuclear receptors: molecular strategies for transcriptional activation, Mol Endocrinol 17 (2003) 1901-1909.

119. D. N. Lavery, and I. J. McEwan, Structure and function of steroid receptor AF1 transactivation domains: induction of active conformations, Biochem J 391 (2005) 449-464.

120. R. Kumar, and E. B. Thompson, Transactivation functions of the N-terminal domains of nuclear hormone receptors: protein folding and coactivator interactions, Mol Endocrinol 17 (2003) 1-10.

121. D. Picard, Chaperoning steroid hormone action, Trends Endocrinol Metab 17 (2006) 229-235.

122. N. J. McKenna, R. B. Lanz, and B. W. O'Malley, Nuclear receptor coregulators: cellular and molecular biology, Endocr Rev 20 (1999) 321-344.

123. M. Ptashne, and A. A. Gann, Activators and targets, Nature 346 (1990) 329-331.

124. D. M. Lonard, and B. W. O'Malley, The expanding cosmos of nuclear receptor coactivators, Cell 125 (2006) 411-414.

125. D. M. Lonard, and B. W. O'Malley, Expanding functional diversity of the coactivators, Trends Biochem Sci 30 (2005) 126-132.

126. M. R. Stallcup, J. H. Kim, C. Teyssier, Y. H. Lee, H. Ma, and D. Chen, The roles of protein-protein interactions and protein methylation in transcriptional activation by nuclear receptors and their coactivators, J Steroid Biochem Mol Biol 85 (2003) 139-145.

127. E. M. McInerney, D. W. Rose, S. E. Flynn, S. Westin, T. M. Mullen, A. Krones, J. Inostroza, J. Torchia, R. T. Nolte, N. Assa-Munt, M. V. Milburn, C. K. Glass, and M. G. Rosenfeld, Determinants of coactivator LXXLL motif specificity in nuclear receptor transcriptional activation, Genes Dev 12 (1998) 3357-3368.

128. Z. Wu, K. O. Martin, N. B. Javitt, and J. Y. Chiang, Structure and functions of human oxysterol 7alpha-hydroxylase cDNAs and gene CYP7B1, J Lipid Res 40 (1999) 2195-2203.

129. S. Misiti, L. Schomburg, P. M. Yen, and W. W. Chin, Expression and hormonal regulation of coactivator and corepressor genes, Endocrinology 139 (1998) 2493-2500.

130. P. Puigserver, Tissue-specific regulation of metabolic pathways through the transcriptional coactivator PGC1-alpha, Int J Obes (Lond) 29 Suppl 1 (2005) S5-9.

131. H. Pilegaard, T. Osada, L. T. Andersen, J. W. Helge, B. Saltin, and P. D. Neufer, Substrate availability and transcriptional regulation of metabolic genes in human skeletal muscle during recovery from exercise, Metabolism 54 (2005) 1048-1055.

132. I. U. Agoulnik, A. Vaid, W. E. Bingman, 3rd, H. Erdeme, A. Frolov, C. L. Smith, G. Ayala, M. M. Ittmann, and N. L. Weigel, Role of SRC-1 in the promotion of prostate cancer cell growth and tumor progression, Cancer Res 65 (2005) 7959-7967.

133. M. T. Tilli, R. Reiter, A. S. Oh, R. T. Henke, K. McDonnell, G. I. Gallicano, P. A. Furth, and A. T. Riegel, Overexpression of an N-terminally truncated isoform of the nuclear receptor coactivator amplified in breast cancer 1 leads to altered proliferation of mammary epithelial cells in transgenic mice, Mol Endocrinol 19 (2005) 644-656.

134. S. Misiti, N. Koibuchi, M. Bei, A. Farsetti, and W. W. Chin, Expression of steroid receptor coactivator-1 mRNA in the developing mouse embryo: a possible role in olfactory epithelium development, Endocrinology 140 (1999) 1957-1960.

135. L. C. Murphy, S. L. Simon, A. Parkes, E. Leygue, H. Dotzlaw, L. Snell, S. Troup, A. Adeyinka, and P. H. Watson, Altered expression of estrogen receptor coregulators during human breast tumorigenesis, Cancer Res 60 (2000) 6266-6271.

136. H. Gronemeyer, Control of transcription activation by steroid hormone receptors, Faseb J 6 (1992) 2524-2529.

137. B. M. Jaber, R. Mukopadhyay, and C. L. Smith, Estrogen receptor-alpha interaction with the CREB binding protein coactivator is regulated by the cellular environment, J Mol Endocrinol 32 (2004) 307-323.

138. C. M. Klinge, S. C. Jernigan, K. A. Mattingly, K. E. Risinger, and J. Zhang, Estrogen response element-dependent regulation of transcriptional activation of estrogen receptors alpha and beta by coactivators and corepressors, J Mol Endocrinol 33 (2004) 387-410.

139. F. Blaschke, Y. Takata, E. Caglayan, R. E. Law, and W. A. Hsueh, Obesity, peroxisome proliferator-activated receptor, and atherosclerosis in type 2 diabetes, Arterioscler Thromb Vasc Biol 26 (2006) 28-40.

140. B. Pourcet, J. C. Fruchart, B. Staels, and C. Glineur, Selective PPAR modulators, dual and pan PPAR agonists: multimodal drugs for the treatment of type 2 diabetes and atherosclerosis, Expert Opin Emerg Drugs 11 (2006) 379-401.

141. P. Zimmet, D. Magliano, Y. Matsuzawa, G. Alberti, and J. Shaw, The metabolic syndrome: a global public health problem and a new definition, J Atheroscler Thromb 12 (2005) 295-300.

142. M. T. Nakamura, Y. Cheon, Y. Li, and T. Y. Nara, Mechanisms of regulation of gene expression by fatty acids, Lipids 39 (2004) 1077-1083.

143. T. Ide, K. Egan, L. C. Bell-Parikh, and G. A. FitzGerald, Activation of nuclear receptors by prostaglandins, Thromb Res 110 (2003) 311-315.

144. M. Quinkler, I. J. Bujalska, J. W. Tomlinson, D. M. Smith, and P. M. Stewart, Depot-specific prostaglandin synthesis in human adipose tissue: a novel possible mechanism of adipogenesis, Gene 380 (2006) 137-143.

145. S. Hummasti, and P. Tontonoz, The peroxisome proliferator-activated receptor N-terminal domain controls isotype-selective gene expression and adipogenesis, Mol Endocrinol 20 (2006) 1261-1275.

146. R. Nielsen, L. Grontved, H. G. Stunnenberg, and S. Mandrup, Peroxisome proliferator-activated receptor subtype- and cell-type-specific activation of genomic target genes upon adenoviral transgene delivery, Mol Cell Biol 26 (2006) 5698-5714.

147. S. Mandard, M. Muller, and S. Kersten, Peroxisome proliferator-activated receptor alpha target genes, Cell Mol Life Sci 61 (2004) 393-416.

148. R. F. Morrison, and S. R. Farmer, Role of PPARgamma in regulating a cascade expression of cyclin-dependent kinase inhibitors, p18(INK4c) and p21(Waf1/Cip1), during adipogenesis, J Biol Chem 274 (1999) 17088-17097.

149. K. T. Dalen, K. Schoonjans, S. M. Ulven, M. S. Weedon-Fekjaer, T. G. Bentzen, H. Koutnikova, J. Auwerx, and H. I. Nebb, Adipose tissue expression of the lipid droplet-associating proteins S3-12 and perilipin is controlled by peroxisome proliferator-activated receptor-gamma, Diabetes 53 (2004) 1243-1252.

150. K. Schoonjans, J. Peinado-Onsurbe, A. M. Lefebvre, R. A. Heyman, M. Briggs, S. Deeb, B. Staels, and J. Auwerx, PPARalpha and PPARgamma activators direct a distinct tissue-specific transcriptional response via a PPRE in the lipoprotein lipase gene, Embo J 15 (1996) 5336-5348.

151. A. R. Vasudevan, and A. Balasubramanyam, Thiazolidinediones: a review of their mechanisms of insulin sensitization, therapeutic potential, clinical efficacy, and tolerability, Diabetes Technol Ther 6 (2004) 850-863.

152. N. Maeda, M. Takahashi, T. Funahashi, S. Kihara, H. Nishizawa, K. Kishida, H. Nagaretani, M. Matsuda, R. Komuro, N. Ouchi, H. Kuriyama, K. Hotta, T. Nakamura, I. Shimomura, and Y. Matsuzawa, PPARgamma ligands increase expression and plasma concentrations of adiponectin, an adipose-derived protein, Diabetes 50 (2001) 2094-2099.

153. H. I. Kim, and Y. H. Ahn, Role of peroxisome proliferator-activated receptor-gamma in the glucose-sensing apparatus of liver and beta-cells, Diabetes 53 Suppl 1 (2004) S60-65.

154. S. Y. Kim, H. I. Kim, S. K. Park, S. S. Im, T. Li, H. G. Cheon, and Y. H. Ahn, Liver glucokinase can be activated by peroxisome proliferator-activated receptor-gamma, Diabetes 53 Suppl 1 (2004) S66-70.

155. H. I. Kim, J. W. Kim, S. H. Kim, J. Y. Cha, K. S. Kim, and Y. H. Ahn, Identification and functional characterization of the peroxisomal proliferator response element in rat GLUT2 promoter, Diabetes 49 (2000) 1517-1524.

156. A. J. Gilde, J. C. Fruchart, and B. Staels, Peroxisome proliferator-activated receptors at the crossroads of obesity, diabetes, and cardiovascular disease, J Am Coll Cardiol 48 (2006) A24-32.

157. J. Berger, M. D. Leibowitz, T. W. Doebber, A. Elbrecht, B. Zhang, G. Zhou, C. Biswas, C. A. Cullinan, N. S. Hayes, Y. Li, M. Tanen, J. Ventre, M. S. Wu, G. D. Berger, R. Mosley, R. Marquis, C. Santini, S. P. Sahoo, R. L. Tolman, R. G. Smith, and D. E. Moller, Novel peroxisome proliferator-activated receptor (PPAR) gamma and PPARdelta ligands produce distinct biological effects, J Biol Chem 274 (1999) 6718-6725.

158. W. R. Oliver, Jr., J. L. Shenk, M. R. Snaith, C. S. Russell, K. D. Plunket, N. L. Bodkin, M. C. Lewis, D. A. Winegar, M. L. Sznaidman, M. H. Lambert, H. E. Xu, D. D. Sternbach, S. A. Kliewer, B. C. Hansen, and T. M. Willson, A selective peroxisome proliferator-activated receptor delta agonist promotes reverse cholesterol transport, Proc Natl Acad Sci U S A 98 (2001) 5306-5311.

159. M. D. Leibowitz, C. Fievet, N. Hennuyer, J. Peinado-Onsurbe, H. Duez, J. Bergera, C. A. Cullinan, C. P. Sparrow, J. Baffic, G. D. Berger, C. Santini, R. W. Marquis, R. L. Tolman, R. G. Smith, D. E. Moller, and J. Auwerx, Activation of PPARdelta alters lipid metabolism in db/db mice, FEBS Lett 473 (2000) 333-336.

160. O. Braissant, F. Foufelle, C. Scotto, M. Dauca, and W. Wahli, Differential expression of peroxisome proliferator-activated receptors (PPARs): tissue distribution of PPAR-alpha, -beta, and -gamma in the adult rat, Endocrinology 137 (1996) 354-366.

161. Y. X. Wang, C. L. Zhang, R. T. Yu, H. K. Cho, M. C. Nelson, C. R. Bayuga-Ocampo, J. Ham, H. Kang, and R. M. Evans, Regulation of muscle fiber type and running endurance by PPARdelta, PLoS Biol 2 (2004) e294.

162. T. Tanaka, J. Yamamoto, S. Iwasaki, H. Asaba, H. Hamura, Y. Ikeda, M. Watanabe, K. Magoori, R. X. Ioka, K. Tachibana, Y. Watanabe, Y. Uchiyama, K. Sumi, H. Iguchi, S. Ito, T. Doi, T. Hamakubo, M. Naito, J. Auwerx, M. Yanagisawa, T. Kodama, and J. Sakai, Activation of peroxisome proliferator-activated receptor delta induces fatty acid beta-oxidation in skeletal muscle and attenuates metabolic syndrome, Proc Natl Acad Sci U S A 100 (2003) 15924-15929.

163. B. A. Janowski, P. J. Willy, T. R. Devi, J. R. Falck, and D. J. Mangelsdorf, An oxysterol signalling pathway mediated by the nuclear receptor LXR alpha, Nature 383 (1996) 728-731.

164. J. M. Lehmann, S. A. Kliewer, L. B. Moore, T. A. Smith-Oliver, B. B. Oliver, J. L. Su, S. S. Sundseth, D. A. Winegar, D. E. Blanchard, T. A. Spencer, and T. M. Willson, Activation of the nuclear receptor LXR by oxysterols defines a new hormone response pathway, J Biol Chem 272 (1997) 3137-3140.

165. L. J. Millatt, V. Bocher, J. C. Fruchart, and B. Staels, Liver X receptors and the control of cholesterol homeostasis: potential therapeutic targets for the treatment of atherosclerosis, Biochim Biophys Acta 1631 (2003) 107-118.

166. J. J. Repa, S. D. Turley, J. A. Lobaccaro, J. Medina, L. Li, K. Lustig, B. Shan, R. A. Heyman, J. M. Dietschy, and D. J. Mangelsdorf, Regulation of absorption and ABC1-mediated efflux of cholesterol by RXR heterodimers, Science 289 (2000) 1524-1529.

167. J. J. Repa, K. E. Berge, C. Pomajzl, J. A. Richardson, H. Hobbs, and D. J. Mangelsdorf, Regulation of ATP-binding cassette sterol transporters ABCG5 and ABCG8 by the liver X receptors alpha and beta, J Biol Chem 277 (2002) 18793-18800.

168. G. Cao, Y. Liang, C. L. Broderick, B. A. Oldham, T. P. Beyer, R. J. Schmidt, Y. Zhang, K. R. Stayrook, C. Suen, K. A. Otto, A. R. Miller, J. Dai, P. Foxworthy, H. Gao, T. P. Ryan, X. C. Jiang, T. P. Burris, P. I. Eacho, and G. J. Etgen, Antidiabetic action of a liver x receptor agonist mediated by inhibition of hepatic gluconeogenesis, J Biol Chem 278 (2003) 1131-1136.

169. T. Yoshikawa, H. Shimano, M. Amemiya-Kudo, N. Yahagi, A. H. Hasty, T. Matsuzaka, H. Okazaki, Y. Tamura, Y. Iizuka, K. Ohashi, J. Osuga, K. Harada, T. Gotoda, S. Kimura, S. Ishibashi, and N. Yamada, Identification of liver X receptor-retinoid X receptor as an activator of the sterol regulatory element-binding protein 1c gene promoter, Mol Cell Biol 21 (2001) 2991-3000.

170. M. Makishima, A. Y. Okamoto, J. J. Repa, H. Tu, R. M. Learned, A. Luk, M. V. Hull, K. D. Lustig, D. J. Mangelsdorf, and B. Shan, Identification of a nuclear receptor for bile acids, Science 284 (1999) 1362-1365.

171. T. T. Lu, M. Makishima, J. J. Repa, K. Schoonjans, T. A. Kerr, J. Auwerx, and D. J. Mangelsdorf, Molecular basis for feedback regulation of bile acid synthesis by nuclear receptors, Mol Cell 6 (2000) 507-515.

172. J. Grober, I. Zaghini, H. Fujii, S. A. Jones, S. A. Kliewer, T. M. Willson, T. Ono, and P. Besnard, Identification of a bile acid-responsive element in the human ileal bile acid-binding protein gene. Involvement of the farnesoid X receptor/9-cis-retinoic acid receptor heterodimer, J Biol Chem 274 (1999) 29749-29754.

173. M. Ananthanarayanan, N. Balasubramanian, M. Makishima, D. J. Mangelsdorf, and F. J. Suchy, Human bile salt export pump promoter is transactivated by the farnesoid X receptor/bile acid receptor, J Biol Chem 276 (2001) 28857-28865.

174. J. L. Staudinger, B. Goodwin, S. A. Jones, D. Hawkins-Brown, K. I. MacKenzie, A. LaTour, Y. Liu, C. D. Klaassen, K. K. Brown, J. Reinhard, T. M. Willson, B. H. Koller, and S. A. Kliewer, The nuclear receptor PXR is a lithocholic acid sensor that protects against liver toxicity, Proc Natl Acad Sci U S A 98 (2001) 3369-3374.

175. D. Jung, D. J. Mangelsdorf, and U. A. Meyer, Pregnane X receptor is a target of farnesoid X receptor, J Biol Chem 281 (2006) 19081-19091.

176. S. Modica, and A. Moschetta, Nuclear bile acid receptor FXR as pharmacological target: are we there yet?, FEBS Lett 580 (2006) 5492-5499.

177. B. Cariou, K. van Harmelen, D. Duran-Sandoval, T. H. van Dijk, A. Grefhorst, M. Abdelkarim, S. Caron, G. Torpier, J. C. Fruchart, F. J. Gonzalez, F. Kuipers, and B. Staels, The farnesoid X receptor modulates adiposity and peripheral insulin sensitivity in mice, J Biol Chem 281 (2006) 11039-11049.

178. Y. Zhang, F. Y. Lee, G. Barrera, H. Lee, C. Vales, F. J. Gonzalez, T. M. Willson, and P. A. Edwards, Activation of the nuclear receptor FXR improves hyperglycemia and hyperlipidemia in diabetic mice, Proc Natl Acad Sci U S A 103 (2006) 1006-1011.

179. K. E. Matsukuma, M. K. Bennett, J. Huang, L. Wang, G. Gil, and T. F. Osborne, Coordinated control of bile acids and lipogenesis through FXR-dependent regulation of fatty acid synthase, J Lipid Res 47 (2006) 2754-2761.

180. G. L. Kennedy, Jr., J. L. Butenhoff, G. W. Olsen, J. C. O'Connor, A. M. Seacat, R. G. Perkins, L. B. Biegel, S. R. Murphy, and D. G. Farrar, The toxicology of perfluorooctanoate, Crit Rev Toxicol 34 (2004) 351-384.

181. S. L. Becker, The role of pharmacological enhancement in protease inhibitor-based highly active antiretroviral therapy, Expert Opin Investig Drugs 12 (2003) 401-412.

182. D. J. Kempf, K. C. Marsh, G. Kumar, A. D. Rodrigues, J. F. Denissen, E. McDonald, M. J. Kukulka, A. Hsu, G. R. Granneman, P. A. Baroldi, E. Sun, D. Pizzuti, J. J. Plattner, D. W. Norbeck, and J. M. Leonard, Pharmacokinetic enhancement of inhibitors of the human immunodeficiency virus protease by coadministration with ritonavir, Antimicrob Agents Chemother 41 (1997) 654-660.

183. C. L. Cooper, R. P. van Heeswijk, K. Gallicano, and D. W. Cameron, A review of low-dose ritonavir in protease inhibitor combination therapy, Clin Infect Dis 36 (2003) 1585-1592.

184. J. M. Lehmann, D. D. McKee, M. A. Watson, T. M. Willson, J. T. Moore, and S. A. Kliewer, The human orphan nuclear receptor PXR is activated by compounds that regulate CYP3A4 gene expression and cause drug interactions, J Clin Invest 102 (1998) 1016-1023.

185. I. Dussault, M. Lin, K. Hollister, E. H. Wang, T. W. Synold, and B. M. Forman, Peptide mimetic HIV protease inhibitors are ligands for the orphan receptor SXR, J Biol Chem 276 (2001) 33309-33312.

186. J. M. Rosenfeld, R. Vargas, Jr., W. Xie, and R. M. Evans, Genetic profiling defines the xenobiotic gene network controlled by the nuclear receptor pregnane X receptor, Mol Endocrinol 17 (2003) 1268-1282.

187. J. Zhou, Y. Zhai, Y. Mu, H. Gong, H. Uppal, D. Toma, S. Ren, R. M. Evans, and W. Xie, A Novel Pregnane X Receptor-mediated and Sterol Regulatory Element-binding Protein-independent Lipogenic Pathway, J Biol Chem 281 (2006) 15013-15020.

188. M. Sporstol, G. Tapia, L. Malerod, S. A. Mousavi, and T. Berg, Pregnane X receptor-agonists down-regulate hepatic ATP-binding cassette transporter A1 and scavenger receptor class B type I, Biochem Biophys Res Commun 331 (2005) 1533-1541.

189. S. Kodama, C. Koike, M. Negishi, and Y. Yamamoto, Nuclear receptors CAR and PXR cross talk with FOXO1 to regulate genes that encode drug-metabolizing and gluconeogenic enzymes, Mol Cell Biol 24 (2004) 7931-7940.

190. R. Blomhoff, M. H. Green, T. Berg, and K. R. Norum, Transport and storage of vitamin A, Science 250 (1990) 399-404.

191. J. Lengqvist, A. Mata De Urquiza, A. C. Bergman, T. M. Willson, J. Sjovall, T. Perlmann, and W. J. Griffiths, Polyunsaturated fatty acids including docosahexaenoic and arachidonic acid bind to the retinoid X receptor alpha ligand-binding domain, Mol Cell Proteomics 3 (2004) 692-703.

192. S. Kitareewan, L. T. Burka, K. B. Tomer, C. E. Parker, L. J. Deterding, R. D. Stevens, B. M. Forman, D. E. Mais, R. A. Heyman, T. McMorris, and C. Weinberger, Phytol metabolites are circulating dietary factors that activate the nuclear receptor RXR, Mol Biol Cell 7 (1996) 1153-1166.

193. D. J. Mangelsdorf, and R. M. Evans, The RXR heterodimers and orphan receptors, Cell 83 (1995) 841-850.

194. R. Mukherjee, P. J. Davies, D. L. Crombie, E. D. Bischoff, R. M. Cesario, L. Jow, L. G. Hamann, M. F. Boehm, C. E. Mondon, A. M. Nadzan, J. R. Paterniti, Jr., and R. A. Heyman, Sensitization of diabetic and obese mice to insulin by retinoid X receptor agonists, Nature 386 (1997) 407-410.

195. P. Kastner, J. M. Grondona, M. Mark, A. Gansmuller, M. LeMeur, D. Decimo, J. L. Vonesch, P. Dolle, and P. Chambon, Genetic analysis of RXR alpha developmental function: convergence of RXR and RAR signaling pathways in heart and eye morphogenesis, Cell 78 (1994) 987-1003.

196. T. Imai, M. Jiang, P. Chambon, and D. Metzger, Impaired adipogenesis and lipolysis in the mouse upon selective ablation of the retinoid X receptor alpha mediated by a tamoxifen-inducible chimeric Cre recombinase (Cre-ERT2) in adipocytes, Proc Natl Acad Sci U S A 98 (2001) 224-228.

197. Y. J. Wan, D. An, Y. Cai, J. J. Repa, T. Hung-Po Chen, M. Flores, C. Postic, M. A. Magnuson, J. Chen, K. R. Chien, S. French, D. J. Mangelsdorf, and H. M. Sucov, Hepatocyte-specific mutation establishes retinoid X receptor alpha as a heterodimeric integrator of multiple physiological processes in the liver, Mol Cell Biol 20 (2000) 4436-4444.

198. Y. J. Wan, Y. Cai, W. Lungo, P. Fu, J. Locker, S. French, and H. M. Sucov, Peroxisome proliferator-activated receptor alpha-mediated pathways are altered in hepatocyte-specific retinoid X receptor alpha-deficient mice, J Biol Chem 275 (2000) 28285-28290.

199. K. V. Heath, R. S. Hogg, K. J. Chan, M. Harris, V. Montessori, M. V. O'Shaughnessy, and J. S. Montanera, Lipodystrophy-associated morphological, cholesterol and triglyceride abnormalities in a population-based HIV/AIDS treatment database, Aids 15 (2001) 231-239.

200. A. Ammassari, A. Antinori, A. Cozzi-Lepri, M. P. Trotta, G. Nasti, A. L. Ridolfo, F. Mazzotta, A. W. Wu, A. d'Arminio Monforte, and M. Galli, Relationship between HAART adherence and adipose tissue alterations, J Acquir Immune Defic Syndr 31 Suppl 3 (2002) S140-144.

201. A. K. Agarwal, and A. Garg, A novel heterozygous mutation in peroxisome proliferator-activated receptor-gamma gene in a patient with familial partial lipodystrophy, J Clin Endocrinol Metab 87 (2002) 408-411.

202. A. K. Agarwal, and A. Garg, Genetic basis of lipodystrophies and management of metabolic complications, Annu Rev Med 57 (2006) 297-311.

203. S. Kersten, B. Desvergne, and W. Wahli, Roles of PPARs in health and disease, Nature 405 (2000) 421-424.

204. F. M. Gregoire, C. M. Smas, and H. S. Sul, Understanding adipocyte differentiation, Physiol Rev 78 (1998) 783-809.

205. A. Hammarstedt, C. X. Andersson, V. Rotter Sopasakis, and U. Smith, The effect of PPARgamma ligands on the adipose tissue in insulin resistance, Prostaglandins Leukot Essent Fatty Acids 73 (2005) 65-75.

206. T. Sher, H. F. Yi, O. W. McBride, and F. J. Gonzalez, cDNA cloning, chromosomal mapping, and functional characterization of the human peroxisome proliferator activated receptor, Biochemistry 32 (1993) 5598-5604.

207. R. Mukherjee, L. Jow, G. E. Croston, and J. R. Paterniti, Jr., Identification, characterization, and tissue distribution of human peroxisome proliferator-activated receptor (PPAR) isoforms PPARgamma2 versus PPARgamma1 and activation with retinoid X receptor agonists and antagonists, J Biol Chem 272 (1997) 8071-8076.

208. A. Schmidt, N. Endo, S. J. Rutledge, R. Vogel, D. Shinar, and G. A. Rodan, Identification of a new member of the steroid hormone receptor superfamily that is activated by a peroxisome proliferator and fatty acids, Mol Endocrinol 6 (1992) 1634-1641.

209. P. J. Willy, K. Umesono, E. S. Ong, R. M. Evans, R. A. Heyman, and D. J. Mangelsdorf, LXR, a nuclear receptor that defines a distinct retinoid response pathway, Genes Dev 9 (1995) 1033-1045.

210. D. J. Mangelsdorf, E. S. Ong, J. A. Dyck, and R. M. Evans, Nuclear receptor that identifies a novel retinoic acid response pathway, Nature 345 (1990) 224-229.

211. R. Mukherjee, S. Sun, L. Santomenna, B. Miao, H. Walton, B. Liao, K. Locke, J. H. Zhang, S. H. Nguyen, L. T. Zhang, K. Murphy, H. O. Ross, M. X. Xia, C. Teleha, S. Y. Chen, B. Selling, R. Wynn, T. Burn, and P. R. Young, Ligand and coactivator recruitment preferences of peroxisome proliferator activated receptor alpha, J. Steroid. Biochem. Mol. Biol. 81 (2002) 217-225.

212. P. J. Brown, L. W. Stuart, K. P. Hurley, M. C. Lewis, D. A. Winegar, J. G. Wilson, W. O. Wilkison, O. R. Ittoop, and T. M. Willson, Identification of a subtype selective human PPARalpha agonist through parallel-array synthesis, Bioorg Med Chem Lett 11 (2001) 1225-1227.

213. K. A. D. Ji-Hu Zhang, Richard Harrison and Gerard M. McGeehan, Co-activator LXXLL peptide preference on subtypes of peroxisome proliferator-activated receptors: An *in vitro* recruitment study, (in-process).

214. C. Yu, L. Chen, H. Luo, J. Chen, F. Cheng, C. Gui, R. Zhang, J. Shen, K. Chen, H. Jiang, and X. Shen, Binding analyses between Human PPARgamma-LBD and ligands, Eur J Biochem 271 (2004) 386-397.

215. B. R. Henke, S. G. Blanchard, M. F. Brackeen, K. K. Brown, J. E. Cobb, J. L. Collins, W. W. Harrington, Jr., M. A. Hashim, E. A. Hull-Ryde, I. Kaldor, S. A. Kliewer, D. H. Lake, L. M. Leesnitzer, J. M. Lehmann, J. M. Lenhard, L. A. Orband-Miller, J. F. Miller, R. A. Mook, Jr., S. A. Noble, W. Oliver, Jr., D. J. Parks, K. D. Plunket, J. R. Szewczyk, and T. M. Willson, N-(2-Benzoylphenyl)-L-tyrosine PPARgamma agonists. 1. Discovery of a novel series of potent antihyperglycemic and antihyperlipidemic agents, J Med Chem 41 (1998) 5020-5036.

216. K. A. Drake, J. H. Zhang, R. K. Harrison, and G. M. McGeehan, Development of a homogeneous, fluorescence resonance energy transfer-based in vitro recruitment assay for peroxisome proliferator-activated receptor delta via selection of active LXXLL coactivator peptides, Anal Biochem 304 (2002) 63-69.

217. P. Delerive, Y. Wu, T. P. Burris, W. W. Chin, and C. S. Suen, PGC-1 functions as a transcriptional coactivator for the retinoid X receptors, J Biol Chem 277 (2002) 3913-3917.

218. W. Bourguet, M. Ruff, D. Bonnier, F. Granger, M. Boeglin, P. Chambon, D. Moras, and H. Gronemeyer, Purification, functional characterization, and crystallization of the ligand binding domain of the retinoid X receptor, Protein Expr Purif 6 (1995) 604-608.

219. X. Gan, R. Kaplan, J. G. Menke, K. MacNaul, Y. Chen, C. P. Sparrow, G. Zhou, S. D. Wright, and T. Q. Cai, Dual mechanisms of ABCA1 regulation by geranylgeranyl pyrophosphate, J Biol Chem 276 (2001) 48702-48708.

220. D. J. Peet, B. A. Janowski, and D. J. Mangelsdorf, The LXRs: a new class of oxysterol receptors, Curr Opin Genet Dev 8 (1998) 571-575.

221. K. H. Cho, J. Y. Park, J. I. Han, and T. S. Jeong, Ligand-binding domain of farnesoid X receptor (FXR) had the highest sensitivity and activity among FXR variants in a fluorescence-based assay, Lipids 38 (2003) 1149-1156.

222. D. J. Parks, S. G. Blanchard, R. K. Bledsoe, G. Chandra, T. G. Consler, S. A. Kliewer, J. B. Stimmel, T. M. Willson, A. M. Zavacki, D. D. Moore, and J. M. Lehmann, Bile acids: natural ligands for an orphan nuclear receptor, Science 284 (1999) 1365-1368.

223. B. Goodwin, E. Hodgson, and C. Liddle, The orphan human pregnane X receptor mediates the transcriptional activation of CYP3A4 by rifampicin through a distal enhancer module, Mol Pharmacol 56 (1999) 1329-1339.

224. T. M. Willson, P. J. Brown, D. D. Sternbach, and B. R. Henke, The PPARs: from orphan receptors to drug discovery, J. Med. Chem. 43 (2000) 527-550.

225. G. Allenby, M. T. Bocquel, M. Saunders, S. Kazmer, J. Speck, M. Rosenberger, A. Lovey, P. Kastner, J. F. Grippo, P. Chambon, and et al., Retinoic acid receptors and retinoid X receptors: interactions with endogenous retinoic acids, Proc Natl Acad Sci U S A 90 (1993) 30-34.

226. D. G. Lemay, and D. H. Hwang, Genome-wide identification of peroxisome proliferator response elements using integrated computational genomics, J Lipid Res 47 (2006) 1583-1587.

227. J. D. Horton, N. A. Shah, J. A. Warrington, N. N. Anderson, S. W. Park, M. S. Brown, and J. L. Goldstein, Combined analysis of oligonucleotide microarray data from transgenic and knockout mice identifies direct SREBP target genes, Proc Natl Acad Sci U S A 100 (2003) 12027-12032.

228. U. E. Gibson, C. A. Heid, and P. M. Williams, A novel method for real time quantitative RT-PCR, Genome Res 6 (1996) 995-1001.

229. C. A. Heid, J. Stevens, K. J. Livak, and P. M. Williams, Real time quantitative PCR, Genome Res 6 (1996) 986-994.

230. T. Chen, W. Xie, M. Agler, and M. Banks, Coactivators in assay design for nuclear hormone receptor drug discovery, Assay Drug Dev Technol 1 (2003) 835-842.

231. M. J. Clemens, M. Bushell, I. W. Jeffrey, V. M. Pain, and S. J. Morley, Translation initiation factor modifications and the regulation of protein synthesis in apoptotic cells, Cell Death Differ 7 (2000) 603-615.

232. T. Fujino, Y. Sato, M. Une, T. Kanayasu-Toyoda, T. Yamaguchi, K. Shudo, K. Inoue, and T. Nishimaki-Mogami, In vitro farnesoid X receptor ligand sensor assay using surface plasmon resonance and based on ligand-induced coactivator association, J Steroid Biochem Mol Biol 87 (2003) 247-252.

233. D. J. Kempf, K. C. Marsh, J. F. Denissen, E. McDonald, S. Vasavanonda, C. A. Flentge, B. E. Green, L. Fino, C. H. Park, X. P. Kong, and et al., ABT-538 is a potent inhibitor of human immunodeficiency virus protease and has high oral bioavailability in humans, Proc Natl Acad Sci U S A 92 (1995) 2484-2488.

234. K. Jones, P. G. Hoggard, S. D. Sales, S. Khoo, R. Davey, and D. J. Back, Differences in the intracellular accumulation of HIV protease inhibitors in vitro and the effect of active transport, Aids 15 (2001) 675-681.

235. H. E. Xu, M. H. Lambert, V. G. Montana, K. D. Plunket, L. B. Moore, J. L. Collins, J. A. Oplinger, S. A. Kliewer, R. T. Gampe, Jr., D. D. McKee, J. T. Moore, and T. M. Willson, Structural determinants of ligand binding selectivity between the peroxisome proliferator-activated receptors, Proc Natl Acad Sci U S A 98 (2001) 13919-13924.

236. A. D. Kelleher, A. K. Sewell, and D. A. Price, Dyslipidemia due to retroviral protease inhibitors, Nat Med 8 (2002) 308; author reply 308-309.

237. G. Dore, Antiretroviral therapy-related hepatotoxicity: predictors and clinical management, J HIV Ther 8 (2003) 96-100.

238. R. S. Autar, M. Boffito, E. Hassink, F. W. Wit, J. Ananworanich, U. Siangphoe, A. Pozniak, D. A. Cooper, P. Phanuphak, J. M. Lange, K. Ruxrungtham, and D. M. Burger, Interindividual variability of once-daily ritonavir boosted saquinavir pharmacokinetics in Thai and UK patients, J Antimicrob Chemother 56 (2005) 908-913.

239. S. Wilkening, F. Stahl, and A. Bader, COMPARISON OF PRIMARY HUMAN HEPATOCYTES AND HEPATOMA CELL LINE HEPG2 WITH REGARD TO THEIR BIOTRANSFORMATION PROPERTIES, Drug Metab Dispos 31 (2003) 1035-1042.

240. R. Jover, R. Bort, M. J. Gomez-Lechon, and J. V. Castell, Cytochrome P450 regulation by hepatocyte nuclear factor 4 in human hepatocytes: a study using adenovirus-mediated antisense targeting, Hepatology 33 (2001) 668-675.

241. B. A. Jessen, J. S. Mullins, A. De Peyster, and G. J. Stevens, Assessment of hepatocytes and liver slices as in vitro test systems to predict in vivo gene expression, Toxicol Sci 75 (2003) 208-222.

242. R. Gutierrez-Juarez, A. Pocai, C. Mulas, H. Ono, S. Bhanot, B. P. Monia, and L. Rossetti, Critical role of stearoyl-CoA desaturase-1 (SCD1) in the onset of diet-induced hepatic insulin resistance, J Clin Invest 116 (2006) 1686-1695.

243. L. T. LaFave, L. B. Augustin, and C. N. Mariash, S14: insights from knockout mice, Endocrinology 147 (2006) 4044-4047.

244. J. Patel, B. Buddha, S. Dey, D. Pal, and A. K. Mitra, In vitro interaction of the HIV protease inhibitor ritonavir with herbal constituents: changes in P-gp and CYP3A4 activity, Am J Ther 11 (2004) 262-277.

245. C. Juge-Aubry, A. Pernin, T. Favez, A. G. Burger, W. Wahli, C. A. Meier, and B. Desvergne, DNA binding properties of peroxisome proliferator-activated receptor subtypes on various natural peroxisome proliferator response elements. Importance of the 5'-flanking region, J Biol Chem 272 (1997) 25252-25259.

246. S. P. Anderson, C. Dunn, A. Laughter, L. Yoon, C. Swanson, T. M. Stulnig, K. R. Steffensen, R. A. Chandraratna, J. A. Gustafsson, and J. C. Corton, Overlapping transcriptional programs regulated by the nuclear receptors peroxisome proliferator-activated receptor alpha, retinoid X receptor, and liver X receptor in mouse liver, Mol Pharmacol 66 (2004) 1440-1452.

247. T. Yoshikawa, T. Ide, H. Shimano, N. Yahagi, M. Amemiya-Kudo, T. Matsuzaka, S. Yatoh, T. Kitamine, H. Okazaki, Y. Tamura, M. Sekiya, A. Takahashi, A. H. Hasty, R. Sato, H. Sone, J. Osuga, S. Ishibashi, and N. Yamada, Cross-talk between peroxisome proliferator-activated receptor (PPAR) alpha and liver X receptor (LXR) in nutritional regulation of fatty acid metabolism. I. PPARs suppress sterol regulatory element binding protein-1c promoter through inhibition of LXR signaling, Mol Endocrinol 17 (2003) 1240-1254.

248. E. S. Goetzman, L. Tian, T. R. Nagy, B. A. Gower, T. R. Schoeb, A. Elgavish, E. P. Acosta, M. S. Saag, and P. A. Wood, HIV protease inhibitor ritonavir induces lipoatrophy in male mice, AIDS Res Hum Retroviruses 19 (2003) 1141-1150.

249. S. S. Im, J. W. Kim, T. H. Kim, X. L. Song, S. Y. Kim, H. I. Kim, and Y. H. Ahn, Identification and characterization of peroxisome proliferator response element in the mouse GLUT2 promoter, Exp Mol Med 37 (2005) 101-110.

250. C. Bonny, N. Thompson, P. Nicod, and G. Waeber, Pancreatic-specific expression of the glucose transporter type 2 gene: identification of cis-elements and islet-specific trans-acting factors, Mol Endocrinol 9 (1995) 1413-1426.

251. N. E. Rubins, J. R. Friedman, P. P. Le, L. Zhang, J. Brestelli, and K. H. Kaestner, Transcriptional Networks in the Liver: Hepatocyte Nuclear Factor 6 Function Is Largely Independent of Foxa2, Mol. Cell. Biol. 25 (2005) 7069-7077.

252. V. J. Lannoy, J. F. Decaux, C. E. Pierreux, F. P. Lemaigre, and G. G. Rousseau, Liver glucokinase gene expression is controlled by the onecut transcription factor hepatocyte nuclear factor-6, Diabetologia 45 (2002) 1136-1141.

253. G. Waeber, N. Thompson, P. Nicod, and C. Bonny, Transcriptional activation of the GLUT2 gene by the IPF-1/STF-1/IDX-1 homeobox factor, Mol Endocrinol 10 (1996) 1327-1334.

254. C. Postic, M. Shiota, and M. A. Magnuson, Cell-specific roles of glucokinase in glucose homeostasis, Recent Prog Horm Res 56 (2001) 195-217.

255. F. C. Schuit, P. Huypens, H. Heimberg, and D. G. Pipeleers, Glucose sensing in pancreatic beta-cells: a model for the study of other glucose-regulated cells in gut, pancreas, and hypothalamus, Diabetes 50 (2001) 1-11.

256. M. Mueckler, Facilitative glucose transporters, Eur J Biochem 219 (1994) 713-725.

257. L. L. Levitsky, Q. Zheng, K. Mink, and D. B. Rhoads, GLUT-1 and GLUT-2 mRNA, protein, and glucose transporter activity in cultured fetal and adult hepatocytes, Am J Physiol 267 (1994) E88-94.

258. C. Bouche, S. Serdy, C. R. Kahn, and A. B. Goldfine, The cellular fate of glucose and its relevance in type 2 diabetes, Endocr Rev 25 (2004) 807-830.

259. C. M. Garcia-Herrero, M. Galan, O. Vincent, B. Flandez, M. Gargallo, E. Delgado-Alvarez, E. Blazquez, and M. A. Navas, Functional analysis of human glucokinase gene mutations causing MODY2: exploring the regulatory mechanisms of glucokinase activity, Diabetologia 50 (2007) 325-333.

260. G. Velho, K. F. Petersen, G. Perseghin, J.-H. Hwang, D. L. Rothman, M. E. Pueyo, G. W. Cline, P. Froguel, and G. I. Shulman, Impaired Hepatic Glycogen Synthesis in Glucokinase-deficient (MODY-2) Subjects, J. Clin. Invest. 98 (1996) 1755-1761.

261. J. F. Caro, S. Triester, V. K. Patel, E. B. Tapscott, N. L. Frazier, and G. L. Dohm, Liver glucokinase: decreased activity in patients with type II diabetes, Horm Metab Res 27 (1995) 19-22.

262. A. Basu, R. Basu, P. Shah, A. Vella, C. Johnson, K. Nair, M. Jensen, W. Schwenk, and R. Rizza, Effects of type 2 diabetes on the ability of insulin and glucose to regulate splanchnic and muscle glucose metabolism: evidence for a defect in hepatic glucokinase activity, Diabetes 49 (2000) 272-283.

263. A. Basu, R. Basu, P. Shah, A. Vella, C. M. Johnson, M. Jensen, K. S. Nair, W. F. Schwenk, and R. A. Rizza, Type 2 Diabetes Impairs Splanchnic Uptake of Glucose but Does Not Alter Intestinal Glucose Absorption During Enteral Glucose Feeding: Additional Evidence for a Defect in Hepatic Glucokinase Activity, Diabetes 50 (2001) 1351-1362.

264. J. Seoane, A. Barbera, S. Telemaque-Potts, C. B. Newgard, and J. J. Guinovart, Glucokinase Overexpression Restores Glucose Utilization and Storage in Cultured Hepatocytes from Male Zucker Diabetic Fatty Rats, J. Biol. Chem. 274 (1999) 31833-31838.

265. T. Ferre, E. Riu, F. Bosch, and A. Valera, Evidence from transgenic mice that glucokinase is rate limiting for glucose utilization in the liver, Faseb J 10 (1996) 1213-1218.

266. N. Hariharan, D. Farrelly, D. Hagan, D. Hillyer, C. Arbeeny, T. Sabrah, A. Treloar, K. Brown, S. Kalinowski, and K. Mookhtiar, Expression of human hepatic glucokinase in transgenic mice liver results in decreased glucose levels and reduced body weight, Diabetes 46 (1997) 11-16.

267. K. J. Brocklehurst, V. A. Payne, R. A. Davies, D. Carroll, H. L. Vertigan, H. J. Wightman, S. Aiston, I. D. Waddell, B. Leighton, M. P. Coghlan, and L. Agius, Stimulation of hepatocyte glucose metabolism by novel small molecule glucokinase activators, Diabetes 53 (2004) 535-541.

268. K. R. Guertin, and J. Grimsby, Small molecule glucokinase activators as glucose lowering agents: a new paradigm for diabetes therapy, Curr Med Chem 13 (2006) 1839-1843.

269. G. C. Weir, A. Sharma, D. H. Zangen, and S. Bonner-Weir, Transcription factor abnormalities as a cause of beta cell dysfunction in diabetes: a hypothesis, Acta Diabetol 34 (1997) 177-184.

270. A. De Vos, H. Heimberg, E. Quartier, P. Huypens, L. Bouwens, D. Pipeleers, and F. Schuit, Human and rat beta cells differ in glucose transporter but not in glucokinase gene expression, J Clin Invest 96 (1995) 2489-2495.

271. Of mice and men: GLUT2 highlights differences in diabetes, Gastroenterology 114 (1998) 429.

272. S. Del Guerra, R. Lupi, L. Marselli, M. Masini, M. Bugliani, S. Sbrana, S. Torri, M. Pollera, U. Boggi, F. Mosca, S. Del Prato, and P. Marchetti, Functional and molecular defects of pancreatic islets in human type 2 diabetes, Diabetes 54 (2005) 727-735.

273. R. Santer, S. Groth, M. Kinner, A. Dombrowski, G. T. Berry, J. Brodehl, J. V. Leonard, S. Moses, S. Norgren, F. Skovby, R. Schneppenheim, B. Steinmann, and J. Schaub, The mutation spectrum of the facilitative glucose transporter gene SLC2A2 (GLUT2) in patients with Fanconi-Bickel syndrome, Hum Genet 110 (2002) 21-29.

274. J. Y. Cha, H. S. Kim, H. I. Kim, S. S. Im, S. Y. Kim, J. W. Kim, B. I. Yeh, and Y. H. Ahn, Analysis of polymorphism of the GLUT2 promoter in NIDDM patients and its functional consequence to the promoter activity, Ann Clin Lab Sci 32 (2002) 114-122.

275. J. C. Koster, M. S. Remedi, H. Qiu, C. G. Nichols, and P. W. Hruz, HIV Protease Inhibitors Acutely Impair Glucose-Stimulated Insulin Release, Diabetes 52 (2003) 1695-1700.

276. M. A. Noor, T. Seneviratne, F. T. Aweeka, J. C. Lo, J. M. Schwarz, K. Mulligan, M. Schambelan, and C. Grunfeld, Indinavir acutely inhibits insulin-stimulated glucose disposal in humans: a randomized, placebo-controlled study, Aids 16 (2002) F1-8.

277. G. A. Lee, T. Seneviratne, M. A. Noor, J. C. Lo, J. M. Schwarz, F. T. Aweeka, K. Mulligan, M. Schambelan, and C. Grunfeld, The metabolic effects of lopinavir/ritonavir in HIV-negative men, Aids 18 (2004) 641-649.

278. R. Walli, G. M. Michl, D. Muhlbayer, L. Brinkmann, and F. D. Goebel, Effects of troglitazone on insulin sensitivity in HIV-infected patients with protease inhibitor-associated diabetes mellitus, Res Exp Med (Berl) 199 (2000) 253-262.

279. M. C. Gelato, D. C. Mynarcik, J. L. Quick, R. T. Steigbigel, J. Fuhrer, C. E. Brathwaite, J. S. Brebbia, M. R. Wax, and M. A. McNurlan, Improved insulin sensitivity and body fat distribution in HIV-infected patients treated with rosiglitazone: a pilot study, J Acquir Immune Defic Syndr 31 (2002) 163-170.

280. B. Desvergne, and W. Wahli, Peroxisome proliferator-activated receptors: nuclear control of metabolism, Endocr. Rev. 20 (1999) 649-688.

281. R. M. Evans, G. D. Barish, and Y. X. Wang, PPARs and the complex journey to obesity, Nat. Med. 10 (2004) 355-361.

282. M. H. Hsu, U. Savas, K. J. Griffin, and E. F. Johnson, Identification of peroxisome proliferator-responsive human genes by elevated expression of the peroxisome proliferator-activated receptor alpha in HepG2 cells, J. Biol. Chem. 276 (2001) 27950-27958.

283. G. Krey, O. Braissant, F. L'Horset, E. Kalkhoven, M. Perroud, M. G. Parker, and W. Wahli, Fatty acids, eicosanoids, and hypolipidemic agents identified as ligands of peroxisome proliferator-activated receptors by coactivator-dependent receptor ligand assay, Mol. Endocrinol. 11 (1997) 779-791.

284. J. C. Corton, S. P. Anderson, and A. Stauber, Central role of peroxisome proliferator-activated receptors in the actions of peroxisome proliferators, Annu. Rev. Pharmacol. Toxicol. 40 (2000) 491-518.

285. R. K. Harrison, S. Lin, H. M. Seidel, J. Zhang, L. Zhang, and G. McGeehan, Cell-free and cell-based methods for characterizing nuclear receptor ligands, Curr. Med. Chem.- Imun., Endoc. & Metab. Agents 2 (2002) 23-31.

286. G. Zhou, R. Cummings, J. Hermes, and D. E. Moller, Use of homogeneous time-resolved fluorescence energy transfer in the measurement of nuclear receptor activation, Methods 25 (2001) 54-61.

287. M. Fritsch, C. M. Leary, J. D. Furlow, H. Ahrens, T. J. Schuh, G. C. Mueller, and J. Gorski, A ligand-induced conformational change in the estrogen receptor is localized in the steroid binding domain, Biochemistry 31 (1992) 5303-5311.

288. I. Sadowski, J. Ma, S. Triezenberg, and M. Ptashne, GAL4-VP16 is an unusually potent transcriptional activator, Nature 335 (1988) 563-564.

289. A. R. Bapat, and D. E. Frail, Full-length estrogen receptor alpha and its ligand-binding domain adopt different conformations upon binding ligand, J. Steroid. Biochem. Mol. Biol. 86 (2003) 143-149.

290. G. Mathis, Probing molecular interactions with homogeneous techniques based on rare earth cryptates and fluorescence energy transfer, Clin. Chem. 41 (1995) 1391-1397.

291. D. M. Heery, E. Kalkhoven, S. Hoare, and M. G. Parker, A signature motif in transcriptional co-activators mediates binding to nuclear receptors, Nature 387 (1997) 733-736.

292. R. e. a. Mukherjee, Abstract of the Keystone symposia: PPARs-a Transcriptional Odyssey, (2001) 64.

293. C. E. Juge-Aubry, S. Kuenzli, J. C. Sanchez, D. Hochstrasser, and C. A. Meier, Peroxisomal bifunctional enzyme binds and activates the activation function-1 region of the peroxisome proliferator-activated receptor alpha, Biochem. J. 353 (2001) 253-258.

294. C. E. Juge-Aubry, E. Hammar, C. Siegrist-Kaiser, A. Pernin, A. Takeshita, W. W. Chin, A. G. Burger, and C. A. Meier, Regulation of the transcriptional activity of the peroxisome proliferator-activated receptor alpha by phosphorylation of a ligand-independent trans-activating domain, J. Biol. Chem. 274 (1999) 10505-10510.

295. A. Tremblay, G. B. Tremblay, F. Labrie, and V. Giguere, Ligand-independent recruitment of SRC-1 to estrogen receptor beta through phosphorylation of activation function AF-1, Mol. Cell 3 (1999) 513-519.

296. L. Gelman, G. Zhou, L. Fajas, E. Raspe, J. C. Fruchart, and J. Auwerx, p300 interacts with the N- and C-terminal part of PPARgamma2 in a ligand-independent and -dependent manner, respectively, J. Bio.l Chem. 274 (1999) 7681-7688.

297. R. Hi, S. Osada, N. Yumoto, and T. Osumi, Characterization of the amino-terminal activation domain of peroxisome proliferator-activated receptor alpha. Importance of alpha-helical structure in the transactivating function, J. Biol. Chem. 274 (1999) 35152-35158.

Vita

Jennifer Berbaum (Born: Jennifer Smith, Philadelphia, PA)

Professional Experience:

Research Scientist 4/06 to present
Senior Research Associate 3/02 to 4/06
Vitae Pharmaceuticals, Discovery Biology, Ft. Washington, PA
Project leader. Led the development and implementation of biochemical methods to identify and characterize inhibitors of hydroxysteroid dehydrogenases.

Senior Staff Scientist 8/01 to 12/01
Staff Scientist 10/98 to 8/01
DuPont Pharmaceuticals, Research and Development, Antimicrobials, Wilmington, DE
Experience in antimicrobial areas involving Glu-tRNA^{Gln} amidotransferase and tRNA synthetases.

Research Assistant 6/95 to 9/97
Immune Response Corporation, Process Development, King of Prussia, PA
Production scale growth, inactivation and purification of HIV-1.

Laboratory Assistant 12/94 to 6/95
Drexel University, Department of Bioscience and Biotechnology, Philadelphia, PA
Investigation of the mechanisms involved in the induction of the *sfi*-independent pathway of *E. coli.*

Laboratory Technician 3/93 to 9/93
SmithKline Beecham Pharmaceuticals, Department of Infectious Diseases, Upper Merion, PA
Analysis of HSV-2 levels in mice brainstems to determine effects of inhibitor therapy.

Publications and Posters:

1. **Berbaum, Jennifer** and Richard K. Harrison. 2007. Effect of HIV drugs on the activation of metabolic nuclear receptors. Manuscript in-process.

2. **Berbaum, Jennifer,** Joseph Bruno and Richard K. Harrison. 2007. Kinetic characterization of 3βHSD2. Manuscript in-process.

3. **Berbaum, Jennifer** and Richard K. Harrison. 2005. Comparison of full-length versus ligand binding domain constructs in cell-free and cell-based peroxisome proliferators-activated receptor alpha assays. Anal. Biochem. 339(1):121-8.

4. Ekins, Sean, **J. Berbaum**, R. K. Harrison, M. Zecher, J. Yuan, A. V. Ishchenko, K. Berezin, V. Chubukov, J. D. Lawson, and a. M. A. Hupcey. 2004. *in* Pharmaceutical Profiling in Drug Discovery for Lead Selection (Ronald T. Bouchardt, E.H. Kerns, C.A. Lipinski, D.R. Thakker, and Wang, B., Eds.), Vol. 1, pp. 361-389, American Association of Pharmaceutical Scientists, Arlington.

5. Ekins, Sean, **Jennifer Berbaum**, and Richard K. Harrison. 2003. Generation and validation of rapid computational filters for cyp2D6 and cyp3A4. Drug Metab. Dispos. 31(9): 1077-80.

6. Hill, Thomas M., Bela Sharma, Majda Valjavec-Gratian and **Jennifer Smith**. 1997. *Sfi*-independent filamentation in *Escherichia coli* is *lexA* dependent and requires DNA damage for induction. J. Bacteriol. 179:1931-1939.

7. Uncoupling the Catalytic Activities of the Glu-tRNA^{Gln} Amidotransferase from *Streptococcus pyogenes.* Mason, Jennifer L., **Jennifer Berbaum**, Fay Yu, Kathy Wang, Debra Burdick, Kelley Rogers, and David Pompliano. Poster presented at annual tRNA conference in Oxford, England 2000.